

Sarah Kimmina, Klaus Nebendahl (ed.)

Laboratory Animal Science – Main Focus: Neuroscience

Proceedings of the 41th Annual Symposium of the Society for
Laboratory Animal Science (GV-SOLAS), 7.–10.09.2003 Göttingen



Universitätsdrucke Göttingen

Sarah Kimmina und Klaus Nebendahl (Hg.)
Laboratory Animal Science – Main focus: Neuroscience

Except where otherwise noted, this work is
licensed under a [Creative Commons License](#)



erschieden in der Reihe der Universitätsdrucke
im Universitätsverlag Göttingen 2006

Sarah Kimmina und Klaus Nebendahl (Hg.)

Laboratory Animal Science – Main focus: Neuroscience

Proceedings of the 41th Annual
Symposium of the Society for
Laboratory Animal Science
(GV-SOLAS)
7.-10.09.2003 Göttingen



Universitätsverlag Göttingen
2006

Bibliographische Information der Deutschen Nationalbibliothek

Die Deutsche Nationalbibliothek verzeichnet diese Publikation in der Deutschen Nationalbibliographie; detaillierte bibliographische Daten sind im Internet über <http://dnb.ddb.de> abrufbar

Address of the Editors

Dr. Sarah Kimmina

e-mail: kimmina@med.uni-goettingen.de

Dr. Klaus Nebendahl

e-mail: knebenda@med.uni-goettingen.de

This work is protected by German Intellectual Property Right Law. It is also available as an Open Access version through the publisher's homepage and the Online Catalogue of the State and University Library of Goettingen (<http://www.sub.uni-goettingen.de>). Users of the free online version are invited to read, download and distribute it [if licenced: under the licence agreement shown in the online version]. Users may also print a small number for educational or private use. However they may not sell print versions of the online book.

Satz und Layout: Sarah Kimmina

Umschlaggestaltung: Kilian Klapp

© 2006 Universitätsverlag Göttingen

<http://univerlag.uni-goettingen.de>

ISBN-13: 978-3-938616-66-6

Preface

It was a great pleasure to organize the 41st meeting of the Laboratory Animal Society (GV-SOLAS) in Göttingen. The organisers and participants have been impressed by the high level of the presented scientific work. For this reason we had to meet the demands of the requests for a commonly accessible publication. After quite a long time of preparation we can now present this documentation.

The main topic of the meeting “Neuroscience” was focussed on the region of Göttingen, due to the different institutes working with laboratory animals such as the Max Planck Institutes for experimental medicine and biophysical chemistry, the German Primate Center, the European Neuroscience Institute and finally the Georg August University (Medical Department). A large variety of issues was discussed in the course of this congress, e.g. stroke, neurodegenerative disorders, TSE, stem-cells and infectious diseases in laboratory animals, which can be found in the congress book now.

We hope that this publication will be of interest for a lot of people working in the field of Laboratory Animal Science.

Finally we would like to thank all authors, participants and helping hands, who made this congress successful.

Göttingen, August 2006
S. Kimmina and K. Nebendahl

Index of contents

Magnetic Resonance Imaging of Animal Brain In Vivo	1
<i>Jens Frahm, Oliver Natt, Takashi Watanabe, Susann Boretius, Thomas Michaelis</i>	
Relevance of small animal models for TSE Research	15
<i>W.J. Schulz-Schaeffer</i>	
Animal models for multiple sclerosis	19
<i>C. Stadelmann</i>	
Treatment trials for stroke: Preclinical and clinical models	34
<i>Anna-Leena Sirén and Hannelore Ehrenreich</i>	
Non-Invasive Quantification of Brain Edema and the Space-Occupying effect in a permanent rat stroke model using magnetic resonance imaging	43
<i>M. Walberer, T. Gerriets, E. Stolz, M. Kaps, C. Müller, A. Kluge, A. Bachmann, M. Fisher, M. Kaps, G. Bachmann</i>	
Chronic rat models of cerebral oligaemia	47
<i>Konstanze Plaschke, Hubert J. Bardenheuer, Eike Martin, Michael Knauth</i>	
Hypothalamic injury and Hyperthermia (side effects of the suture model for MCA occlusion) can confound the evaluation of neuroprotective drugs	51
<i>M. Walberer, T. Gerriets, E. Stolz, M. Kaps, M. Fisher, G. Bachmann</i>	
Superselective diagnostic and interventional angiography in rats	56
<i>M. Knauth, A. Mohr, K. Plaschke</i>	
Intracoronary transplantation of autologous mesenchymal stem cells in a swine ischemic heart model	62
<i>K. Guan, V. Zyba, T. Becker, S. Won, D. Lages, A.B. Buchwald, G. Hasenfuß</i>	
Hepatocyte transplantation model and induction of intrahepatic stem cells	64
<i>Sarah König, Petra Krause</i>	
Recombination analysis in porcine endogenous retroviruses	68
<i>B. Aigner, N. Klymiuk, M. Müller, G. Brem</i>	

Investigation of the efficacy of rodent microbiological monitoring methods in a ventilated cage rack system	72
<i>Susan R Compton, Felix Homberger, Judy MacArthur Clark, Frank X Paturzo.</i>	
Optimization of the detection of Helicobacter spp. using PCR	74
<i>K. Jacobsen, E. Mahabir, M. Brielmeier, P. Wilhelm, K. Seidel, J. Schmidt</i>	
In utero infection of pseudopregnant mice recipients with Mouse Hepatitis Virus and Mouse Minute Virus	76
<i>E. Mahabir, A. Mayer, J. Needham1, J. Schmidt</i>	
Health monitoring of laboratory rodents: incidence and relevance of bacterial isolates from the trachea	78
<i>M. Brielmeier, P. Wilhelm and J. Schmidt</i>	
Changes in differential haemogram after infusion of mean and low molecular weight hydroxyethyl starch (HES) in rats	81
<i>M. Wagenblast, A. Theisen, Ch. Tandi, H. Forester</i>	
Does inhalation anesthesia act beneficial in preventing distress from tail biopsy in laboratory mice?	85
<i>M. Arras, A. Rettich, B. Seifert, T. Rühlcke</i>	
Animal Experimentation: A Comparison of the Attitude of the German and the British Population	87
<i>C. Exner and G. Heldmaier</i>	
WOKW rats: an excellent animal model for the complete metabolic syndrome	91
<i>Ingrid Klötting and Nora Klötting</i>	
The proinflammatory cytokine interferon- γ induces chronic active myocarditis and cardiomyopathy in transgenic mice	96
<i>S. Ott, J. Löhler, K. Yamamura und K. Reifenberg</i>	
Genetics of the Metabolic Syndrome in NZO Mice	99
<i>R. Kluge, M. Grothe, S. Scherneck, K. Schmolz, K. Giesen, L. Plum, H.G. Joost</i>	
Differences of pathogenicity of Pasteurella pneumotropica biotypes	105
<i>H. Meyer, S. Ott</i>	
Health monitoring results obtained from mice and rats from commercial breeders	108
<i>Werner Nicklas</i>	

The sheep as a chronic animal model for the long-term test of left ventricular assist device	112
<i>C Ballat, H. Alekuzzei, K. Steinke, J. Schmitto, H. Doerge, F Schoendube</i>	
Reconstitution of immunodeficient mice	114
<i>Beuter, C., Stauffer, U., Kwiatkowski, H., Joswig, N., Mossmann, H.</i>	
4 Major candidate genes for experimental IBD identified by microarray analysis in combination with quantitative trait locus (CTL) mapping data in mice	115
<i>André Bleich, Jörg Lauber, Jan Buer, Hans Hedrich, Michael Mähler</i>	
Health problems in South African Clawed Frogs (<i>Xenopus laevis</i>): Pathological, microbiological, and parasitological findings	117
<i>Ines Bolle, Gero Hilken</i>	
The influence of changed cage structuring on fighting and basic physiological parameters of the Athymic Nude-nu/nu mouse	119
<i>T. Büрге, L. Fozard</i>	
Genetical characterization of the LEW/Ztm-ci2 (circling2) and the BH.7A/Ztm-ci3 (circling3) rats as animal models for syndromic deafness (USH1) respectively lateralization of brain function and hyperlocomotion	128
<i>W.T. Chwalisz, D. Wedekind, H.J. Hedrich</i>	
Induced Intracerebral Haemorrhage in Rats: Comparison of the Validity of Computertomography (CT) and Magnetresonanztomographie (MRI)	131
<i>V. Elste</i>	
PyRAT- Python based relational animal tracking – a new web-based solution for animal facility management	135
<i>J. Helppi, J. Oegema, J. Duperon</i>	
The dorsal skinfold chamber as useful model for the investigation of microcirculation and angiogenesis	136
<i>Markus Heuser, Gerhard Zöller, Rolf H. Ringert, Bernhard Hemmerlein</i>	

Spontaneous tumours in a colony of Cynomolgus monkeys (<i>Macaca fascicularis</i>) observed during a 10-year period (1992-2002), with a survey of the literature	137
<i>J.Kaspareit, S.Friderichs-Gromoll, E.Buse, G.Habermann and F. Vogel</i>	
Mycobacterium marinum infection in <i>Xenopus laevis</i> – a case study	140
<i>Sarah Kimmina</i>	
Determination of circadian rhythm of body temperature in laboratory mice and rats by rectal probe	141
<i>M. Klein¹, T. Tillmann¹, P. P. Tsai, H. Hackbarth, C. Dasenbrock</i>	
Subcutaneously implanted transponders/microchips – a new minimally invasive method of body temperature measurement?	143
<i>M. Klein, T. Tillmann, P. P. Tsai, H. Hackbarth, C. Dasenbrock</i>	
The polydactyly luxate syndrome of the rat: Morphological and genetical findings	145
<i>C. Krüger, D. Büttner, H. Böhme, K. Militzer</i>	
Detection of MHV and MMV in mice: Comparison of a viral plaque assay with the MAP-test and PCR	147
<i>E. Mahabir, K. Jacobsen, D. Peters, J. Needham, J. Schmidt</i>	
Individually Ventilated Cages and Open Cages with or without environmental enrichment: a comparative study on body weight, major organs weight and blood parameters in Hsd:ICR(CD-1) [®] mice	149
<i>Gianpaolo Milite</i>	
Investigations on the effect of inhalative formaldehyde exposure on the open field behavior in rats	150
<i>K.-U. Möritz, F. A. Malek, J. Fanghänel</i>	
TierBase: A program for computer-assisted management of an animal breeding and experimentation facility	151
<i>P. Nielsen und H. Mossmann</i>	
Neuropathological results in laboratory mice	153
<i>S. Ott, H. Meyer, N. Gerstmayr, G. Spindler</i>	
<i>Pasteurella pneumotropica</i> – Pathology of Virulent Biotypes	154
<i>S. Ott, H. Meyer, J. Brodbeck, P. Nusser, G. Spindler</i>	

New mouse models derived from the Munich ENU mouse mutagenesis project for iron metabolism research	155
<i>B. Rathkolb, M. Klempt, M. Mohr, D. Soewarto, S. Hoffmann, S. Wagner, M. Hrabé de Angelis, E. Wolf, B. Aigner</i>	
Effects of soy-containing rat chow on estrogen receptive organs	157
<i>G. Rimoldi, J. Chistoffel, D. Seidlova-Wuttke, W. Wuttke</i>	
Enrichment in the housing of laboratory dogs	158
<i>L. Schmid, D. Döring-Schätzl, M. H. Erhard</i>	
The Effect of Hyperventilation on Cognitive Performance, Motor Function and Lesion Volume After Controlled Cortical Impact in the Rat	160
<i>E. Eberspächer, M. Blobner, S. Ruf, K. Engelhard, B. Eckel, C. Werner</i>	
Right ventricular pressure load in pigs	162
<i>C. Sellin, H. Doerge, M. Coulibaly, C. Muehlfeld, C. Ballat1, F.A. Schoendube</i>	
Increased cancer risk in the B6C3F1 progeny of female mice exposed to X-rays before conception?	164
<i>T. Tillmann, H. Ernst, C. Dasenbrock</i>	
EEG monitoring of anaesthetic depth using Bispectral Index® (BIS™) measurement in large experimental surgery in swine	166
<i>M. Wagenblast, H. Winklmaier and A. Theisen</i>	
Changes in differential haemogram after infusion of mean and low molecular weight hydroxyethyl starch (HES) in rats	171
<i>M. Wagenblast, A. Theisen, Ch. Tandi, H. Forester</i>	
Middle cerebral artery occlusion during MR-imaging (in-bore occlusion) -A new stroke model in rats	175
<i>M. Walberer, T. Gerriets, E. Stolz, C. Müller, A. Kluge, A. Bachmann, M. Kaps, G. Bachmann</i>	
Cryopreservation of transgenic mouse embryos	178
<i>K. Ways, M. Klefenz, J. Schenkel</i>	
Understanding and Controlling for Background Strain Effects on Phenotype	179
<i>C. Cutler Linder, B. Witham</i>	

Magnetic Resonance Imaging of Animal Brain In Vivo

Jens Frahm, Oliver Natt, Takashi Watanabe, Susann Boretius, Thomas Michaelis
Biomedizinische NMR Forschungs GmbH am MPI für biophysikalische Chemie,
Göttingen

Since the fundamental discovery of spatial resolution in nuclear magnetic resonance by the 2003 Nobel laureates Paul C. Lauterbur (1) and Peter Mansfield (2) in 1972/73, non-invasive magnetic resonance imaging (MRI) has undergone a tremendous development from a physical tool with potential medical applications to the method of choice and premier modality for diagnostic imaging. Apart from technical advances in instrumentation such as the availability of large-bore superconducting magnets and high-performance gradient coils for spatial discrimination, this development was based on several breakthroughs in MRI physics, in particular the invention of rapid gradient-echo imaging in 1985 (3-5). The underlying principles allowed for a wide range of new applications ranging from breathhold MRI of the thorax and abdomen to EKG-synchronized dynamic imaging of the heart as well as high-resolution three-dimensional (3D) imaging of complex anatomical structures.

Many of the important improvements have first been made in applications to the central nervous system where methods are available that by far extend the possibilities of structural imaging. In fact, such approaches complement the excellent soft-tissue contrast and high pathological sensitivity of conventional MRI by a more specific characterization of brain tissue. For example, aspects of focal brain chemistry may be studied by localized proton MR spectroscopy. Pertinent measurements yield patterns of cerebral metabolites in the millimolar concentration range which are indicative of both the cellular composition and intracellular metabolism. Recently, the axonal connectivities between brain systems became accessible via the diffusion properties of water within white matter. The technique exploits the anisotropic motion of water molecules inside myelinated axons to discriminate white matter from gray matter and to determine the actual fiber direction. And finally, a most significant contribution to cognitive neuroscience stems from the capability to map the functional anatomy of the human brain. The underlying visualization of task- or stimulus-related activations in networks of cortical and subcortical gray matter is based on the use of an

endogenous contrast provided by differences in the concentration of paramagnetic deoxyhemoglobin in the microvasculature.

Why neuroimaging of animals?

Despite the fact that many technical advances in MRI have originally been developed using small-bore magnets suitable for studying laboratory animals, the tremendous success and commercial impact of human MRI has largely masked the fact that - parallel to medical applications – research in neuroimaging of small animals progressed at similar speed. Its key potential and strategic role is to provide a link between system-oriented neurobiology, molecular neurobiology and neurogenetics, and secondly, to close the gap between research on animal models of human disorders and future clinical applications to human patients.

Similar to studies of the human brain, *in vivo* magnetic resonance examinations of anesthetized animals allow for the assessment of anatomic, metabolic, and even functional aspects of the intact central nervous system. The central problems result from the small brain size and correspondingly lower signal-to-noise ratio than obtainable in humans, and the need for anesthesia which in functional studies may hamper the use of the blood flow-mediated approaches commonly in use for humans. For recent applications in rodents see (6).

A main area of research is devoted to neuroimaging of genetically manipulated animals (mice). Complementary to histologic and behavioural studies, MRI is expected to contribute to a better understanding of the morphologic and functional consequences in the intact system. Mutant animal models are designed to allow for a more detailed investigation of the pathophysiology of a particular disorder and a corresponding assessment of novel therapeutic regimens. In this context, the specific potential of MRI is based on its noninvasiveness which offers not only *in vivo* findings but also intraindividual follow-up evaluations which often are more relevant for human applications than mere group analyses. Moreover, the similarity of MRI techniques and image properties for animal and human brain ensures an almost immediate transfer of experimental methods and findings to whole-body MRI systems and patient studies. The following sections briefly discuss selected examples from our laboratory including primates, mice, and insects.

Methodological considerations

MRI requires the positioning of the animal into a strong magnetic field in order to polarize the nuclear spins of water protons. Short radiofrequency pulses are

then used to disturb the resulting equilibrium magnetization. The subsequent return to equilibrium is termed relaxation and associated with the emission of a radiofrequency signal from the sample itself.

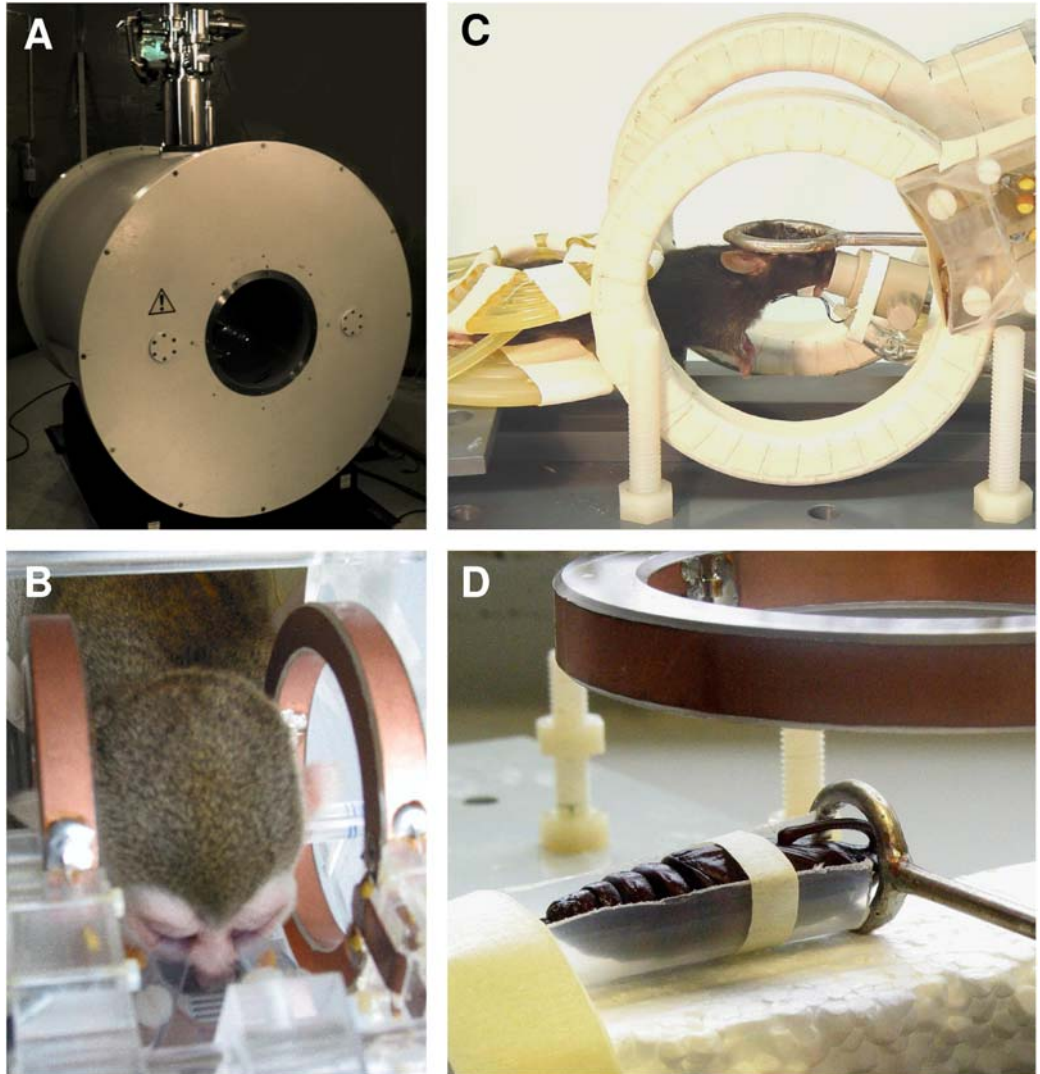


Figure 1.

(A) Small bore (40 cm diameter) magnet for *in vivo* MRI of laboratory animals. The maximum accessible bore has a diameter of 20 cm because of the magnetic gradient coils required for spatial assignment. (B-D) Experimental setup (B) for small primates using a single homogeneous Helmholtz coil (10 cm diameter) for radiofrequency excitation and signal reception, (C) for mice using a Helmholtz coil (10 cm diameter) for excitation and an elliptical surface coil (12 mm short axis, 20 mm long axis) for reception, and (D) for insects using a similar arrangement with a circular surface coil (16 mm diameter) oriented perpendicular to the long axis of the animal.

While primates and rodents are studied under general anesthesia, narcosis is not required for *Manduca sexta* in the pupal state.

Excitation and detection are accomplished by antennae circumscribing the head of the animal. While homogeneous signal excitation is performed with a large coil, signal reception benefits

from the use of a small coil matched to the size of the brain to obtain an optimal signal-to-noise ratio. Figure 1 shows the coil arrangements for MRI of the brain of small primates, mice, and insects, respectively. During radiofrequency excitation and signal reception the MRI experiment employs three orthogonal and spatially varying magnetic fields for a spatial discrimination of the signal. Multiple signals with different spatial encodings need to be recorded for image reconstruction.

It turns out that neuroimaging of small animals clearly benefits from 3D MRI sequences. They provide access to a sufficiently high (and preferably isotropic) spatial resolution in order to resolve the major cerebral structures of interest (7). Typically, high-resolution *in vivo* studies with adequate signal require measuring times of about 30 min (small primates) to 3 hours (insects). It is possible to achieve a similar range of contrasts as in humans including image weightings with T1, T2, and T2* relaxation times as well as spin density (that is water concentration), magnetization transfer with information about the macromolecular content (8), and diffusion indicating differences in water mobility (9-11). Functional studies rely on changes in deoxyhemoglobin (6) or the application of exogenous contrast agents (12-16).

Primate brain: diffusion tensor mapping of axonal connectivities

Figure 2 shows a sagittal and (slightly magnified) coronal section from a T1-weighted 3D MRI acquisition of the brain of a squirrel monkey at 234 μm isotropic resolution. The anatomy is clearly depicted with high intensities for white matter structures and lower intensities for gray matter. Bright spots refer to water protons in flowing blood which are continuously refreshed during the imaging process and therefore mark major vessels.

The good signal-to-noise ratio at the relatively low magnetic field strength of 2.35 T is due to the much longer T2* relaxation time of brain tissue than observed at higher fields. Thus, the use of optimized MRI sequences with small receiver bandwidths and correspondingly reduced noise level effectively counterbalances the (linear) decrease of the equilibrium magnetization at lower fields. Moreover, lower magnetic fields exhibit a reduced sensitivity to magnetic field

inhomogeneities and associated susceptibility artefacts. Such problems occur at air-tissue boundaries and may severely degrade the quality of high-field gradient-echo images of animal brain.

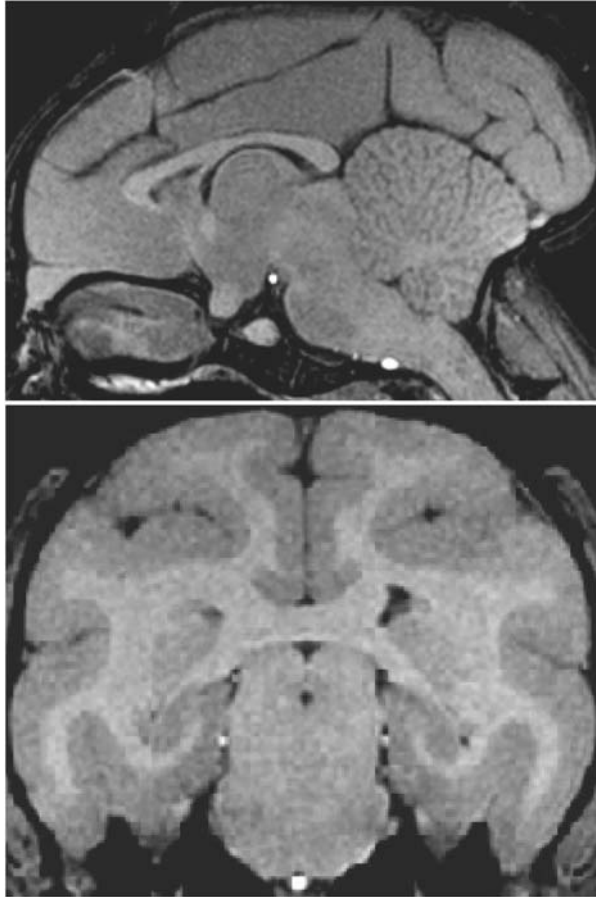


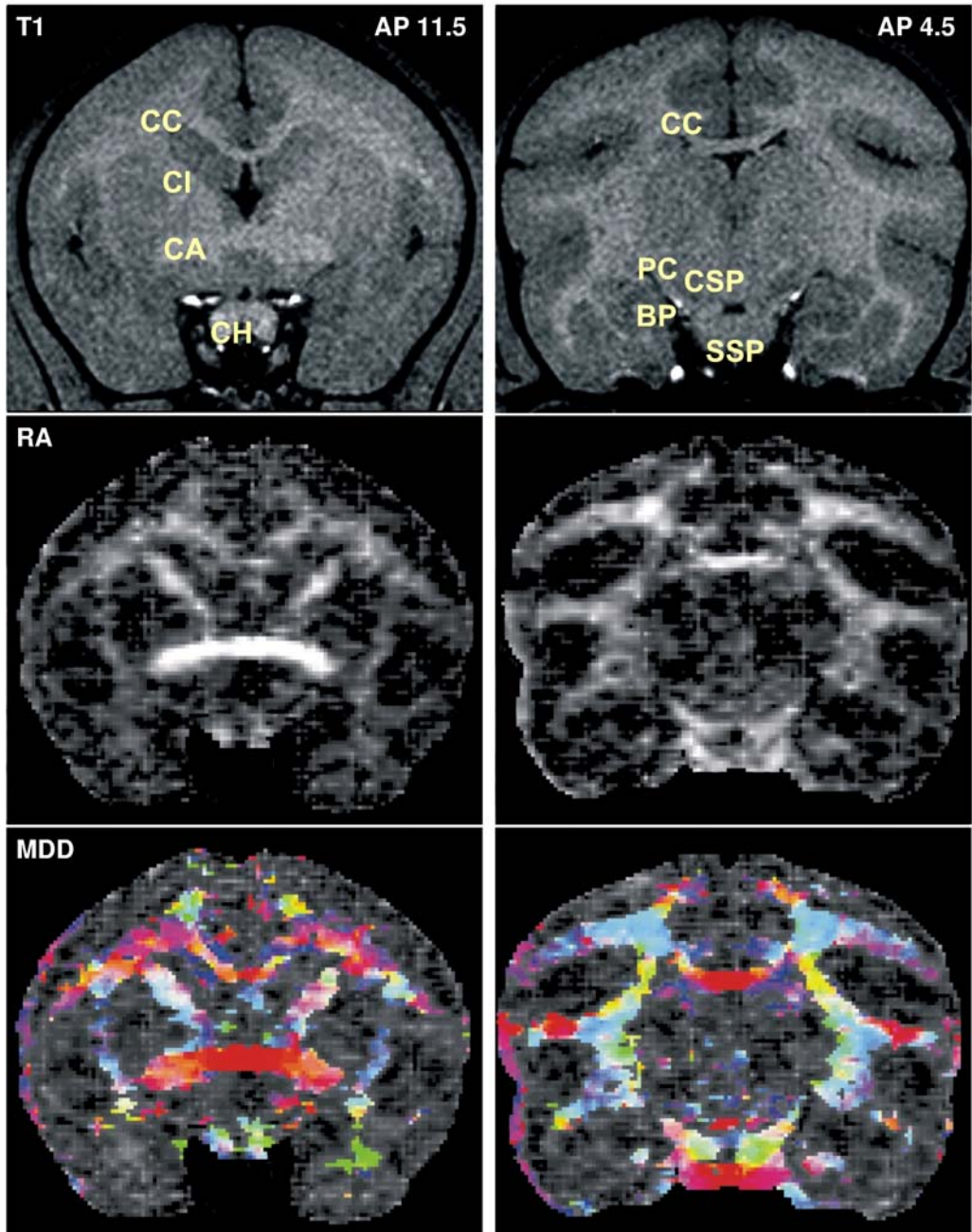
Figure 2. T1-weighted 3D MRI (FLASH, TR/TE = 23/10.1 ms, 25° flip angle) of the brain of a squirrel monkey *in vivo* at 234 μm isotropic resolution in (top) a sagittal and (bottom) a coronal section orientation. Although the central nervous system exhibits a much less pronounced gyrification than a human brain, it closely resembles its structural organization. In particular, the coronal section reveals good contrast between cortical gray matter (gray intensity) and white matter (bright intensity).

Diffusion-weighted MRI allows for a more detailed look into the structural organization of white matter in animal brain *in vivo* (9-11). Diffusion measures the microscopic motion of water (protons) within brain tissue. Rather than simply determining the mean speed or motion-induced positional displacement for a given diffusion time, diffusion MRI studies that employ multiple gradient directions offer the advantage of mapping the diffusion tensor, that is a set of orientation-dependent diffusion coefficients along 6 principal axes. This quantity may be used to identify regions of anisotropic water mobility which in brain tissue mainly applies to white matter where bundles of elongated and heavily myelinated axons facilitate the motion of water molecules along the long axis of the axon but not perpendicular to it.

In comparison with T1-weighted anatomical images of the brain of a squirrel monkey (top), Figure 3 confirms that motional anisotropy in diffusion anisotropy maps (middle) predominantly refers to white matter. In the selected sections the highest degree of anisotropy (coded in bright intensities) is seen in the anterior commissure connecting both hemispheres. Gray matter exhibits no pronounced motional anisotropy, at least not over the spatial dimension of an MRI voxel.

Figure 3.

(Top) MRI anatomy (T1), (middle) relative anisotropy (RA) of the water diffusion highlighting white matter, and (bottom) color-coded mean diffusion direction (MDD) of nerve fibers in two coronal brain sections of a squirrel monkey *in vivo* (11.5 mm and 4.5 mm anterior to the external auditory meatus). CC = corpus callosum, Ci = internal capsule, CA = anterior commissure, CH = optical chiasm, PC = cerebral peduncle, CSP = corticospinal tract, BP = brachium pontis, SSP = stratum superficiale pontis.



It should also be noted that the scalar value of the diffusion coefficient is very similar in gray and white matter. Marked differences are only seen in pathological situations such as ischemia which renders diffusion MRI an indispensable tool for the early detection of ischemic lesions in acute stroke.

Because the diffusion tensor contains information about the orientation dependence of the molecular motion, it is possible to calculate not only a qualitative anisotropy map (where do we have anisotropic motion?) but also a quantitative map of the main diffusion orientation (in which direction are water molecules preferentially moving?). Using a color code, this information is visualized in the bottom part of Fig. 3. For example, coding the right-to-left (or left-to-right) direction in red identifies the interhemispheric connections in the corpus callosum and anterior commissure. Under the assumption that these main diffusion directions coincide with the long axis of white matter fiber tracts, it becomes possible to iteratively 'trace' axonal connections from a starting point in a selected voxel (or region) via suitable neighborhood algorithms. Although pertinent approaches are technically feasible and already led to fascinating maps of the structural connectivity in human brain, they are still very demanding and so far only few attempts have been made to unravel connectivities in animal brain *in vivo*.

Mouse brain: functional mapping of neural projections

When studying murine brain, the key problem is spatial resolution (7,8). Together with a surface coil for signal reception which matches the desired field-of-view, 3D MRI acquisitions with measuring times of 1-1.5 hours provide a sufficiently high signal-to-noise ratio for an isotropic resolution of 100-150 μm . Figure 4 compares corresponding acquisitions for two different mouse strains in selected sagittal, horizontal, and coronal sections. The data unravel pronounced neuroanatomical variations which here refer to much larger ventricular spaces in C57BL/6J mice than in BALB/c mice. In general, many important cerebral microstructures are well delineated including the external capsule, anterior commissure, corpus callosum, hippocampal fimbria, hippocampal formation, and cerebellar sulci (7). Although the results support a slight tendency in favor of T1-weighted gradient-echo MRI sequences for a delineation of the neuroanatomy, the usefulness and sensitivity of T2-weighted spin-echo sequences for the detection of pathologic alterations is well appreciated.

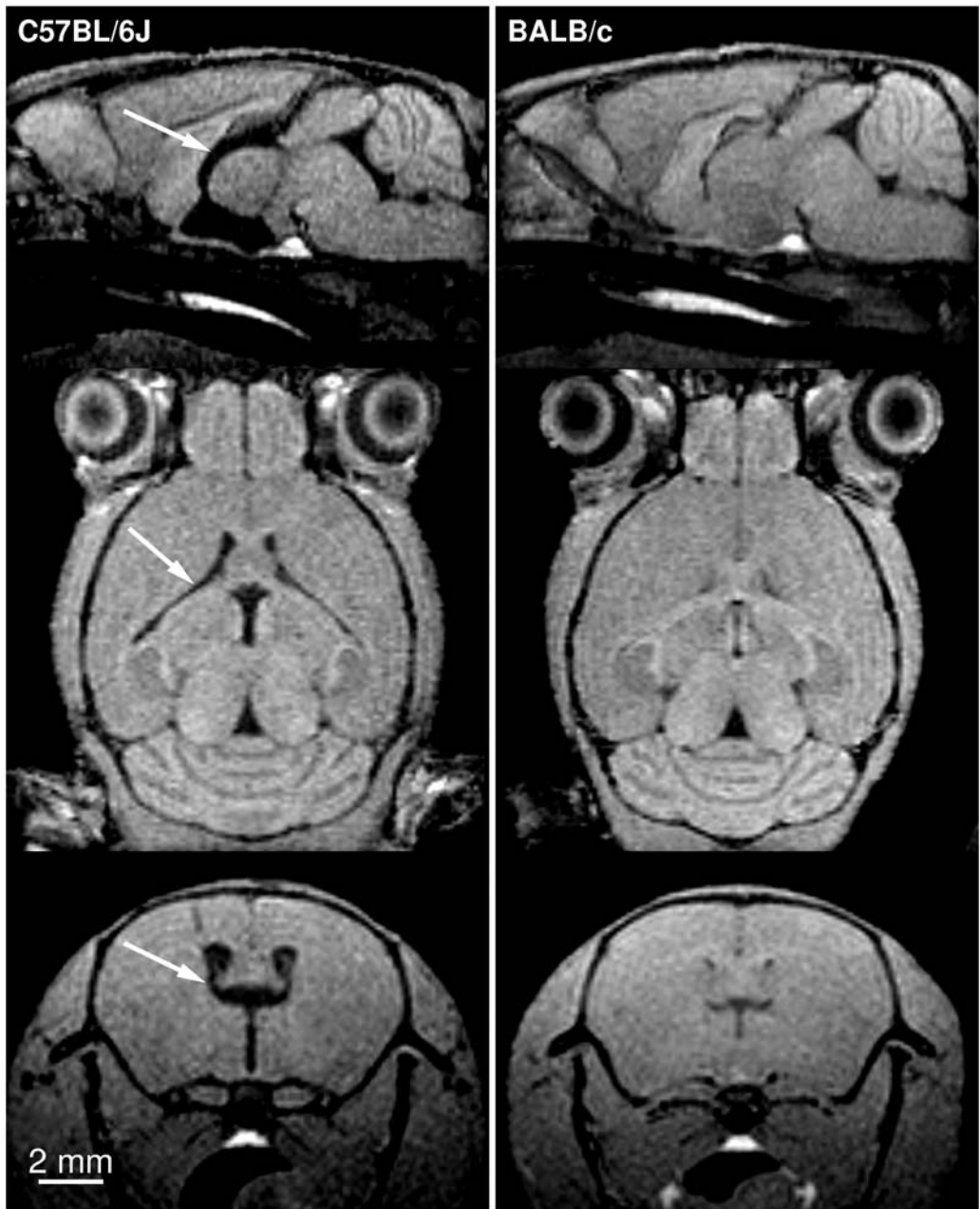


Figure 4. T1-weighted 3D MRI (FLASH, TR/TE = 17/7.6 ms, 25° flip angle) of the brain of (left) a C57BL/6J and (right) a BALB/c mouse *in vivo* at 117 μm isotropic resolution. The comparison demonstrates structural variations in different strains such as larger ventricular spaces in the forebrain of C57BL/6J mice (arrows). The images refer to (top) a mid-sagittal position, (middle) a horizontal section, and (bottom) a coronal section.

In contrast to human studies, functional mapping of mouse brain may be accomplished by using exogenous (paramagnetic) contrast agents such as divalent manganese ions (12-14). These T1-shortening MRI contrast media are known to be taken up by excitable cells (neurons) via voltage-gated calcium channels. Moreover, depending on brain function, manganese ions are transported along axonal projection pathways which therefore become highlighted in T1-weighted images. Because of the limited speed of axonal transport mechanisms, manganese-enhanced MRI is usually performed several hours after the original manganese administration.

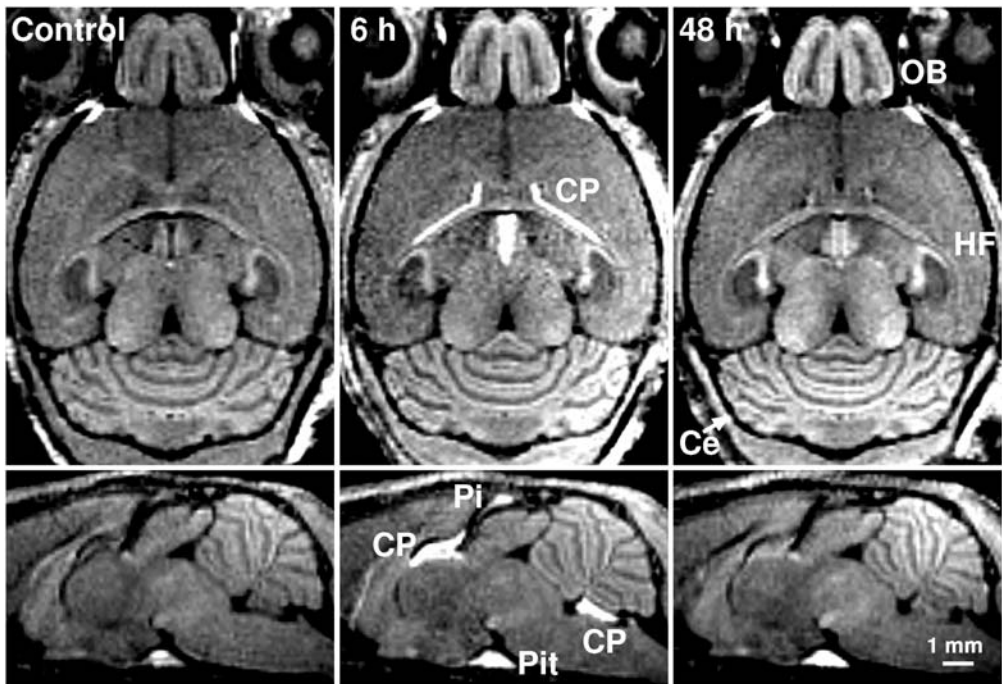


Figure 5.

Manganese-induced MRI signal enhancement of the brain of an NMRI mouse (left) before as well as (middle) 6 hours and (right) 48 hours after subcutaneous injection of 5 ml/kg body weight $MnCl_2$ (20 mM) in (top) horizontal and (bottom) midsagittal sections (T1-weighted 3D FLASH, TR/TE = 22/8.2 ms, 30° flip angle, 120 μm isotropic resolution). In contrast to the transient MRI signal enhancement in the choroid plexus (CP), pineal gland (Pi), and anterior pituitary gland (Pit), brain tissues with a blood-brain barrier such as the olfactory bulb (OB), dentate gyrus and CA3 subregion of the hippocampal formation (HF), and cerebellum (Ce) exhibit a delayed and more persistent enhancement.

Figure 5 reveals both short-term and long-term MRI signal enhancements in mouse brain before as well as 6 hours and 48 hours after systemic (subcutaneous) application of a single dose of MnCl_2 (15). At 6 hours after administration (center column), tissues without a blood-brain barrier such as the choroid plexus, pineal gland, and anterior pituitary gland show a pronounced enhancement. On the other hand, brain regions such as the olfactory bulb, hippocampal formation, and cerebellar cortex reveal an enhancement only in later examinations (right column). For example, at 48 hours, the manganese enhancement improves the delineation of the layered structures within the cerebellum as the outer bright layer circumscribes an interior region without a substantial signal increase. Most likely, the bright signal represents the uptake and accumulation of manganese ions within the cerebellar cortex, while the interior non-enhancing areas refer to white matter. Further insights into the functional connectivity of mouse brain may be gained by direct intracerebral injections into the posterior hippocampus which have been shown to identify the hippocampal projection pathways into the lateral septum (16).

Insect brain: towards mapping neurodevelopment

In comparison with mammals, the insect brain reveals a much simpler organization. With seeing and smelling as key functions which require central processing of sensory information, the optical and antennal lobe form the primary integration centers for the visual and olfactory system, respectively. In this context, *Manduca sexta* serves as a model for the development of the olfactory system which is formed during a 21-day period of metamorphosis. This phase marks the transition from the larva to the adult sphinx moth and is usually divided into pupal stages P0 to P20.

Figure 6 shows selected sections from a 3D MRI acquisition at 100 μm isotropic resolution (1 nl voxel volume) of the brain of a live *Manduca sexta* at pupal stage P12 (17). Apart from highlighting the developing retina, the optical and antennal lobes as well as the antennal nerves are readily discernible in both hemispheres. In fact, after completion of synaptogenesis at about pupal stage P12, even substructures of the central brain such as the calyces of the mushroom bodies (Ca) which possess a similarly high synaptic density as the antennal lobes are well depicted.

Although these findings support the potential of high-resolution 3D MRI to allow for an *in vivo* morphologic characterization of the brain of insects, its use in entomology is not intended to compete with conventional microscopic techniques but to provide new complementary information. For example,

together with the use of T1 contrast agents such as manganese, the MRI protocols are expected to help unravelling the developing neuroaxonal connectivity and brain function during metamorphosis. Current projects focus on functional studies of the evolving olfactory system of *Manduca sexta* after specific labelling of olfactory receptor neurons.

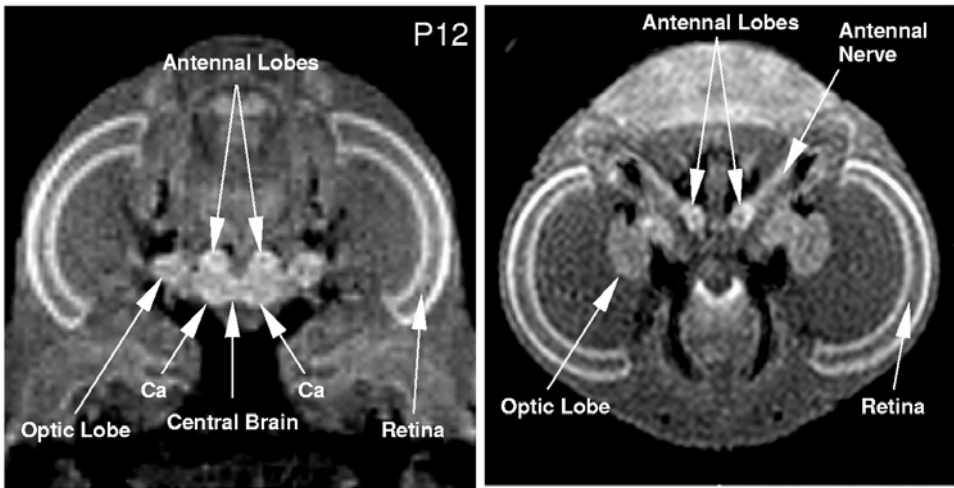


Figure 6.

(Left) Coronal and (right) transverse section of a T1-weighted 3D MRI data set of *Manduca sexta* during metamorphosis at pupal stage P12 (FLASH, TR/TE = 20/7.8 ms, 25° flip angle, 100 μ m isotropic resolution). Apart from visualizing major structures such as the developing retina, 3D MRI allows for the identification of the antennal nerves, antennal lobes, optic lobes, and central brain (Ca = calyxes of the mushroom bodies).

Acknowledgements

The authors would like to thank Dr. Roland Tanner for his support in performing MRI studies of squirrel monkeys and Dr. Joachim Schachtner for his manifold contributions to MRI studies of insect brain.

References

1. Lauterbur PC. Image formation by induced local interactions: Examples employing nuclear magnetic resonance. *Nature* 242: 190-191, 1973.
2. Mansfield P, Grannell PK. 'Diffraction' and microscopy in solids and liquids by NMR. *Phys. Rev.* 12: 3618-3634, 1975.
3. Frahm J, Haase A, Hänicke W, Merboldt KD, Matthaei D. Hochfrequenz-Impuls und Gradienten-Impuls-Verfahren zur Aufnahme von schnellen NMR-Tomogrammen unter Benutzung von Gradientenechos. German Patent Application P 3504734.8, February 12, 1985.
4. Frahm J. Rapid FLASH NMR imaging. *Naturwissenschaften* 74: 415-422, 1987.
5. Frahm J. Toward rapid NMR imaging. *NMR Encyclopedia* 1: 318-322, 1996.
6. Ahrens ET, Narasimhan PT, Nakada T, Jacobs RE. Small animal neuroimaging using magnetic resonance microscopy. *Progr. NMR Spectr.* 40: 275-306, 2002.
7. Natt O, Watanabe T, Boretius S, Radulovic J, Frahm J, Michaelis T. High-resolution 3D MRI of mouse brain reveals small cerebral structures in vivo. *J. Neurosci. Meth.* 120: 203-209, 2002.
8. Natt O, Watanabe T, Boretius S, Frahm J, Michaelis T. Magnetization transfer MRI of mouse brain reveals areas of high neural density. *Magn. Reson. Imaging* 21:1113-1120, 2003.
9. Nolte UG, Finsterbusch J, Frahm J. Rapid isotropic diffusion mapping without susceptibility artifacts. Whole brain studies using diffusion-weighted single-shot STEAM MR imaging. *Magn. Reson. Med.* 44: 731-736, 2000.
10. Boretius S, Watanabe T, Natt O, Michaelis T, Finsterbusch J, Frahm J. Diffusion tensor mapping of living mouse brain using half-Fourier single-shot STEAM MRI. *Proc. Intl. Soc. Magn. Reson. Med.* 10:1231, 2002.

11. Boretius S, Natt O, Watanabe T, Frahm J, Tammer R, Ehrenreich L, Michaelis T. Diffusion tensor MR imaging: Preliminary applications to mice, rats, and squirrel monkeys. *Proc. Göttingen Neurobiol. Conf.* 29: 682, 2003.
12. Lin YJ, Koretsky AP. Manganese ion enhances T1-weighted MRI during brain activation: an approach to direct imaging of brain function. *Magn. Reson. Med.* 38: 378-388, 1997.
13. Pautler RG, Silva AC, Koretsky AP. *In vivo* neuronal tract tracing using manganese-enhanced magnetic resonance imaging. *Magn. Reson. Med.* 40: 740-748, 1998.
14. Watanabe T, Michaelis T, Frahm J. Mapping of retinal projections in the living rat using high-resolution 3D gradient-echo MRI with Mn²⁺-induced contrast. *Magn. Reson. Med.* 46: 424-429, 2001.
15. Watanabe T, Natt O, Boretius S, Frahm J, Michaelis T. *In vivo* 3D MRI staining of mouse brain after subcutaneous application of MnCl₂. *Magn. Reson. Med.* 48: 852-859, 2002.
16. Watanabe T, Natt O, Radulovic J, Spiess J, Boretius S, Michaelis T, Frahm J. 3D MRI of murine hippocampal subfields and projections *in vivo* using Mn²⁺ contrast. *Proc. Intl. Soc. Magn. Reson. Med.* 10: 1254, 2002.
17. Michaelis T, Watanabe T, Natt O, Boretius S, Frahm J, Utz S, Schachtner J. Brain development during metamorphosis: A 3D MRI study of *Manduca Sexta* at 1 nl resolution. *Proc. Intl. Soc. Magn. Reson. Med.* 11: 500, 2003.

Relevance of small animal models for TSE Research

W.J. Schulz-Schaeffer

Prion and Dementia Research Unit, Department of Neuropathology, Faculty of Medicine, Georg August University of Göttingen

Transmissible spongiform encephalopathies (TSEs) such as Creutzfeldt-Jakob disease (CJD) and its variant form (vCJD) in humans, scrapie in sheep, bovine spongiform encephalopathy (BSE) in cattle or chronic wasting disease (CWD) in elk and deer are a group of fatal neurodegenerative disorders of the central nervous system (CNS). The organs involved in the disease are characterized by the deposition of a misfolded form of prion protein (PrP), which is known as the scrapie isoform PrP^{Sc} and which is associated with the infectivity of the organ. PrP^{Sc} is the only molecule consistently found in infectious preparations and is believed to be the only component of the transmissible agent which has been termed prion (prion hypothesis established by S. Prusiner (1)). The prion hypothesis is the most conclusive explanation for a group of diseases that occurs either sporadic or in association with mutations of the prion protein gene and in which the host produces an infectious agent that transmits the disease to other individuals (2). PrP^{Sc} is derived through an posttranslational process involving conformational changes from the physiological cellular isoform of the prion protein (PrP^C). PrP^{Sc} can be distinguished from PrP^C by its high content in beta-sheet structure and its partial resistance to protease digestion (3,4). According to the prion hypothesis the host cellular prion protein succumbs to the conformational change into the disease-associated PrP^{Sc}. Indeed, mice lacking the physiological prion protein (transgenic PrP-knock out mice) are not able to acquire a transmissible spongiform encephalopathy (5). PrP knock out mice with a graft of PrP-competent brain tissue showed neuropathological changes exclusively in the tissue graft (6). In transgenic mice that express prion protein of different species it could be shown that the conversion process of the cellular prion protein into the disease-associated form is easier within one species than between different species (7). Serial passages of PrP^{Sc} after crossing the species barrier shows marked shortening of the incubation time as a phenomenon of adaption to the host.

Using small animal models, it was possible to obtain knowledge about the link between the newly recognized BSE in cattle (known since 1986) and variant CJD

(recognized in 1996). Besides the epidemiological figures with regard to time and regional incidence of these two new TSE forms it was possible to show identical lesion profiles of BSE and vCJD in inbred mouse strains that differ from sporadic (classical) CJD and scrapie in sheep (8). Transmission of vCJD to bovine PrP-transgenic mice shows the same incubation time and the same lesion profile in the host animals as the BSE agent and is different from scrapie of sheep (9).

Using transgenic mice, it was possible to elucidate the role of different cellular components of the lymphoreticular system in the spread of the infection after peripheral administration of the infectious agent (for review see 10). Furthermore, it was possible to show that peripheral nerves need to express the physiological prion protein as a prerequisite for peripheral infection entering the central nervous system (11).

A recently established hamster model for TSEs based on oral challenge of syrian hamsters with the 263K scrapie strain provided key insights on the spread of infection through the body after uptake in the gastrointestinal tract. It was possible to demonstrate the retrograde spread from the gastrointestinal tract via the splanchnic nerve to the thoracic spinal cord and via the vagus nerve to the brain stem (12). This pattern of spread could be confirmed in naturally occurring ovine scrapie, orally transmitted BSE in primates, orally transmitted or naturally occurring CWD and for the first sites of CNS-targeting in BSE (13). Furthermore, it is relevant for peripheral PrP^{Sc} routing in vCJD in humans (Wadsworth, Lancet). Using this hamster model, we were recently able to demonstrate that PrP^{Sc} in muscles of animals orally infected with scrapie can be already detectable before the onset of clinical symptoms. An improved method for the detection of PrP^{Sc} with the paraffin embedded tissue (PET) blot and immunohistochemical studies provided detailed information about the intramuscular location of PrP^{Sc} and the involvement of motoric nerves. These findings led to the new pathophysiological concept that after uptake in the gastrointestinal tract and retrograde spread via the autonomous nervous system to the CNS the infectious agent disperses from spinal and cerebral motor neurons anterogradely via efferent neural projections to motor units of muscle fibers (14).

In conclusion, the key findings of the pathophysiological concept of transmissible spongiform encephalopathies and the risk assessment for humans are based on

small animal experiments. The importance of animal experiments becomes evident by the fact, that uncertainties of the danger of BSE has caused severe economical disturbances in the past. We hope that increasing knowledge will help the society to act more precisely to overcome the TSE problem.

References

- (1) Prusiner SB: Novel proteinaceous infectious particle cause scrapie. *Science* 1982;216:136-144.
- (2) Schulz-Schaeffer: BSE und variante CJK – von den Schwierigkeiten, ein neues Krankheitsprinzip zu etablieren. *Dtsch Med Wochenschr* 2002;127:344-346
- (3) Pan KM, Baldwin M, Ngyen J, Gasset M, Serban A, Groth D, Mehlhorn I, Huang Z, Fletterick RJ, Cohen FE: Conversion of α -helices into β -sheet features in the formation of the scrapie prion protein. *Proc Natl Acad Sci USA* 1993;90:10962-10966.
- (4) Meyer RK, McKinley MP, Bowman KA, Braunfeld MB, Barry RA, Prusiner SB: Separation and properties of cellular and scrapie prion protein. *Proc Natl Acad Sci USA* 1986;83:2310-2314.
- (5) Büeler H, Aguzzi A, Sailer A, Greiner RA, Autenried P, Aguet M, Weissmann C: Mice devoid of PrP are resistant to scrapie. *Cell* 1993;73:1339-1347.
- (6) Brandner S, Isenmann S, Raeber A, Fischer M, Sailer A, Kobayashi Y, Weissmann C, Aguzzi A: Normal host prion protein necessary for scrapie-induced neurotoxicity. *Nature* 1996;379:339-343
- (7) Weissmann C: Spongiform encephalopathies. The prions progress [news]. *Nature* 1991;349:569-571.
- (8) Bruce ME, Will RG, Ironside JW, McConnell I, Drummond D, Suttie A, NCCardle L, Chree A, Hope J, Birkett C, Cousins S, Fraser H, Bostock CJ: Transmission to mice indicate that ‘new variant’ CJD is caused by the BSE agent. *Nature* 1997;389:498-501.

(9) Scott MR, Will R, Ironside J, Nguyen HO, Tremblay P, DeArmond SJ, Prisiner SB: Compelling transgenic evidence for transmission of bovine spongiform encephalopathy prions to humans. *Proc Natl Acad Sci USA* 1999;96:15137-15142.

(10) Aguzzi A: Prion diseases, blood and the immune system: concern and reality. *Haematologica* 2000;86:3-10.

(11) Blättler T, Brandner S, Raeber AJ, Klein MA, Voigtländer T, Weissmann C, Aguzzi A: PrP-expressing tissue required for transfer of scrapie infectivity from spleen to brain. *Nature* 1997;389:69-73.

(12) McBride PA, Schulz-Schaeffer WJ, Donaldson M, Bruce M, Diringer H, Kretzschmar HA, Beekes M: Early spread of scrapie from the gastrointestinal tract to the central nervous system involves autonomic fibers of the splanchnic and vagus nerves. *J Virol* 2001;75:9320-9327.

(13) Schulz-Schaeffer W, Fatzner R, Vandeveldel M, Kretzschmar H: Detection of PrP^{Sc} in subclinical BSE with the paraffin-embedded tissue (PET) blot. *Arch Virol Suppl* 2000;16:173-180.

(14) Thomzig A, Schulz-Schaeffer WJ, Kratzel C, Mai J, Beekes M: Preclinical deposition of pathological prion protein PrP^{Sc} in muscles of hamsters orally exposed to scrapie. *JCI* 2004;113:1465-1472.

Animal models for multiple sclerosis

C. Stadelmann

Institute of neuropathology, University of Goettingen

Abstract

Autoimmune, viral, and toxic animal models have been devised to mimic the inflammatory-demyelinating CNS pathology of multiple sclerosis (MS). During the past decades, animal models for MS have helped to develop and elucidate key immunological concepts, such as the immune privilege of the CNS, the entry of antigen-specific T-cells into the brain, the role of T-cells in inducing CNS autoimmune disease and the role of local parenchymal cells in sustaining and/or downregulating brain inflammation. Recent work in animal models has furthermore paved the way for important advances in MS therapy. However, since the etiology of MS is still unknown, no existing animal model equips the researcher with a perfect imitation of the human disease. Therefore, the experimental model has to be carefully selected depending on the scientific question.

Multiple Sclerosis – features of the human disease

MS is a chronic inflammatory-demyelinating disease of the CNS generally starting in young adulthood. The clinical course is unpredictable, leaving about one third of the patients with serious disabilities after 10 years of disease. The typical relapsing-remitting disease often evolves into a secondary progressive course with insidious clinical deterioration. In the beginning of the disease, bouts tend to resolve without residual deficits, however, with time, sensory, sensible and/or motor deficits remain (Lublin and Reingold 1996; Ebers 1998). Pathologically, MS is characterized by circumscribed disseminated CNS lesions with a predilection for periventricular brain areas, brain stem, and spinal cord. The individual lesions consist of demyelinated brain areas with various degrees of inflammation, predominantly comprising macrophages and T-cells, axonal loss, and gliosis. Oligodendrocytes are preserved to a variable degree. Around 30% of the lesions show signs of remyelination at the lesional edge albeit often incomplete (Kornek and Lassmann 2003; Prineas 1985).

Why do we need animal models for MS research?

Via the modelling of the immunological and structural features of the human disease, experimental models of MS aim at the elucidation of disease pathogenesis and evaluation of new treatment options. Unfortunately, so far no single animal model perfectly reflects all the features of the human disease, e.g. inflammation, demyelination, relapsing-remitting disease course, etc.. Currently, the appropriate animal model has to be selected according to the scientific question. Oftentimes a combination of different animal models has to be employed to reach conclusive results. Important questions that have been addressed in the past include the fundamentals of immune surveillance of the brain (Wekerle *et al.* 1986) and the specific cellular and molecular players involved in brain inflammation (Gaupp *et al.* 2003; Karnezis *et al.* 2004; Yan *et al.* 2003). Ongoing research projects aim at modelling newly discovered aspects of the human disease, such as its pathological heterogeneity, axonal and neuronal damage, and cortical MS lesions (Lassmann *et al.* 2001; Bo *et al.* 2003; Peterson *et al.* 2001). The complexity of the interaction between the immune and the nervous systems makes the use of living animals as experimental systems indispensable for MS research.

Different animal models for MS

The most commonly used animal model for MS is experimental autoimmune encephalomyelitis (EAE) induced in susceptible species by active immunization with myelin proteins or adoptive transfer of activated antigen-specific T-cells. However, there are also virally induced models of chronic inflammatory CNS demyelination in mice (Theiler's murine encephalomyelitis virus, Corona-virus, mouse hepatitis virus) that are based either on a direct cytolytic effect on oligodendrocytes or an immune reaction against viral and CNS proteins (Oleszak *et al.* 2004). Other models to study aspects of MS include models of chemically induced demyelination with a lack of the – in the other models – dominant inflammatory response. There, the focal application of myelinolytic substances, such as lysolecithine and ethidium bromide, induces focal demyelination with relatively few axonal damage (Woodruff and Franklin 1999b). In a further non-inflammatory model of widespread demyelination, mice are fed with the copper chelator cuprizone for 5-6 weeks which induces a metabolic disturbance of the oligodendrocyte and cell death. After discontinuation of the cuprizone feeding, extensive remyelination occurs within 3 weeks. However, if the cuprizone feeding is continued, a complete depletion of oligodendrocytes occurs with subsequent persistent demyelination (Matsushima and Morell 2001; 't Hart and Amor 2003).

Induction of EAE and basic pathomechanisms

More than 70 years ago, observations of paralysis after rabies immunization led to the notion that the brain homogenate employed to propagate the virus *in vitro* induced an allergic reaction (Remlinger 1928; Steinman 2003). Rivers performed immunizations of Rhesus monkeys with rabbit brain homogenate to induce acute disseminated leucoencephalomyelitis (ADEM) with ensuing paralysis, round cell infiltrates in the brain, and only scarce demyelination (Rivers *et al.* 1933). Later on, with the help of adjuvants (Kabat *et al.* 1947), immunization was performed using spinal cord homogenate, whole myelin preparations, purified myelin proteins, e.g., proteolipid protein (PLP) and myelin basic protein (MBP), recombinant myelin proteins, e.g., myelin oligodendrocyte glycoprotein (MOG), and peptides (for review see Steinman 2003). Furthermore, also glial and neuronal proteins were found to elicit inflammatory responses, e.g., S100 and Thy1 (Kojima *et al.* 1997). In the 80ies, the adoptive transfer of CD4-positive T-cells established the key role of T helper cells in the induction of autoimmune disease (Ben Nun *et al.* 1981).

Subcutaneous injection of an emulsion of a CNS protein with complete or incomplete Freund's adjuvant leads to peripheral T-cell priming and expansion. Activated, antigen-specific T-cells enter the CNS and pave the way for non antigen-specific T-cells and macrophages. The encephalitogenic T-cell response can be traced down to encephalitogenic peptides that suffice for EAE induction. Transfer of encephalitogenic T-cells between syngeneic rodents with subsequent development of brain inflammation is the main evidence that CD4-positive T-cells play a central role in the pathogenesis of MS. This passive or adoptive transfer EAE is induced by transfer of *in vitro* re-stimulated polyclonal spleen or lymph node cells. By limiting dilution techniques and repeated antigenic and growth factor stimulation, encephalitogenic T-cell lines and clones can be generated (for review see Gold *et al.* 2000; Lassmann and Wekerle 1998; Rao and Segal 2004).

EAE can be induced in a variety of animal species, most frequently rodents (mice, rats, guinea pigs). However, the use of non-human primates, especially marmosets (*Callithrix jacchus*), is increasing because of closer similarities to the human disease and, even more importantly, the possibility to test humanized therapies (Genain and Hauser 2001). Depending on the genetic background between different species and strains, the pathology induced by immunization with even the same antigen differs markedly. Central to the pathogenesis of all EAE models is the activation and expansion of autoreactive CD4-positive TH1 T-cells in the periphery. After entering the CNS and encountering their respective myelin antigen, unspecific effector cells are recruited from the peripheral blood

via the secretion of cyto- and chemokines. The release of proinflammatory and cytotoxic mediators and macrophage phagocytic activity leads to disseminated inflammatory lesions with various degrees of demyelination and axonal loss. In most rodents models, inflammatory pathology is targeted to the spinal cord. Apart from CD4- and macrophage mediated effector mechanisms, antibody and complement-mediated myelin destruction take place in MOG-induced EAE models. New data furthermore reveal that also CD4-positive Th2 T-cells and CD8-T-cells may play a role in the pathogenesis of EAE and probably MS (Huseby *et al.* 2001; Sun *et al.* 2001; Lafaille *et al.* 1997). Most EAE models are apt to examine the effects of acute CNS inflammation (Steinman 1999). To model the chronic disease phase, special models, such as PLP₁₃₉₋₁₅₁ peptide EAE in SJL mice and cyclosporine A treatment in Lewis rats immunized with myelin components have been devised (Stanley and Pender 1991; Tuohy *et al.* 1989).

Similarities and differences to MS

In recent years, experimental models were developed that reflect many features of the human disease (Table 1). In contrast to immunization with MBP, which leads to perivascular round cell infiltrates with only limited demyelination reminiscent of ADEM, immunization with recombinant MOG in BN and DA rats and marmosets leads to a severe, acute and highly inflammatory disease with the formation of confluent demyelinated plaques in later disease stages. Demyelinating anti-MOG antibodies play a key pathogenic role (Stefflerl *et al.* 1999; Stefflerl *et al.* 2000). In contrast, MOG₃₅₋₅₅ peptide EAE in the B6 mouse rather is a widespread inflammatory disease of the spinal cord with little T-cell and macrophage mediated primary demyelination, but prominent axonal damage (Mendel *et al.* 1995). In the human disease, lesion characteristics vary between individual MS patients: on the one hand, different effector mechanisms of demyelination (e.g. T-cell/macrophage and/or antibody mediated demyelination) are believed to operate (Lassmann *et al.* 2001); on the other hand, the extent of tissue destruction (e.g. oligodendrocyte destruction, axonal damage) and remyelination varies considerably between patients (Ozawa *et al.* 1994). Thus, different EAE models may serve to study different variants of the disease.

The EAE model has proven extremely useful to evaluate a number of questions in MS immunology and immunopathology. However, there are still clear differences between the animal models generated and the human disease. In EAE, lesions are generally smaller, often more inflammatory than demyelinating and mostly located in the spinal cord. Also, cortical lesions are not readily present in experimental models of MS. EAE in non-human primates and some rat strains shows a higher probability of brain involvement (Hart *et al.* 1998; Storch *et al.*

1998). EAE in experimental animals - in contrast to MS - is generally a self limiting disease: the disease course is mostly acute with a chronic persistent neurological deficit and only rarely relapsing-remitting. Special human disease forms, such as primary progressive MS with its later onset and insidious course are especially difficult to model.

Therapeutic strategies for MS developed in experimental models

Animal models for MS have been in use for quite a while, however, only relatively few MS therapies tested in EAE found their way into clinical practice. Surprisingly, some of the therapeutic agents highly successful in EAE proved to be disappointing in humans (for review see Steinman 1999; Hohlfeld and Wekerle 2004): anti-TNF α strategies for example, that were effective in EAE and also in experimental and rheumatoid arthritis, were unsuccessful in MS. Anti-T-cell receptor strategies, such as altered peptide ligands, were equally disappointing in MS. Furthermore, the most frequently used immunomodulatory substances in MS, the β -interferons, arose from clinical observations in patients with tumors and viral disease (Jacobs and Johnson 1994). However, glatiramer acetate (Copaxone®), a synthetic random copolymer of four amino acids, was developed in EAE – in search for the minimum immunogenic MBP peptide (Teitelbaum *et al.* 1971). Recently, a drug developed in EAE and specifically blocking leucocyte entry into the brain (anti- α 4-integrin; Natalizumab®), proved highly effective in MS (Miller *et al.* 2003; Yednock *et al.* 1992). Further highly selective drugs targeting pro-inflammatory molecules are currently being tested for use in humans, e.g. anti-IL-2 receptor alpha and anti-IL12. Surprisingly, lipid-lowering drugs, such as the HMG-CoA-reductase inhibitor simvastatin have recently been shown to exhibit anti-inflammatory effects and ameliorate EAE and probably MS (Youssef *et al.* 2002; Neuhaus *et al.* 2004). Given the importance of axonal damage for the permanent clinical disability of the patients, also neuroprotective and remyelinating therapeutic strategies are currently evaluated. A better understanding of human pathology and pathomechanisms in concert with the development of more suitable experimental models is promising a much higher yield of effective therapeutic substances in the near future.

Recent developments and outlook

Currently, the use of knock-out and transgenic animals in MS research is growing exponentially (for review see Owens *et al.* 2001). More sophisticated molecular biology techniques will further allow to dissect inflammatory pathways in the CNS (Robinson *et al.* 2003; Lock *et al.* 2002; Cabarrocas *et al.* 2003). Imaging and cell tracing techniques are currently applied to study lesional development and inflammatory cell entry into the CNS (Anderson *et al.* 2004; Flugel *et al.* 1999).

Interest has especially grown in the pre-entry phase, where lymphocytes apparently acquire the receptor and activation profile necessary for entry into the CNS (Flugel *et al.* 2001a). To better study the effect of an inflammatory lesion on axonal pathways, a model of focal EAE has been generated that allows the time- and region specific induction of an MS-like lesion. The development of one isolated lesion is in contrast to the mostly disseminated EAE models and also to the human disease, but favors imaging studies and the analysis of regenerative processes (Kerschensteiner *et al.* 2004). Recently, coming from human pathology, interest has grown in the neuro- and axondegenerative aspect of MS that is very well reflected in EAE (Meyer *et al.* 2001; Zhu *et al.* 2003). Interest has furthermore grown in growth factor therapy of EAE and cell replacement strategies (Linker *et al.* 2002; Pluchino *et al.* 2003; Flugel *et al.* 2001b). Routinely, animals with EAE are evaluated using a rather coarse motor test (“score”). Upcoming neuroprotective therapeutic strategies and a new focus on tissue repair ask for more refined behavioral read-out systems to assess the disease course and clinical improvement in animals with EAE (Buddeberg *et al.* 2004).

Conclusion

Animals models for MS have been developed quite some time ago, are widely distributed, and come in a plethora of different forms. New encouraging developments in the fields of immunology, molecular biology, cell biology, and neurobiology still render them very useful to dissect mechanisms of autoimmunity and brain inflammation. However, a close interaction between clinical scientists working with MS patients and scientists working on animal models has to be maintained to identify relevant research topics and ensure the translation of findings from the experimental models to the human condition.

Acknowledgements

Many thanks to Doron Merkler and Stefan Nessler for critical reading of the manuscript. CS is supported by a grant from the Gemeinnützige Hertie-Stiftung and the Medical Faculty of the University of Göttingen.

Autoimmune								
Species	Strain	Antigen	T-cell transfer	Disease Course	Similarities to MS	Differences to MS	Selected References	
Mouse	C57Bl/6	MOG ₁₋₁₂₈ MOG ₃₅₋₅₈	MOG-specific T-cells	Acute EAE with residual deficits	- Subpial infiltration with T-cells and macrophages - Axonal damage	- Predominantly spinal cord involvement - Confluent primary demyelination rare - acute disease with residualia	Mendel <i>et al.</i> 1995	
	SJL	PLP ₁₃₉₋₁₅₁ MBP ₈₉₋₁₀₁	PLP ₁₃₉₋₁₅₁ specific T-cells MBP ₈₉₋₁₀₁ specific T-cells	Chronic; relapsing- remitting EAE	- T-cell/macrophage mediated inflammation - Confluent demyelination - Axonal loss - Relapsing-remitting disease with persistent clinical deficits	- Predominantly spinal cord involvement	Tuohy <i>et al.</i> 1989 Sakai <i>et al.</i> 1988	
Rat	Lewis	MOG ₁₋₁₂₈ MBP PLP	PLP-, MOG-, MBP-specific T- cells	Acute	T-cell/macrophage mediated inflammation	Inflammatory disease with only mild perivenous/subpial demyelination resembling ADEM	Vandenbark and Hirriehs 1974	

Rat	BN			Acute; relapsing-remitting	- Confluent demyelination with relative axonal preservation - T-cell/macrophage and antibody mediated demyelination - Extensive remyelination - Cerebrum, cerebellum, and spinal cord	- Acute, severe disease - Mostly monophasic with persistent deficits or recovery	Storch <i>et al.</i> 1998
	DA						Lorentzen <i>et al.</i> 1997
Marmoset		MOG ₁₋₁₂₅ MBP	MBP-specific T-cells	Acute; non-remitting; relapsing-remitting	- Multifocal brain and spinal cord disease - T-cell/macrophage and antibody mediated demyelination	- MOG ₁₋₁₂₅ : Acute, severe disease, often no remission - MBP: only mild perivascular demyelination	Genain and Hauser 2001

Viral							
Species	Strain	Virus	Mode of action	Disease Course	Similarities to MS	Differences to MS	Selected References
Mouse	SJL	Theiler Murine Encephalomyelitis Virus (TMEV; picornaviridae) Strains: BeAn, DA	Viral infection and persistence in the CNS	Biphasic: acute encephalitis; chronic demyelination	- Chronic inflammatory demyelinating lesions with axonal damage - T-cell/macrophage mediated demyelination	- Viral persistence? - Spinal cord predominance	Oleszak <i>et al.</i> 2004
	C57Bl/6 BALB/c	mouse hepatitis virus (coronaviridae) Strain: JHM	Viral infection and persistence in the CNS	Monophasic: Acute encephalitis with primary demyelination; chronic demyelination	- Acute inflammatory demyelinating lesions with relative axonal preservation - Chronic demyelination - Oligodendrocyte damage - T-cell/macrophage mediated demyelination	- Viral persistence? - Spinal cord predominance	Dandekar <i>et al.</i> 2004; Stohman and Hinton 2001; Haring and Perlman 2001

Toxic							
Species	Strain	Toxin	Mode of action	Disease Course	Similarities to MS	Differences to MS	Selected References
Mouse	C57 Bl/6	Cuprizone	Cu ²⁺ chelator, oligodendroglia toxicity	No apparent clinical CNS symptoms	<ul style="list-style-type: none"> - Oligodendrocyte damage - Demyelination - Microglia activation - Remyelination 	<ul style="list-style-type: none"> - Lack of inflammation - No plaque-like distribution 	Matsushima and Morell 2001
Mouse, rat	various	Lyssolecithin	Focal application: myelinolysis	Symptoms according to focal lesion	<ul style="list-style-type: none"> - Demyelination with axonal preservation - Myelin phagocytosis 	Lack of inflammation	Woodruff and Franklin 1999b
Mouse, rat	various	Ethidium bromide	Focal application: selective destruction of glial cells	Symptoms according to focal lesion	<ul style="list-style-type: none"> - Demyelination with axonal preservation - Myelin phagocytosis - Oligodendrocyte damage 	<ul style="list-style-type: none"> - Lack of inflammation - Oligodendrocyte and astrocyte depletion 	Woodruff and Franklin 1999a; Blakemore <i>et al.</i> 1995

References

- 't Hart BA, Amor0 S. The use of animal models to investigate the pathogenesis of neuroinflammatory disorders of the central nervous system. *Curr.Opin.Neurol.* 2003; 16: 375-383.
- Anderson SA, Shukaliak-Quandt J, Jordan EK *et al.* Magnetic resonance imaging of labeled T-cells in a mouse model of multiple sclerosis. *Ann.Neurol.* 2004; 55: 654-659.
- Ben Nun A, Wekerle H, Cohen IR. The rapid isolation of clonable antigen-specific T lymphocyte lines capable of mediating autoimmune encephalomyelitis. *Eur.J.Immunol.* 1981; 11: 195-199.
- Blakemore WF, Olby NJ, Franklin RJ. The use of transplanted glial cells to reconstruct glial environments in the CNS. *Brain Pathol.* 1995; 5: 443-450.
- Bo L, Vedeler CA, Nyland HI, Trapp BD, Mork SJ. Subpial demyelination in the cerebral cortex of multiple sclerosis patients. *J.Neuropathol.Exp.Neurol.* 2003; 62: 723-732.
- Buddeberg BS, Kerschensteiner M, Merkler D, Stadelmann C, Schwab ME. Behavioral testing strategies in a localized animal model of multiple sclerosis. *J.Neuroimmunol.* 2004; 153: 158-170.
- Cabarrocas J, Bauer J, Piaggio E, Liblau R, Lassmann H. Effective and selective immune surveillance of the brain by MHC class I-restricted cytotoxic T lymphocytes. *Eur.J.Immunol.* 2003; 33: 1174-1182.
- Dandekar AA, Anghelina D, Perlman S. Bystander CD8 T-cell-mediated demyelination is interferon-gamma-dependent in a coronavirus model of multiple sclerosis. *Am.J.Pathol.* 2004; 164: 363-369.
- Ebers G. Natural history of multiple sclerosis. In: Compston A, editor. *McAlpine's Multiple Sclerosis*. London: Curchill Livingstone, 1998: 191-221.
- Flugel A, Berkowicz T, Ritter T *et al.* Migratory activity and functional changes of green fluorescent effector cells before and during experimental autoimmune encephalomyelitis. *Immunity.* 2001a; 14: 547-560.
- Flugel A, Matsumuro K, Neumann H *et al.* Anti-inflammatory activity of nerve growth factor in experimental autoimmune encephalomyelitis: inhibition of monocyte transendothelial migration. *Eur.J.Immunol.* 2001b; 31: 11-22.
- Flugel A, Willem M, Berkowicz T, Wekerle H. Gene transfer into CD4+ T lymphocytes: green fluorescent protein-engineered, encephalitogenic T cells illuminate brain autoimmune responses. *Nat.Med.* 1999; 5: 843-847.
- Gaupp S, Pitt D, Kuziel WA, Cannella B, Raine CS. Experimental autoimmune encephalomyelitis (EAE) in CCR2(-/-) mice: susceptibility in multiple strains. *Am.J.Pathol.* 2003; 162: 139-150.
- Genain CP, Hauser SL. Experimental allergic encephalomyelitis in the New World monkey *Callithrix jacchus*. *Immunol.Rev.* 2001; 183: 159-172.

Gold R, Hartung HP, Toyka KV. Animal models for autoimmune demyelinating disorders of the nervous system. *Mol.Med.Today* 2000; 6: 88-91.

Haring J, Perlman S. Mouse hepatitis virus. *Curr.Opin.Microbiol.* 2001; 4: 462-466.

Hart BA, Bauer J, Muller HJ *et al.* Histopathological characterization of magnetic resonance imaging-detectable brain white matter lesions in a primate model of multiple sclerosis: a correlative study in the experimental autoimmune encephalomyelitis model in common marmosets (*Callithrix jacchus*). *Am.J.Pathol.* 1998; 153: 649-663.

Hohlfeld R, Wekerle H. Autoimmune concepts of multiple sclerosis as a basis for selective immunotherapy: From pipe dreams to (therapeutic) pipelines. *Proc.Natl.Acad.Sci.U.S.A* 2004.

Huseby ES, Liggitt D, Brabb T, Schnabel B, Ohlen C, Goverman J. A pathogenic role for myelin-specific CD8(+) T cells in a model for multiple sclerosis. *J.Exp.Med.* 2001; 194: 669-676.

Jacobs L, Johnson KP. A brief history of the use of interferons as treatment of multiple sclerosis. *Arch.Neurol.* 1994; 51: 1245-1252.

Kabat EA, Wolf A, Bezer AL. The rapid production of acute disseminated encephalomyelitis in rhesus monkeys by injection of heterologous and homologous brain tissue with adjuvants. *J.Exp.Med.* 1947; 85: 117-129.

Karnezis T, Mandemakers W, McQualter JL *et al.* The neurite outgrowth inhibitor Nogo A is involved in autoimmune-mediated demyelination. *Nat.Neurosci.* 2004; 7: 736-744.

Kerschensteiner M, Stadelmann C, Buddeberg BS *et al.* Targeting experimental autoimmune encephalomyelitis lesions to a predetermined axonal tract system allows for refined behavioral testing in an animal model of multiple sclerosis. *Am.J.Pathol.* 2004; 164: 1455-1469.

Kojima K, Wekerle H, Lassmann H, Berger T, Linington C. Induction of experimental autoimmune encephalomyelitis by CD4+ T cells specific for an astrocyte protein, S100 beta. *J.Neural Transm.Suppl* 1997; 49: 43-51.

Kornek B, Lassmann H. Neuropathology of multiple sclerosis-new concepts. *Brain Res.Bull.* 2003; 61: 321-326.

Lafaille JJ, Keere FV, Hsu AL *et al.* Myelin basic protein-specific T helper 2 (Th2) cells cause experimental autoimmune encephalomyelitis in immunodeficient hosts rather than protect them from the disease. *J.Exp.Med.* 1997; 186: 307-312.

Lassmann H, Bruck W, Lucchinetti C. Heterogeneity of multiple sclerosis pathogenesis: implications for diagnosis and therapy. *Trends Mol.Med.* 2001; 7: 115-121.

Lassmann H, Wekerle H. Experimental models of multiple sclerosis. In: Compston A, editor. *McAlpine's Multiple Sclerosis*. London: Churchill Livingstone, 1998: 409-33.

Linker RA, Maurer M, Gaupp S *et al.* CNTF is a major protective factor in demyelinating CNS disease: a neurotrophic cytokine as modulator in neuroinflammation. *Nat.Med.* 2002; 8: 620-624.

Lock C, Hermans G, Pedotti R *et al.* Gene-microarray analysis of multiple sclerosis lesions yields new targets validated in autoimmune encephalomyelitis. *Nat.Med.* 2002; 8: 500-508.

Lorentzen JC, Andersson M, Issazadeh S *et al.* Genetic analysis of inflammation, cytokine mRNA expression and disease course of relapsing experimental autoimmune encephalomyelitis in DA rats. *J.Neuroimmunol.* 1997; 80: 31-37.

Lublin FD, Reingold SC. Defining the clinical course of multiple sclerosis: results of an international survey. National Multiple Sclerosis Society (USA) Advisory Committee on Clinical Trials of New Agents in Multiple Sclerosis. *Neurology* 1996; 46: 907-911.

Matsushima GK, Morell P. The neurotoxicant, cuprizone, as a model to study demyelination and remyelination in the central nervous system. *Brain Pathol.* 2001; 11: 107-116.

Mendel I, Kerlero dR, Ben Nun A. A myelin oligodendrocyte glycoprotein peptide induces typical chronic experimental autoimmune encephalomyelitis in H-2b mice: fine specificity and T cell receptor V beta expression of encephalitogenic T cells. *Eur.J.Immunol.* 1995; 25: 1951-1959.

Meyer R, Weissert R, Diem R *et al.* Acute neuronal apoptosis in a rat model of multiple sclerosis. *J.Neurosci.* 2001; 21: 6214-6220.

Miller DH, Khan OA, Sheremata WA *et al.* A controlled trial of natalizumab for relapsing multiple sclerosis. *N.Engl.J.Med.* 2003; 348: 15-23.

Neuhaus O, Stuve O, Zamvil SS, Hartung HP. Are statins a treatment option for multiple sclerosis? *Lancet Neurol.* 2004; 3: 369-371.

Oleszak EL, Chang JR, Friedman H, Katsetos CD, Platsoucas CD. Theiler's virus infection: a model for multiple sclerosis. *Clin.Microbiol.Rev.* 2004; 17: 174-207.

Owens T, Wekerle H, Antel J. Genetic models for CNS inflammation. *Nat.Med.* 2001; 7: 161-166.

Ozawa K, Suchanek G, Breitschopf H *et al.* Patterns of oligodendroglia pathology in multiple sclerosis. *Brain* 1994; 117 (Pt 6): 1311-1322.

Peterson JW, Bo L, Mork S, Chang A, Trapp BD. Transected neurites, apoptotic neurons, and reduced inflammation in cortical multiple sclerosis lesions. *Ann.Neurol.* 2001; 50: 389-400.

Pluchino S, Quattrini A, Brambilla E *et al.* Injection of adult neurospheres induces recovery in a chronic model of multiple sclerosis. *Nature* 2003; 422: 688-694.

Prineas JW. The neuropathology of multiple sclerosis. In: Koetsier, editor. *Demyelinating Diseases.* Amsterdam: 1985: 337-98.

Rao P, Segal BM. Experimental autoimmune encephalomyelitis. *Methods Mol.Med.* 2004; 102: 363-376.

Remlinger P. Les paralysies du traitement antirabique. *Annals of the Institut Pasteur* 1928; 55 (Suppl): 35-68.

Rivers TM, Sprunt DH, Berry GP. Observations on attempts to produce acute disseminated encephalomyelitis in monkeys. *J.Exp.Med.* 1933; 58: 39-53.

Robinson WH, Fontoura P, Lee BJ *et al.* Protein microarrays guide tolerizing DNA vaccine treatment of autoimmune encephalomyelitis. *Nat.Biotechnol.* 2003; 21: 1033-1039.

Sakai K, Zamvil SS, Mitchell DJ, Lim M, Rothbard JB, Steinman L. Characterization of a major encephalitogenic T cell epitope in SJL/J mice with synthetic oligopeptides of myelin basic protein. *J.Neuroimmunol.* 1988; 19: 21-32.

Stanley GP, Pender MP. The pathophysiology of chronic relapsing experimental allergic encephalomyelitis in the Lewis rat. *Brain* 1991; 114 (Pt 4): 1827-1853.

Stefflerl A, Brehm U, Linington C. The myelin oligodendrocyte glycoprotein (MOG): a model for antibody-mediated demyelination in experimental autoimmune encephalomyelitis and multiple sclerosis. *J.Neural Transm.Suppl* 2000; 123-133.

Stefflerl A, Brehm U, Storch M *et al.* Myelin oligodendrocyte glycoprotein induces experimental autoimmune encephalomyelitis in the "resistant" Brown Norway rat: disease susceptibility is determined by MHC and MHC-linked effects on the B cell response. *J.Immunol.* 1999; 163: 40-49.

Steinman L. Assessment of animal models for MS and demyelinating disease in the design of rational therapy. *Neuron* 1999; 24: 511-514.

Steinman L. Optic neuritis, a new variant of experimental encephalomyelitis, a durable model for all seasons, now in its seventieth year. *J.Exp.Med.* 2003; 197: 1065-1071.

Stohlman SA, Hinton DR. Viral induced demyelination. *Brain Pathol.* 2001; 11: 92-106.

Storch MK, Stefflerl A, Brehm U *et al.* Autoimmunity to myelin oligodendrocyte glycoprotein in rats mimics the spectrum of multiple sclerosis pathology. *Brain Pathol.* 1998; 8: 681-694.

Sun D, Whitaker JN, Huang Z *et al.* Myelin antigen-specific CD8+ T cells are encephalitogenic and produce severe disease in C57BL/6 mice. *J.Immunol.* 2001; 166: 7579-7587.

Teitelbaum D, Meshorer A, Hirshfeld T, Arnon R, Sela M. Suppression of experimental allergic encephalomyelitis by a synthetic polypeptide. *Eur.J.Immunol.* 1971; 1: 242-248.

Tuohy VK, Lu Z, Sobel RA, Laursen RA, Lees MB. Identification of an encephalitogenic determinant of myelin proteolipid protein for SJL mice. *J.Immunol.* 1989; 142: 1523-1527.

Vandenbark AA, Hinrichs DJ. Experimental allergic encephalomyelitis and cellular immunity in the Lewis rat. *Cell Immunol.* 1974; 12: 85-93.

Wekerle H, Linington C, Lassmann H, Meyermann R. Cellular immune reactivity within the CNS. *Trends Neurosci.* 1986; 9: 271-277.

Woodruff RH, Franklin RJ. Demyelination and remyelination of the caudal cerebellar peduncle of adult rats following stereotaxic injections of lysolecithin, ethidium bromide, and complement/anti-galactocerebroside: a comparative study. *Glia* 1999a; 25: 216-228.

Woodruff RH, Franklin RJ. The expression of myelin protein mRNAs during remyelination of lysolecithin-induced demyelination. *Neuropathol.Appl.Neurobiol.* 1999b; 25: 226-235.

Yan SS, Wu ZY, Zhang HP *et al.* Suppression of experimental autoimmune encephalomyelitis by selective blockade of encephalitogenic T-cell infiltration of the central nervous system. *Nat.Med.* 2003; 9: 287-293.

Yednock TA, Cannon C, Fritz LC, Sanchez-Madrid F, Steinman L, Karin N. Prevention of experimental autoimmune encephalomyelitis by antibodies against alpha 4 beta 1 integrin. *Nature* 1992; 356: 63-66.

Youssef S, Stuve O, Patarroyo JC *et al.* The HMG-CoA reductase inhibitor, atorvastatin, promotes a Th2 bias and reverses paralysis in central nervous system autoimmune disease. *Nature* 2002; 420: 78-84.

Zhu B, Luo L, Moore GR, Paty DW, Cynader MS. Dendritic and synaptic pathology in experimental autoimmune encephalomyelitis. *Am.J.Pathol.* 2003; 162: 1639-1650.

Treatment trials for stroke: Preclinical and clinical models

Anna-Leena Sirén^{1,2} and Hannelore Ehrenreich¹

1Division of Clinical Neuroscience, Max-Planck-Institute of Experimental Medicine, Göttingen ; 2Section of Experimental Neurosurgery, Department of Neurosurgery, Julius-Maximilians-University, Würzburg, Germany

Abstract

Stroke is a clinically defined neurological syndrome characterized by rapidly progressing symptoms and signs of focal loss of brain function. Cerebral ischemia invariably underlies ischemic stroke resulting in a wide range of outcomes – from a complete recovery to severe neurological deficits and death. Animal stroke models have been extensively applied to advance our understanding of the mechanisms of ischemic brain injury and to develop novel therapeutic strategies for reducing brain damage after a stroke. Experimental models of stroke in both rodents and larger species (such as cats and primates) include procedures to induce focal (permanent/transient middle cerebral artery occlusion) or global (common carotid artery ligation in gerbils, four-vessel occlusion in rats) cerebral ischemia. Furthermore, genetic models for stroke-risk factors (stroke-prone-spontaneously hypertensive rats - SHR-SP) can be combined with high fat/high salt diets to induce more clinically relevant stroke models. A hypoxia-ischemia model in premature rats is useful for studies of apoptotic cell death signaling after stroke. In primates, the surgical photothrombotic clot model represents a mostly focal ischemia model which may provide the best approximation to human stroke but also the most expensive program. In general, a large number of factors have been found to be protective in animals. The translation of these studies to man, however, failed in most cases: (1) The human study yielded no effect. (2) Non-tolerable toxicity of the compound led to premature cessation of the trial. (3) Outcomes were found to be even inferior to placebo. Based on these grounds and on our own experience with the erythropoietin stroke trial, we propose to design small human pilot studies to test efficacy/proof-of-concept, at least in case of known well tolerated

compounds. Once a compound shows promising results in man, extensive animal work can be initiated.

Stroke - a major clinical problem

Cerebrovascular diseases with stroke as the principal disorder represent the third leading cause of death in industrialized countries and the foremost cause of long-lasting disability 1, 2. The incidence for stroke measures to about 350 per 100 000 in population of the age group 45-89 years 2. There is no doubt that stroke embodies an enormous economic, social and emotional burden both for the society and especially for the affected patient and his/her family. Thus, a major financial investment both by private industry and government agencies has been allocated to study stroke. For example, in the fiscal year 2001, the total research expenditures of the National Institutes of Health (NIH) amounted to almost \$239 million. A major focus of stroke research has been the development of therapeutic strategies to prevent neuronal death and improve functional recovery. Despite the immense clinical importance and the huge financial investments in stroke research, virtually no specific pharmacological therapy that can be safely and commonly used has been introduced for treatment of this disease. Recombinant tissue-plasminogen activator (rt-PA) to improve reperfusion of the thrombosed vessel by clot dissolution is at present the only approved therapy for the treatment of acute ischemic stroke 3-5.

Its use, however, is restricted to application within 3h of stroke onset, a limitation that excludes over 95% of stroke patients from the treatment. Furthermore, the increased risk of hemorrhages significantly limits its applicability 5.

Stroke animal models

Clinically stroke is a defined neurological syndrome characterized by rapidly progressing signs of focal loss of brain function, with symptoms lasting 24h or longer or leading to death, with no apparent cause other than of vascular origin 1. Approximately 85% of all strokes are ischemic caused by cerebral embolism resulting from an occlusion of brain blood vessel by a blood clot from the heart or a diseased artery 1. Accordingly, the major animal models of stroke try to mirror this ischemic physiopathology. They can be divided into two major subgroups: focal and global ischemia models, the latter aiming at modeling of brain effects of cardiac arrest. As models for thromboembolic stroke,

photochemically induced lesions or injections of clotted blood or microspheres have been used (Table 1).

Table 1: Major rodent models of cerebral ischemia

Ischemia:	Procedure:	Species:
Focal transient permanent thrombotic	Middle cerebral artery occlusion (MCAO) Hypoxia-ischemia in juvenile animals	Rats. mice Rats, mice
Global	Transient bilateral common carotid artery occlusion (CCAO) 2-Vessel Occlusion/ 4-Vessel Occlusion Cardiac arrest (KCl, atrial fibrillation, intrathoracic hook etc.)	Gerbils Rats Rats
Thromboembolic	Photochemical Injection of microspheres / blood	Rats

Focal ischemia models

Focal ischemia in both small and large animals is preferentially performed by occluding the middle cerebral artery (MCA). Methods to achieve MCA occlusion (MCAO) include the use of clips, intraluminal thread, snare or cauterization of the blood vessel. Local injection of microspheres, clots or vasospasm inducing agents such as endothelin-1 can also be used 6-8. Another method that is particularly useful in juvenile animals is the hypoxia-ischemia model by one-sided ligation of the common carotid artery followed by exposure to hypoxic atmosphere (8% oxygen) 7, 9, 10. The advantages and disadvantages of these methods are summarized in Table 2. In all these models evaluation of infarct size is routinely achieved by densitometric analysis of the brain tissue upon staining with the vital dye triphenyl tetrasodium chloride (TTC) that colors the intact

brain tissue deep red but leaves infarcted dead tissue unstained 11. This method is especially suitable for fast screening. Histological or MRI techniques have also been frequently used for lesion evaluation 6-8.

Global ischemia models

The most frequently used models of global cerebral ischemia are accomplished by blockage of the major blood vessels that supply the forebrain resulting in ischemia over a large brain area. In gerbils which lack a functional collateral circulation, a bilateral carotid occlusion is sufficient. In rats the bilateral carotid occlusion must be combined with hypotension (2-VO) or with electrocauterization of the vertebral arteries (4-VO) to achieve complete forebrain ischemia 7, 8. Another possibility suitable for use also in larger animals is cardiac arrest achieved by intravenous infusion of potassium chloride or by inducing ventricular fibrillation⁷. In the rat cardio-circulatory arrest is induced by intrathoracal compression by a hook that presses large mediastinal vessels against the inner thoracal wall 7. These models result in delayed (3-7 days) neuronal cell death with selective neuronal vulnerability to ischemic insult in the cerebral cortex, striatum, thalamic nuclei, cerebellum and, in particular, the pyramidal neurons of the hippocampus (CA1>CA4>>>CA3). The advantages and disadvantages of these models are shown in Table 2.

Table 2:
Focal and global models of stroke in rodents: Advantages & Disadvantages

Model:	Advantages	Disadvantages:
Mouse MCAO	low cost, genetic models (transgenes/knock-outs)	limited capacity of physiologic monitoring, blood sampling non-gyroencephalic, surgical techniques extensive
Rat MCAO	low cost, genetic models of stroke risk-factors (hypertension, diabetes, obesity)	non-gyroencephalic, chronic physiologic monitoring difficult, variability of techniques, surgical techniques extensive

Treatment trials for stroke: Preclinical and clinical models

Rat 2-VO	selective, delayed cell death, one-stage surgery, physiological monitoring possible	need to induce hypotension, post-ischemic seizures
Rat 4-VO	selective delayed cell death (hippocampus) physiological monitoring possible	two-stage surgery, variability
Gerbil CCAO	rapid screening, selective delayed neuronal death model	sensitive to temperature manipulation, variability
Cardiac Arrest	clinically relevant, technically easy	whole body ischemia interferes with post-ischemic recovery of the brain, variability

Why has translation from animal to man failed?

Appropriateness of the used animal model

A fundamental problem in translating results from animal studies to clinical use is whether or not the pathophysiological processes in animal models reflect those in human disease. Thus, strain variability in the anatomy of cerebral vasculature and neuronal vulnerability has been suspected to contribute to variability in the outcome of ischemic injury. Genetic models for stroke-risk factors (stroke-prone-spontaneously hypertensive rats - SHR-SP) can be combined with high fat/high salt diets to induce more clinically relevant stroke models instead of using young healthy rodents. These models, however, are not in routine use.

The route of drug application in rodent models (intracerebral administration) is not clinically feasible. Moreover, the therapeutic window in animal models may not predict the human therapeutic window and can thus only be used as a guideline. Methodological problems such as lack of meticulous physiological monitoring (e.g. CBF, brain temperature) and the lack of adherence to major

outcomes (infarct volume and functional recovery) have weakened the predictive value of therapeutic studies in animal models.

Clinical studies – reasons for pitfalls and a first success story

Instead of homogeneous group of young, healthy animals used in preclinical studies, clinical stroke trials typically include patients with different ages, types of stroke and several comorbidities. As therapies may work in one type of disease (gray matter vs, white matter infarct, large vs. small vessel disease) but not in the other, these study designs are doomed for failure. Outcome measures lack standardization, are not sensitive or well defined. It should also be kept in mind that some therapies may be heavily influenced by individual factors such as age and sex. Moreover, many in preclinical animal studies safe compounds have proven to produce severe side effects in patients and their therapeutic window being too small to be feasibly applicable in the clinical setting.

Basically all neuroprotective approaches to human stroke had failed thus far. Reasons for these failures are numerous. As already discussed above they range from general problems in translating animal studies to man (species differences, dose and application, timing, animal model used), toxicity and intolerance reactions, to a tremendously high heterogeneity of the human population, particularly in studies recruiting unclearly defined patient groups 8, 12-15. These negative experiences in translating animal data to human studies motivated us, after having obtained promising results from preclinical studies, to launch without delay a clinical proof-of-concept trial using the clinically safe recombinant human erythropoietin (EPO) for stroke 16. The pharmacological profile of the growth factor EPO in the nervous system makes it an ideal candidate for pharmacotherapeutic neuroprotection: EPO is antiapoptotic, antioxidative, anti-inflammatory, glutamate-inhibitory, neurotrophic, angiogenetic and modulates stem cell differentiation and proliferation (for recent review of EPO literature see 17, 18). Furthermore, we observed a massive increase in EPO and EPO receptor immunoreactivity in neurons, astrocytes and endothelial cells of the infarcted human brain, pointing to an upregulation of this endogenous neuroprotective system in situations of cerebral ischemia 19.

When setting up the first EPO stroke trial 16, we decided to design a study that should come as close as possible to a preclinical animal study. When going from the established MCA (middle cerebral artery) occlusion models of laboratory animals to human stroke we are suddenly confronted with a tremendous

heterogeneity of the test population as compared to the very homogeneous situation in the laboratory, and should therefore at least aim at defining a clear "lesion model" in man. Therefore, and also to make comparability of treatment groups easier, both clinically and with respect to imaging, we decided to restrict

the stroke population in our trial to patients suffering from a stroke in the MCA territory. This was done anticipating that such clear-cut design would be at the cost of a much longer duration of the study. A proof-of-principle trial, restricted to a relatively small number of patients, cannot afford to include patients without a clear diagnosis and a reliable time-window of inclusion after the onset of a stroke. It was therefore necessary and totally exceptional at that time to request magnetic resonance imaging (MRI) for diagnosis and as prerequisite to include a

patient into the study. These two very unusual and restrictive inclusion criteria, stroke in the MCA territory and requirement of MRI for diagnosis, most likely explain the success of this small trial 16.

Conclusions & Outlook

As no single animal model represents human stroke, preclinical testing of novel compounds must include: (1) at least two species, (2) gender, age needs to be explored, (3) combination therapies, (4) at least two independent laboratories should be able to replicate the protective effect of a compound. Moreover, preclinical testing of candidate compounds known to be well-tolerated in other indications in man should: (1) be restricted to clearly defined proof-of-concept experiments, (2) be translated to human pilot trials without delay, (3) after successful translation to man return to animal work with focus on understanding mechanisms of action.

References

1. The World Health Organization MONICA Project (monitoring trends and determinants in cardiovascular disease): a major international collaboration. WHO MONICA Project Principal Investigators. *J Clin Epidemiol* 41, 105-14 (1988).
2. Warlow, C. P. Epidemiology of stroke. *Lancet* 352 Suppl 3, SIII1-4 (1998).
3. Tissue plasminogen activator for acute ischemic stroke. The National Institute of Neurological Disorders and Stroke rt-PA Stroke Study Group. *N Engl J Med* 333, 1581-7 (1995).
4. Hacke, W. et al. Randomised double-blind placebo-controlled trial of thrombolytic therapy with intravenous alteplase in acute ischaemic stroke (ECASS II). Second European-Australasian Acute Stroke Study Investigators. *Lancet* 352, 1245-51 (1998).
5. Wardlaw, J. M., Warlow, C. P. & Counsell, C. Systematic review of evidence on thrombolytic therapy for acute ischaemic stroke. *Lancet* 350, 607-14 (1997).
6. Feuerstein, G. Z. & Wang, X. Animal models of stroke. *Mol Med Today* 6, 133-5 (2000).
7. Hossmann, K. A. Experimental models for the investigation of brain ischemia. *Cardiovasc Res* 39, 106-20 (1998).
8. Green, R. A., Odergren, T. & Ashwood, T. Animal models of stroke: do they have value for discovering neuroprotective agents? *Trends Pharmacol Sci* 24, 402-8 (2003).
9. Levine, S. Anoxic-ischemic encephalopathy in rats. *Am J Pathol* 36, 1-17 (1960).
10. Sirén, A. L. et al. Endothelin B receptor deficiency augments neuronal damage upon exposure to hypoxia-ischemia in vivo. *Brain Res* 945, 144-9 (2002).
11. Isayama, K., Pitts, L. H. & Nishimura, M. C. Evaluation of 2,3,5-triphenyltetrazolium chloride staining to delineate rat brain infarcts. *Stroke* 22, 1394-8 (1991).
12. Albers, G. W., Goldstein, L. B., Hall, D. & Lesko, L. M. Aptiganel hydrochloride in acute ischemic stroke: a randomized controlled trial. *Jama* 286, 2673-82 (2001).
13. Davis, S. M. et al. Selfotel in acute ischemic stroke: possible neurotoxic effects of an NMDA antagonist. *Stroke* 31, 347-54 (2000).

14. De Keyser, J., Sulter, G. & Luiten, P. G. Clinical trials with neuroprotective drugs in acute ischaemic stroke: are we doing the right thing? *Trends Neurosci* 22, 535-40 (1999).
15. Muir, K. W., Lees, K. R., Ford, I. & Davis, S. Magnesium for acute stroke (Intravenous Magnesium Efficacy in Stroke trial): randomised controlled trial. *Lancet* 363, 439-45 (2004).
16. Ehrenreich, H. et al. Erythropoietin therapy for acute stroke is both safe and beneficial. *Mol Med* 8, 495-505 (2002).
17. Brines, M. & Cerami, A. Emerging biological roles for erythropoietin in the nervous system. *Nat Rev Neurosci* 6, 484-94 (2005).
18. Ehrenreich, H. Medicine. A boost for translational neuroscience. *Science* 305, 184-5 (2004).
19. Sirén, A.-L. et al. Erythropoietin and erythropoietin receptor in human ischemic/hypoxic brain. *Acta Neuropathologica* 101, 271-276 (2001).

Correspondence :

Prof. Anna-Leena Sirén, MD., PhD
Section of Experimental Neurosurgery
Department of Neurosurgery, Julius-Maximilians-University, Würzburg
Josef-Schneider-Str. 11, 97080 Würzburg, Germany
Tel: 49-931-201 24579
Fax:49-931-201 24140
E-Mail: siren.a@nch.uni-wuerzburg.de

or

Prof. Hannelore Ehrenreich, MD, DVM
Max-Planck-Institute for Experimental Medicine
Hermann-Rein-Str.3
37075 Göttingen, Germany
Tel: 49-551-389 9628
Fax: 49-551-389 9670
E-Mail: ehrenreich@em.mpg.de

Non-Invasive Quantification of Brain Edema and the Space-Occupying effect in a permanent rat stroke model using magnetic resonance imaging

M. Walberer, T. Gerriets, E. Stolz, M. Kaps, C. Müller, A. Kluge, A. Bachmann,
M. Fisher, M. Kaps, G. Bachmann

Dep. of Radiology / Experimental Neurology Research Group, Kerckhoff Clinic
Bad Nauheim, Germany; Dep. of Neurology, University Giessen, Germany;
Department of Neurology, University of Massachusetts Medical School,
Worcester, MA, USA

Introduction

Brain edema is a life threatening consequence of stroke. It leads to an accumulation of water and thus to a volume increase of the affected tissue. This space occupying effect causes horizontal and vertical displacement of the brain stem and midline structures.

The present study addresses two questions:

1. Can the space occupying effect due to brain edema be quantified by morphometric assessment of the hemispheric volumes on MRI?
2. Is it possible to calculate lesion volumes on MRI corrected for the space-occupying effect of edema?

Methods

Thirty male Sprague-Dawley rats (290 to 350g) were anesthetized with 5% Isofluran delivered in air at 3.0 l/min. Anaesthesia was maintained with 2.5% Isofluran delivered in air at 0.5l/min. Animals were subjected to permanent occlusion of the middle cerebral artery (MCAO) using the suture technique. A 4-0 silicone-coated nylon suture was advanced into the internal carotid artery until its tip blocked blood flow to the middle cerebral artery.

MRI was performed 6 or 24 hours after occlusion to determine hemispheric swelling. Hemispheric volumes were determined on T2-imaging and lesion volumes from ADC-maps by tracing the edges of the hemispheres and the lesions. The areas were then summed and multiplied by the slice thickness.

Lesion volumes were calculated with and without edema correction and expressed as percent of the hemispheric volume. The calculation is based on three assumptions: First, the compression of the contralateral hemisphere is comparable to the compression of the entire healthy brain tissue, whereas the lesion is not compressed. Second, the contralateral hemisphere is compressed to the same extent as the affected hemisphere is extended. The total brain volume does not change. Third, volume extension occurs only within the lesion, not in the unaffected tissue. With these assumptions the following equations were defined:

Uncorrected hemispheric lesion volume: $\%HLV_u = ((2 \cdot LV^u) / (HV_c + HV_i)) \cdot 100$

Corrected hemispheric lesion volume: $\%HLV_e = ((HV_c - HV_i + LV^u) / HV_c) \cdot 100$

Space occupying effect: $\%HSE = \%HLV_u - \%HLV_e$

(LV^u = uncorrected lesion volume, HV_c = volume of the contralateral hemisphere, HV_i = volume of the ipsilateral hemisphere)

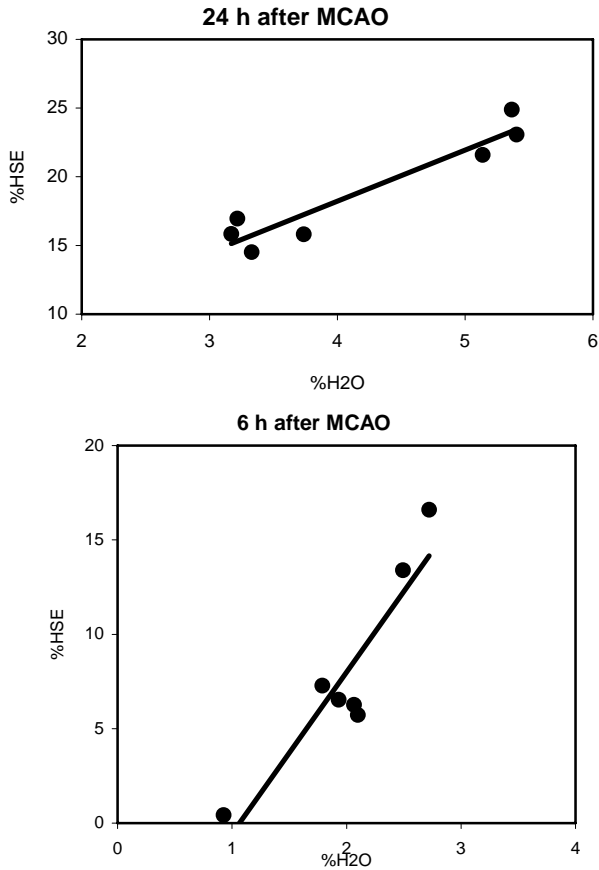
Inter- and intraobserver reproducibility of MRI measurements were assessed.

In study 1 the space-occupying effect, that results from brain edema, was correlated with the hemispheric water content determined by the wet-dry method at 6 or 24 hours after induction of ischemia.

In study 2 the impact of edema correction on lesion volume calculation was determined by comparison with TTC staining.

Results

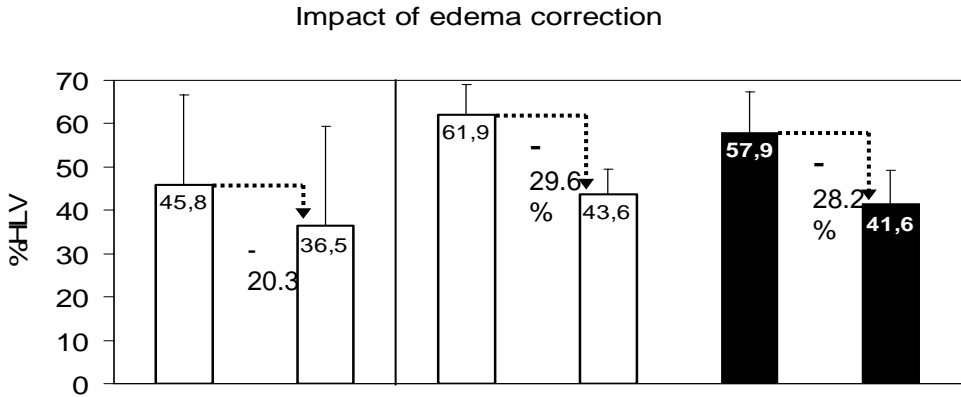
Inter- and intraobserver reproducibility of MRI measurements was excellent ($r \geq 0.97$). Hemispheric water content (wet dry-method) correlated well with hemispheric swelling determined on MRI after 6 and 24 hours of ischemia ($r \geq 0.95$).



Correlation between MRI and wet-dry-method

Correlation between the space-occupying effect as determined on MRI (%HSE) and the absolute hemispheric water content (wet-dry-method; %H₂O) after 6 hours (left) and 24 hours (right) of ischemia.

Lesion volumes calculated from MRI were overestimated by 20.3% after 6 hours and 29.6% after 24 hours of ischemia without edema correction.



Impact of edema correction on lesion volume calculation

This figure illustrates the difference in uncorrected and corrected hemispheric lesion volume 6 and 24 hours after MCAO. Already 6 hours after ischemia, lesion volume is overestimated by 20.3% (9.3%HLV), if edema correction is not performed. After 24 hours, edema correction leads to a reduction of HLV by 18.3 and 16.3%HLV (-29.6% and -28.2%) on MRI and TTC staining, respectively.

Conclusion

Morphometric assessment of hemispheric swelling on MRI provides a non-invasive measure for the increase of absolute water content in the ischemic hemisphere with a good inter- and intraobserver reliability. This technique allows to calculate edema corrected lesion volumes on MRI-scans. Without edema correction, lesion volumes are overestimate by almost 30% at 24 hours and by 20% at 6 hours after induction of cerebral ischemia. These findings emphasize, that edema correction is important for the exact determination of lesion size on MRI scans at sub acute and acute stages of cerebral ischemia. Edema corrected lesion volume calculation is relevant particularly for the interpretation of neuroprotective drug studies in animals.

Chronic rat models of cerebral oligaemia

Konstanze Plaschke*, Hubert J. Bardenheuer*, Eike Martin*, Michael Knauth#

*Clinic of Anaesthesia, Department of Experimental Anaesthesia, University of Heidelberg, Germany, #Department of Neuroradiology, University of Goettingen, Germany

Introduction: Increasing life expectancy has raised health problems with respect to 'normal' ageing, however, and particularly to age-related disorders. Cerebral oligaemia may become a stress factor during ageing leading to functional and structural deterioration in brain. The use of reproducible animal models is crucial to the study of age-related ischaemic or oligoemic brain injury – both the mechanisms governing its occurrence and potential therapeutic strategies. Several laboratory rodent species such as rat, gerbils, or mice which are readily available at relatively low cost, are highly suitable for the investigation of cerebral ischaemia and have been widely employed for this purpose. Although larger animal species (dogs, cats, rabbits, and subhuman primates) have been used to study brain ischaemia, rodents are equally suitable and more desirable from following points: 1.) low cost of the animals, 2.) relative homogeneity within strains owing to inbreeding, 3.) lower cost of the procedures that increase in expense as a function of animal weight e.g. for antibodies in immunohistochemistry or for radioligands), 4.) close resemblance of the cerebrovascular anatomy and physiology to that of higher developed species, 5.) small brain size that is well-suited to fixation procedures, and 6.) greater acceptability from ethical perspectives.

A mostly used rodent species is the rat. In some respects it is difficult to consider the complexity of age- and disease-related changes in rats because of i) the short life expectancy as compared to humans and ii) partial different cerebral compensatory mechanisms (i.e. via the Circles Willis). However, the intraindividual differences in the same rat strain are few, costs for chronic studies compared to larger animal species are lower, and important physiological mechanisms of cerebral regulation are comparable to those in humans. Therefore, the rat species are suitable for long-lasting investigation of age-related processes in cerebral oligoemia. Thus, chronic rat models may have clinical relevance for patients with a high risk of cerebral vessel stenosis or occlusion, e.g.

for patients with uni- or bilateral stenosis of the carotid arteries or for patients with dementia either of vascular or of sporadic Alzheimer's type.

Methods: In the last few years we have used rat models with permanent cerebral 2- or 4-vessel occlusions and different structural and functional parameters were investigated in rat brain (*Plaschke et al., 1999*). A new stepwise procedure of the cerebral 4-vessel occlusion model was established in adult male Wistar rats (*Plaschke et al., 2003*) to illustrate an age-related stepwise degree in cerebral blood supply. Chronic CBF reductions due to cerebrovascular disease are presumed to be stepwisely dependent on the degree of cerebrovascular involvement. Therefore, animal models with different grade of CBF reductions should be evaluated to investigate processes related to cerebral degeneration and adaptation. While rat bilateral common carotid artery occlusion (BCCAO) model was used to investigate chronic changes in cerebral energy state in relation to cognitive function, the new established rat stepwise 4-vessel occlusion model characterize a clinically relevant situation of stepwise deterioration in cerebral blood supply after chronic cerebrovascular disease. In the stepwise 4-vessel occlusion model the focus was laid on morphologic changes in rat brain microvasculature and on macrovessels after chronic cerebral oligoemia.

Results: Using the two-vessel-occlusion rat model, in which both common carotid arteries we have occluded permanently (BCCAO), results during *acute* cerebral oligoemia showed that energy metabolism is upset because the energy stores in the tissue are rapidly depleted. Consequently, there was a significant fall in the concentrations of ATP and phosphocreatine in rat brain (>50%). In parallel to the severe depression of brain energy metabolism, cerebral functions had significantly deteriorated on the first day after BCCAO. Acute oligoemia tremendously reduced rat locomotor activity. In addition, using a holeboard test system, short- and long-term memory capacities were reduced by -95% with acute oligoemia. After 3 weeks of *subchronic* BCCAO, the concentrations of high energy phosphates in rat brain tissue and memory function exhibit a tendency to partial restoration. A close linear correlation between energy rich phosphate concentration and cognitive function was determined. The partial restoration indicate that compensatory mechanisms were activated during subchronic brain oligoemia.

Using the rat stepwise cerebral 4-vessel occlusion model compensatory mechanisms in form of pronounced arterial collateralization were detected and functional and structural cerebral changes were determined after acute, subchronic and chronic time periods (*Plaschke et al., 2003*). For cerebral 4-vessel occlusion, the right carotid artery was ligated and the contralateral vertebral artery

was occluded by electrocoagulation. One week later, the left carotid and the right vertebral artery were occluded permanently. The technique of transfemoral digital subtraction angiography (DSA) was adapted from humans for use in adult rats. The DSA-technique is a modern radiographic method that can demonstrate directly whether the two vertebral arteries are completely and permanently occluded. In addition to acute verification of the degree of cerebral vessel occlusion, the transfemoral DSA technique offers the possibility of demonstrating functional adaptation in the form of pronounced arterial collateralization. This particular compensatory mechanism is based on multiple anastomoses between cervical arteries and on the patency of communicating arteries in the circle of Willis.

Despite the pronounced arterial collateralization, further compensatory mechanisms including neovascularization and the opening of pre-existing collaterals may be important during long-lasting vessel occlusions for counteracting the reduction in CBF after acute vessel occlusion. Although capillary density was not altered in rats with four stepwisely occluded vessels, ultrastructural analysis revealed endothelial cell swelling and activation as well as luminal narrowing. The basal membrane of cerebral microvessels was thickened, which can physically hinder nutrient transport into the neural tissue and may functionally affect the blood-brain barrier. Therefore, according to our hypothesis, energy and neurotransmitter deficits and ultrastructural abnormalities of cerebral capillaries are all involved in oligoemia-related decreases in cerebral function. Thus, this chronic rat model based on stepwise occlusion of four cerebral vessels reveals i) pronounced arterial collateralization, on the one hand, and ii) capillary degeneration after long-lasting vessel occlusion, on the other, which occurs simultaneously.

Summary: Using rat models of permanent cerebral vessel occlusions long-lasting cerebral oligoemia led to: i) disturbed cerebral energy state, ii) discrete changes in neuropathology, iii) moderate cerebral blood flow reduction, and iv) marked deterioration in animal behaviour.

Our findings suggest that many neuronal properties are preserved as a result of adaptive mechanisms and that a series of interdependent factors regulate brain ageing. The challenge to understand the effects of ageing represents the "new frontier" in research, both to prevent degenerative diseases and reduce their consequences. New aspects are considered on the role of rat models of permanent cerebral oligoemia. These numerous multifactorial approaches are essential to understand the process of ageing. The more we learn about it, the more we realize how to achieve "successful" and "adaptive" ageing. In addition, the development of new non-invasive MRI techniques and the use of DSA-technique in rodents will be able to give more insights into brain functional and

structural processes. In the future, these findings could lead to new neuroprotective strategies for counteracting degenerative changes in ageing and in age-associated chronic diseases.

Plaschke K et al. (1999) *Brain Res* 830: 320-329

Plaschke K et al. (2003) *J Neural Transm* 110: 719-732

Hypothalamic injury and Hyperthermia (side effects of the suture model for MCA occlusion) can confound the evaluation of neuroprotective drugs

M. Walberer, T. Gerriets, E. Stolz, M. Kaps, M. Fisher, G. Bachmann

Dep. of Radiology / Experimental Neurology Research Group, Kerckhoff Clinic Bad Nauheim, Germany; Dep. of Neurology, University Giessen, Germany, Dep. of Neurology, University of Massachusetts Medical School, Worcester, MA, USA

Introduction

Animal studies play an important role in the development of neuroprotective drugs. Using the established intraluminal suture technique for permanent occlusion of the middle cerebral artery (MCAO) in rat models causes hypothalamic injury, which is followed by hyperthermia. It is widely accepted that hyperthermia increases infarct volume and worsens functional outcome. These side effects can be avoided by using the recently developed “macrosphere model” that avoids hypothalamic damage and hyperthermia. The present study aims to compare the neuroprotective effects of the NMDA antagonist MK-801 between different MCAO models. We used the suture MCAO technique (that causes hypothalamic damage and hyperthermia, group I) and the new macrosphere model (that avoids these side effects, group II). In group III, the macrosphere model was modified to cause hypothalamic infarction and hyperthermia.

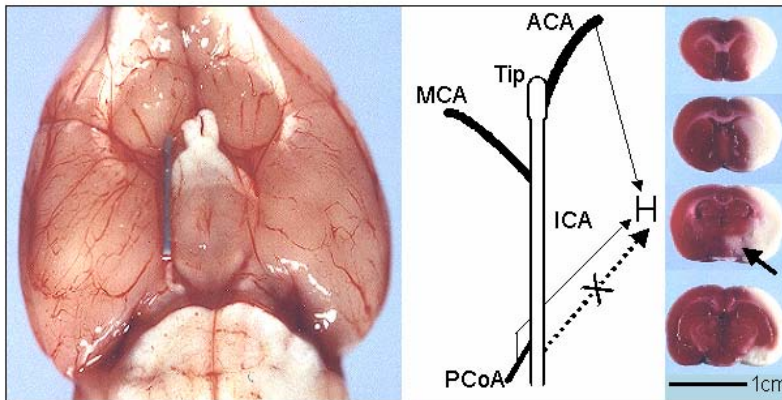
Methods

Sixty male Sprague-Dawley rats, (290 to 350 g), were treated with MK-801 (3 x 1mg/kg i.p.) or placebo. Treatment was started 15 minutes before induction of focal brain ischemia. Animals were anaesthetized with 5% Isofluran delivered in air at 3.0 l/min for 1 minute. Anaesthesia was maintained with 2% Isofluran delivered in air at 0.5 l/min. During surgery body temperature was monitored and maintained at 36.5°C to 37.5°C.

Hypothalamic injury and Hyperthermia (side effects of the suture model for MCA occlusion) can confound the evaluation of neuroprotective drugs

In group I MCAO was achieved using the suture model. In this model, a monofilament was introduced into the internal carotid artery until the tip blocked the blood flow into the MCA.

Suture MCAO

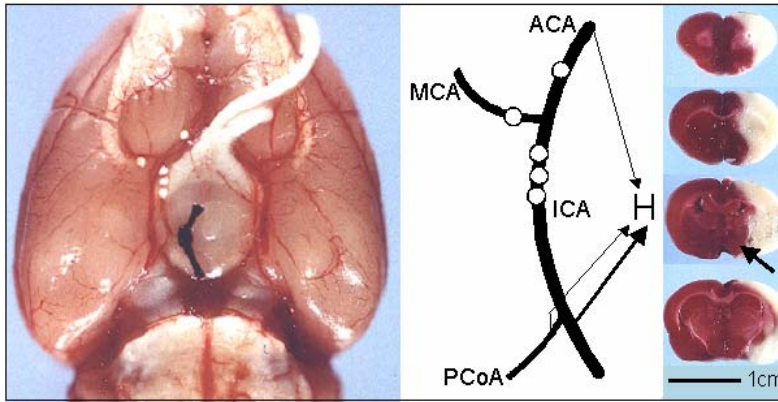


Left: Photography of the basal cerebral arteries following suture induced MCAO. The suture is located in the ICA and the proximal ACA and thus blocks the blood flow to the MCA.

Middle: Diagram of the ipsilateral cerebral arteries. The blood supply to the hypothalamus originating from the ICA is blocked by the suture (X). Hypothalamic branches from the ACA were perfused from the contralateral hemisphere via the anterior communicating artery (crossflow). The hypothalamic blood supply originating from the PCoA is not affected.

Right: The TTC staining 24 hours after MCAO demonstrates an infarction of the MCA territory. The arrow indicates additional ischemic damage of the hypothalamus.

In group II and III MCAO was performed by using the macrosphere model. In this model PE-tubing filled with six (group II) or with ten (group III) macrospheres (diameter 0.315 to 0.355mm, BRACE GmbH, Germany), was inserted through the external carotid artery into the carotid bifurcation without affecting blood flow from the common carotid artery to the internal carotid artery. Then the macrospheres were advanced separately into the internal carotid artery by injecting approximately 0.05ml saline.



Macrosphere MCAO

Left: Photography of the basal cerebral arteries following macrosphere-induced MCAO. The macropheres are located in the MCA, ACA and the distal ICA.

Middle: Diagram of the ipsilateral cerebral arteries. The blood supply to the hypothalamus (arrows) from the ICA and PCoA is not affected by the macropheres. The ACA and its branches to the hypothalamus were perfused from the contralateral hemisphere via the anterior communicating artery (crossflow).

Right: TTC staining 24 hours after MCAO reveals an infarction of the MCA territory. No ischemic lesion could be detected in the hypothalamic area (arrow).

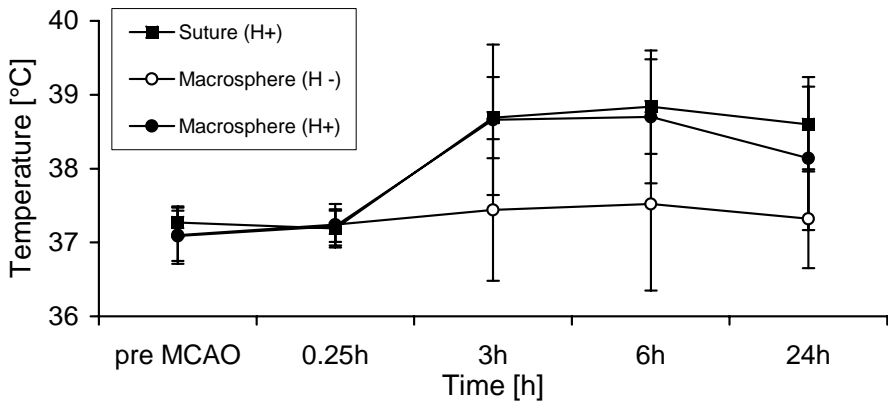
Then the animals were allowed to recover from anaesthesia. Drug injection was repeated 3 and 6 hours after MCAO.

Body temperature measurement and neurological evaluation was performed 3, 6 and 24 hours after induction of focal brain ischemia. The brains were evaluated after 24 hours by TTC-staining. Using image analysis software (Image J 1.25s; National Institutes of Health) the areas of both hemispheres and of the infarcted regions were calculated on each slice. The percent hemispheric lesion volume (%HLV) was calculated and corrected for the space-occupying effect of brain edema by using the equation $\%HLV = LV/HV_i$, where LV is the direct lesion volume and HV_i is the ipsilateral hemispheric volume, which are calculated by multiplying the area by the slice thickness and summing the volumes. Cortical and subcortical lesion volumes were calculated likewise.

Results

Treatment with MK-801 resulted in severe ataxia at 3 and 6 hours after MCAO. This well known side effect appeared in all treatment-groups and resulted in significantly decreased clinical scores compared with placebo. Thus, no significant improvement in clinical outcome could be achieved by MK-801 treatment.

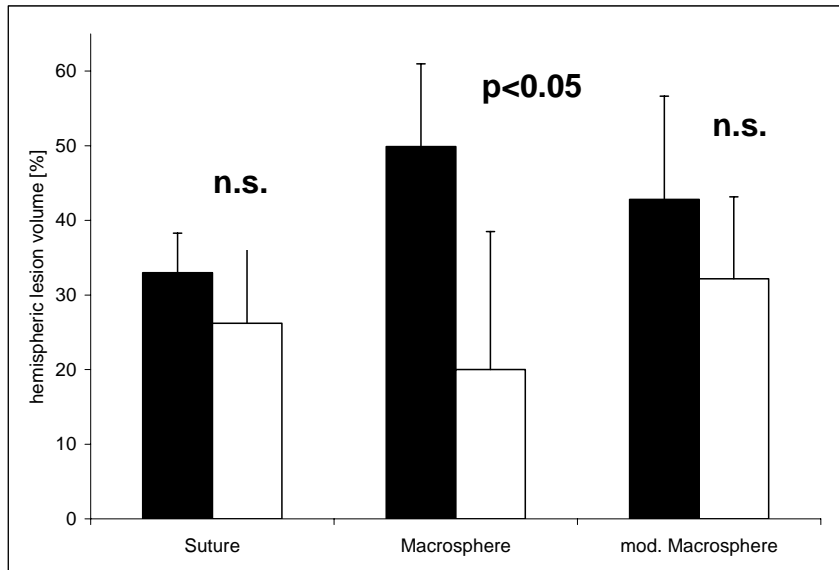
As expected, all animals in group I and III developed hypothalamic lesions with significantly increased body temperature 3, 6 and 24 hours after MCAO. Hypothalamic damage and hyperthermia was avoided in group II.



Time course of body temperature

Body temperature did not differ significantly among the groups at the first two time-points (during anesthesia). Temperature was significantly increased at 3, 6 and 24hours in animals subjected to suture-MCAO (group I) and macrosphere-MCAO with hypothalamic infarction (H+; group III) compared to rats subjected to macrosphere-MCAO without hypothalamic damage (H-; group II).

Compared to placebo, MK-801 provided a highly significant reduction in infarct size (-60%) in group II only.



Lesion volumes

In animals subjected to suture-MCAO (left) and to macrosphere-MCAO with hypothalamic damage (right) MK-801 did not provide a significant reduction of lesion volumes compared to placebo. In contrast, rats subjected to macrosphere-MCAO without hypothalamic damage (middle) showed a highly significant reduction in total, cortical and subcortical infarct size.

The presence of hypothalamic injury was strongly correlated with increased body temperature measured at 3, 6 and 24h after MCAO.

Conclusion

The present study indicates that hypothalamic infarction and subsequent hyperthermia confounds the neuroprotective effect of MK-801 and leads to false-negative results in preclinical drug studies. This typical side-effect of the suture MCAO technique can be avoided by using the new macrosphere model. Thus, this model appears to be more suitable for the evaluation of new neuroprotective approaches in permanent MCAO.

Superselective diagnostic and interventional angiography in rats

M. Knauth, A. Mohr, *K. Plaschke

Dept. of Neuroradiology, Georg-August-Universität Göttingen, University Clinic, Robert-Koch-Str. 40, D 37099 Goettingen, Germany (E-Mail: michael.knauth@med.uni-goettingen.de) *Dept. of Anaesthesiology, Ruprecht-Karls-Universität Heidelberg

Introduction:

Various rat models of acute and chronic brain ischemia include the (surgical) occlusion of brain supplying vessels. However, the surgical occlusion of the vertebral artery is difficult to achieve, as the electrocoagulation of the artery in the „atlas loop“ is performed „blindly“. It is even more difficult to prove the complete occlusion of the vessel. Our study was designed to show that with superselective diagnostic and interventional digital subtraction angiography

- (1) the efficacy of the occlusion of brain supplying vessels can be evaluated.
- (2) patterns of collateralisation and the opening of anastomoses after successful occlusion of brain supplying vessels can be studied and classified.
- (3) by superselective coil embolisation or injection of microspheres reliable vessel occlusions (coils) or hypoperfusion of brain parenchyma (microspheres) can be achieved.

Methods:

The access to the arterial system was via the femoral artery in all animals. With a microcatheter (Tracker 10) the four brain supplying vessels could be catheterized and depicted angiographically. Digital subtraction angiography was performed in a high resolution mode (matrix 1024², FOV 14 cm).

- (1) In the 4-vessel-occlusion rat model of chronic brain hypoperfusion the efficacy of vessel occlusion and the patterns of acute and chronic collateral blood supply to the brain were studied.

- (2) In some animals the minimally invasive angiographic occlusion of the vertebral artery was achieved by superselective embolisation of the vessel with platinum microcoils.
- (3) In two animals we superselectively injected microspheres into the internal carotid artery via a microcatheter (transfemoral approach). The resulting unilateral hemispheric hypoperfusion was evaluated by MRI (T2w, diffusion- and perfusion-weighted imaging)

Results

- (1) In 33% of the rats, in which a surgical occlusion of the vertebral artery had been attempted, DSA showed an only incomplete occlusion (Fig.1).
- (2) In the chronic phase DSA showed the development of collateral blood supply into the anterior and posterior cerebral circulation mainly over branches of the external carotid artery (Fig. 2). However, in some animals collateral blood supply into the posterior cerebral circulation was via spinal radicular arteries and the anterior spinal artery.
- (3) The minimal invasive angiographic occlusion of the vertebral artery by placing platinum microcoils into the artery was feasible (Fig.3) and is an elegant and effective alternative to the surgical electrocoagulation in the atlas loop.
- (4) By angiographic superselective injection of microspheres into the internal carotid artery a hemispheric hypoperfusion (without frank parenchymal infarction) could be achieved and demonstrated by MR perfusion weighted imaging (Fig. 4). Diffusion weighted imaging did not show cytotoxic edema of the hypoperfused brain tissue. The durability of the hemispheric hypoperfusion after microsphere embolisation has not yet been studied.

Conclusions:

- (1) Digital subtraction angiography is an elegant and effective tool to evaluate the completeness of attempted surgical vessel occlusions in rat models of chronic cerebral hypoperfusion. In the posterior circulation the high rate of angiographic vessel patency despite attempted complete surgical occlusion of the vertebral artery reflects the difficulty to achieve a complete occlusion. The high rate of angiographically incomplete occlusions probably (at least partially) explains the high variability of the 4-vessel-occlusion rat model of chronic cerebral hypoperfusion.

- (2) The development of collateral blood supply in the acute and chronic phase after occlusion of the brain supplying vessels can be studied and classified by digital subtraction angiography.
- (3) The surgically difficult occlusion of the vertebral artery can be effectively and minimally invasively achieved by platinum coil embolisation using superselective interventional angiography.



Fig. 1

Digital subtraction angiography of the left subclavian artery of the rat. Two days prior to the angiography an attempt had been made to surgically occlude the vertebral artery at the atlas loop by electrocoagulation. DSA shows a stenosis at the atlas loop of the vertebral artery (arrow). However, the vessel is patent – a complete surgical occlusion has not been achieved.



Fig. 2

Digital subtraction angiography of the left subclavian artery of a rat. An occlusion of all four brain-supplying vessels had been performed several weeks prior to angiography. DSA shows a persisting occlusion of the left vertebral artery (black arrow) and a collateral blood into the basilar artery via spinal radicular arteries and the anterior spinal artery (white arrows).

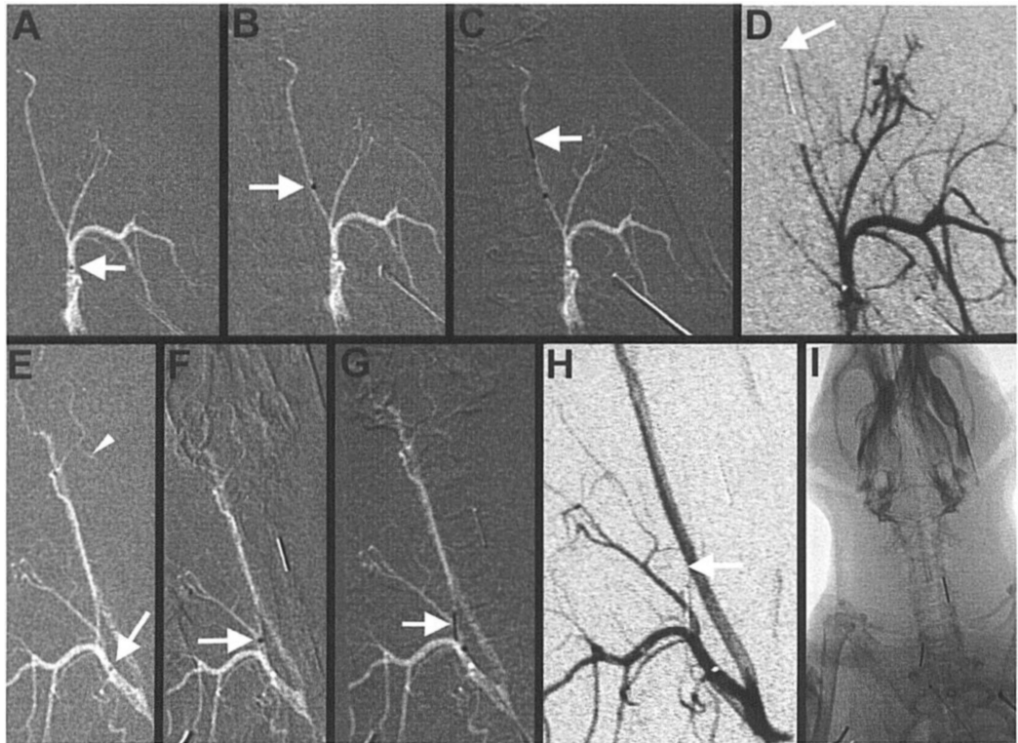


Fig. 3.

Endovascular occlusion of both vertebral arteries.

(A) and (B) shows the advancement of the microcatheter into the vertebral artery. The tip of the microcatheter can be seen in the subclavian artery (A) and in the vertebral artery (B) (white arrows). (C): a platinum coil is placed into the vertebral artery. (D): DSA control series shows a complete occlusion of the left vertebral artery. (E-H): identical procedure on the right side. (I): the unsubtracted image shows platinum coils in the vertebral arteries.

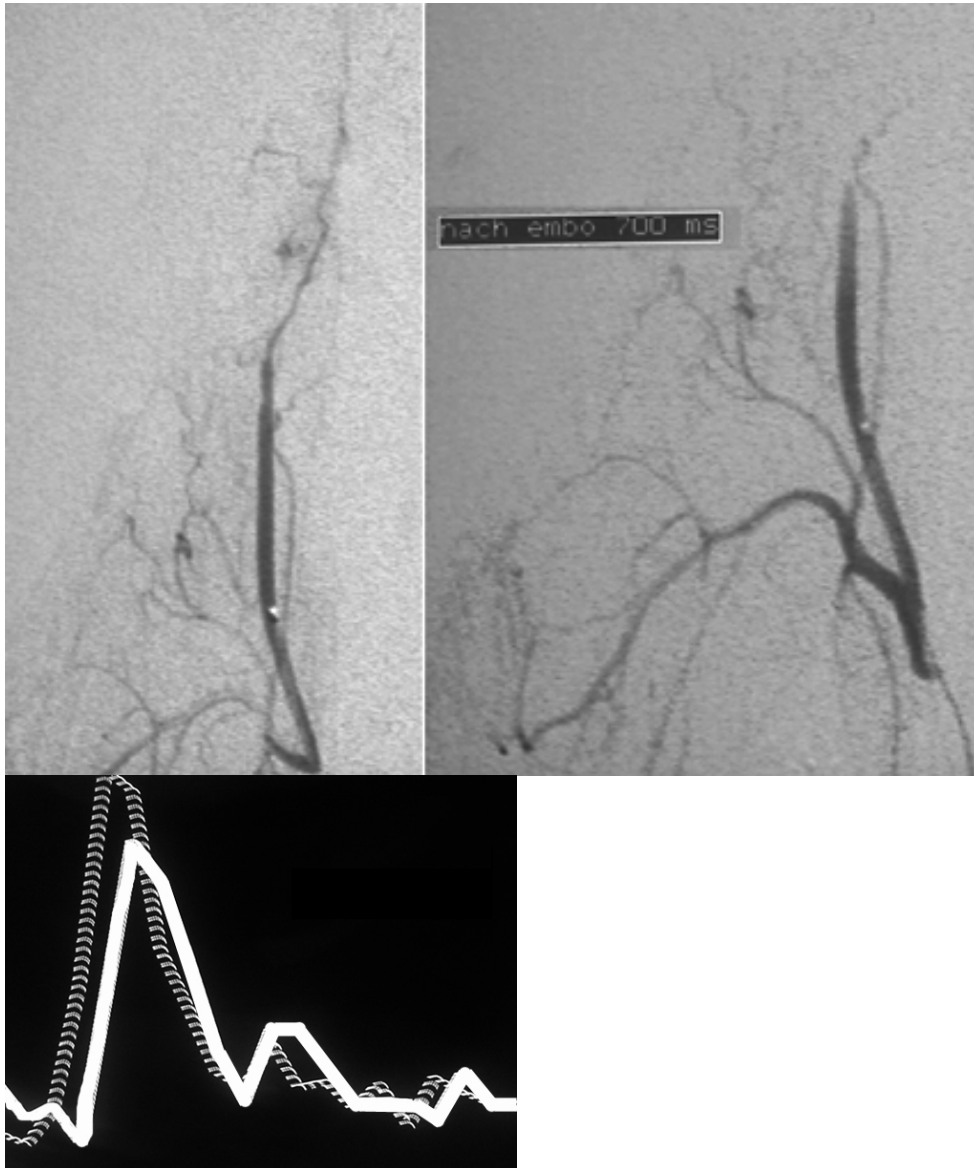


Fig. 4

Mikrosphäre embolisation of the right hemisphere. The upper row shows an angiography of the right common carotid artery before (left) and after (right) embolisation with 700 microspheres. The lower part of the figure shows the inverted time-intensity curves of an MR-perfusion-weighted sequence. The right hemisphere (full line) shows a diminished and delayed perfusion as compared with the left hemisphere (dotted line).

Intracoronary transplantation of autologous mesenchymal stem cells in a swine ischemic heart model

K. Guan, V. Zyba, T. Becker, S. Won, D. Lages, A.B. Buchwald, G. Hasenfuß

Department of Cardiology and Pneumology, Georg-August-University of Goettingen, D-37075 Goettingen, Germany

Cardiomyocyte loss in the adult heart is thought to be irreversible and frequently leads to heart failure refractory to medical therapy. Cell transplantation has emerged as a potential strategy for repairing injured myocardium. The goal of our studies was to use a pig model, which closely resembles the situation in patients to investigate cell labelling methods for in vivo cell tracking, and the survival of autologous mesenchymal stem cells (MSCs) delivered into infarcted heart tissue at two time points.

To isolate MSCs from bone marrow aspirated from the iliac crest of mini-pigs ($n = 18$), the marrow sample was diluted 1:2 with Dulbecco's modified Eagle's medium (DMEM) and loaded onto 20 ml of lymphocyte separation medium. Cell separation was accomplished by centrifugation at 800 g for 15 minutes at 20°C. The nucleated cells were collected from the interface, washed with DMEM twice and cultivated in DMEM containing 15% FCS. MSCs were obtained by their tendency to adhere to tissue culture dishes. Non-adherent cells were washed away during medium changes. The remaining adherent MSC population were expanded in vitro. Myocardial infarction was created by a 60-min occlusion of the diagonal branch of the LAD with a balloon catheter. At the end of 60 minutes, balloon was deflated and the reperfusion was visually confirmed. For in vivo tracking of MSCs isolated from bone marrow, the cells were double-labelled with fluorescent dye CM-DiI and DAPI. The labelling experiments revealed that over 95% of MSCs could be labelled with CM-DiI and DAPI and over 80% of MSCs maintained fluorescence at three weeks. Ten minutes after reperfusion, the labelled MSCs (2×10^7) were autologously delivered into the infarcted hearts via a coronary artery. The DiI-labelled cells (0.32%, $n = 3$) could be found in the infarcted compared to in the non-infarcted heart tissue (0.002%, $n = 6$) at 1 hour after MSC delivery, whereas about 0.43% of the CM-DiI- and DAPI-labelled

cells were found in the infarct at 2 days ($n = 3$). When you investigate the infarcted heart tissue at 2 weeks after MSC delivery, we still could find 0.35% of CM-DiI- and DAPI-positive cells ($n = 3$). In non-infarcted area, we could not find any positive cells at 2 days and 2 weeks. When we study the MSC injection at 7 days after reperfusion, we found that at 1 hour after MSC injection ($n = 2$), about 1.5% of positive cells in the infarcted tissue compared to the non-infarcted (0.2%). In the infarcted tissue, the number of positive cells is about 5 time folds higher after MSC injection at 7 days compared to at 10 min. These data suggest that (1) In the infarcted tissue there are significantly higher number of DiI-positive cells than in the non-infarcted. (2) Later injection is more efficient than early injection.

Hepatocyte transplantation model and induction of intrahepatic stem cells

Sarah König, Petra Krause

Dept. of General Surgery, George-August University of Göttingen, Robert-Koch-Str. 40,
37099 Göttingen, Germany Tel. +49-551-392612 Email: skoenig@surgery-goettingen.de

Introduction

Central to the success of the surgical treatment of numerous liver diseases is the ability of the organ to regenerate. The understanding of the process of self renewal has both progressed and changed over the last few decades. For many years, the assumption was that the liver regenerates primarily through the division of mature liver cells. However, over the last few years there has been increasing evidence of the participation of stem cells.

Intrahepatic stem cells, the so-called oval cells, represent a dormant cell compartment which is activated under conditions of severe or chronic liver disease. In addition, extrahepatic stem cells may migrate from the bone marrow into the liver, when the regenerative capacity of the liver itself is depleted. It is not yet fully clear as to how the different stem cell populations interact both with each other and with the mature liver cell population, in order to achieve homeostatic cell and differentiation equilibrium in the diseased and/or regenerating organ. In any case, the outstanding growth potential of liver stem cells may become a clinically viable option in the field of cell transplantation.

This work reports of a rat animal transplantation model for studying the mechanisms of integration and repopulation after hepatocellular transplantation under regenerative conditions. Furthermore, we provide with a stimulation protocol to induce intrahepatic liver stem cells.

Transplantation model to evaluate the repopulation capacity of transplanted cells

To investigate mechanisms of integration and repopulation of transplanted liver cells in the recipient parenchyma, a special rat model has been developed based on two strains of Fischer rats (see figure 1). The recipient is naturally deficient of the enzyme dipeptidyl peptidase IV (DPPIV). DPPIV is an exopeptidase located

in the basolateral membrane of fully differentiated and metabolically active hepatocytes. The donors are standard wild type Fischer rats. Normal hepatocytes are isolated from the donors and injected into the portal vein of the recipients. This model involves a syngeneic transplantation and thus requires no immunosuppressive measures. To guarantee the selective proliferation of donor cells recipients rats are pretreated with retrorsine. This substance is a cell division blocking agent, which is administered at a dosage of 30mg/kg 6 and 4 weeks prior to cell transplantation. In addition, a partial hepatectomy of 30% at the time of transplantation triggers the regenerative response. Transplanted hepatocytes and their descendents may be detected using histochemical staining or alternatively through immunofluorescence with an antibody to DPPIV. Transplantation of 8Mio adult hepatocytes leads to repopulation of up to 40% after two months.

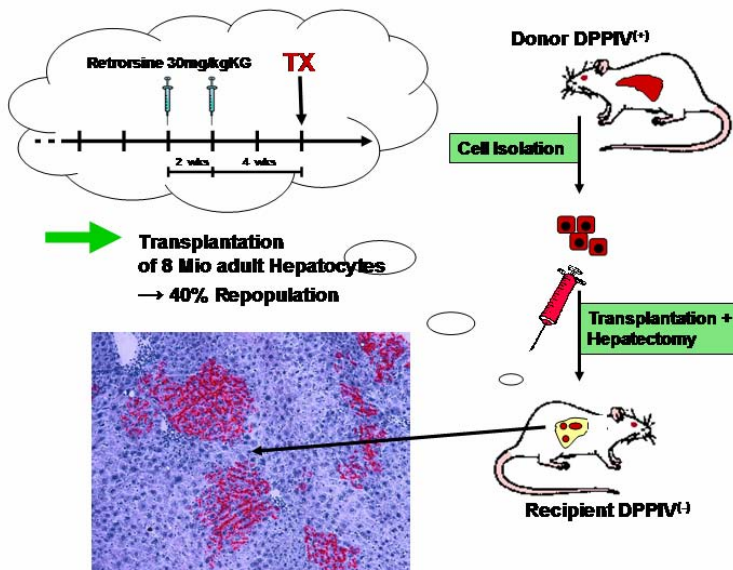


Figure 1: Transplantation and repopulation model of DPPIV-deficient Fischer rat pre-treated with retrorsine and partial hepatectomy to enable selective proliferation of donor cells

In vivo induction of intrahepatic stem cells

Intrahepatic stem cell activation only occurs when the proliferation of mature hepatocytes is massively impaired. To prime the liver for these conditions, a carcinogenic stimulus needs to be combined with substantial hepatocellular cell

loss (see figure 2). Therefore, a 2-acetylaminofluorene time release pellet (Innovative Research of America, Sarasota USA) is inserted subcutaneously in the

neck region of the stimulated rat. The pellet allows constant and gentle release of the carcinogenic substance (2,5mg per day) to suppress the proliferation of hepatocytes. A single dose of tetrachloromethane (CCl_4 1,5g per kg body weight) applied one week later and induces acute hepatic injury. Subsequently, the resistant progenitor cells start to proliferate. The organ can be harvested after 20 days.

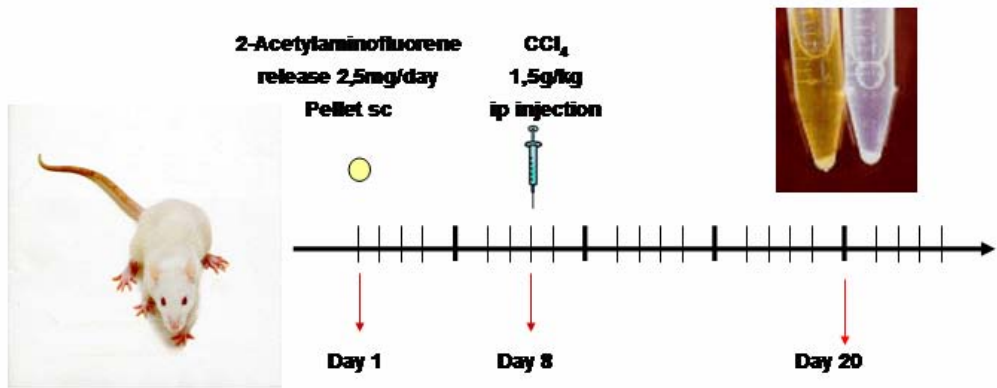


Figure 2:
Protocol to induce intrahepatic stem cell (= oval cells)

The stimulation protocol results in cell proliferation in the periportal regions. Duct like structures can be clearly seen, which stain positively for bile duct markers such as cytokeratin 7. It appears that intrahepatic stem cells develop as oval cells from these ductules and migrate further into the parenchyma. As their name indicates, the proliferating cells display oval-shaped nucleus and scant cytoplasm.

Oval cells may well be classified as an intrahepatic progenitor compartment, but one can not exclude an extrahepatic, hematopoietic origin as they express various hematopoietic stem cell markers as e. g. Thy-1 (= CD90). Thy-1 represents a cell surface protein which is not normally expressed on any cells in the adult rat liver. In stimulated rat liver, Thy-1 antigen can be used to visualise oval cells with immunostaining methods. As shown in figure 3, clusters of Thy-1 positive cells growth out from the periportal fields. In additional characterisation studies, these cells display the hepatocyte markers albumin and cytokeratin 18 and demonstrate

the fetal liver development marker alpha-fetoprotein. In contrast, the intrahepatic stem cells lack the liver specific differentiation markers dipeptidyl peptidase IV und Connexin 32.

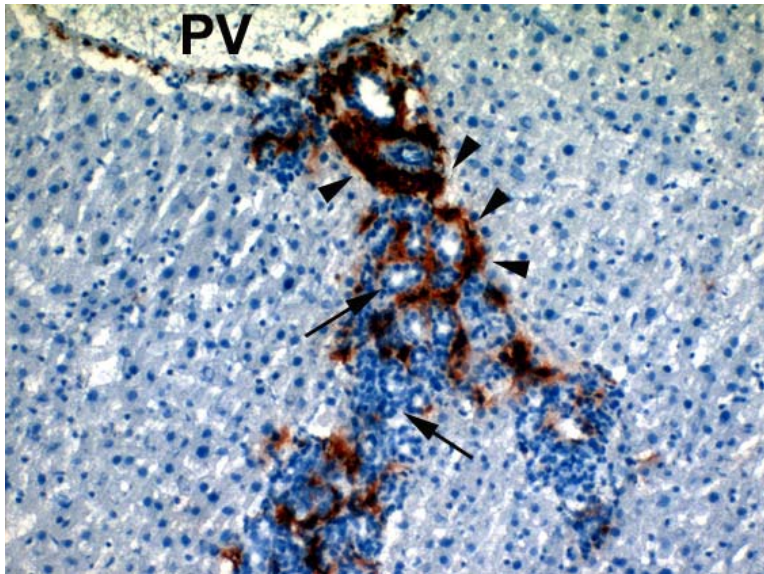


Figure 3:
Immunohistochemical staining of Thy-1 positive oval cells (arrowheads) in stimulated rat liver (original magnification x100). Duct like structures that appear as origin of oval cells are marked with arrows. PV = portal vein.

Prospects

We certainly need to clarify the mechanisms of hepatic stem cell activation to fully understand their potency of differentiation and interaction within the host parenchyma. The next step will be to track their fate after transplantation into the above described rat animal liver regeneration model. We surely do not yet know whether liver precursor cells really repopulate the recipient liver more rapidly and effectively than adult hepatocytes.

Recombination analysis in porcine endogenous retroviruses

B. Aigner¹, N. Klymiuk^{2,3}, M. Müller³, G. Brem²

¹Lehrstuhl für Molekulare Tierzucht und Biotechnologie, Ludwig-Maximilians-Universität München, D-85764 Oberschleißheim, ²ApoGene Biotechnologie, D-86567 Hilgertshausen, ³Institut für Tierzucht und Genetik, Veterinärmedizinische Universität Wien, A-1210 Wien

Abstract

Prevention of cross-species infection of porcine endogenous retroviruses (PERV) is crucial for xenotransplantation. The potential risk of infection is caused by replication competent PERV as well as by hybrid viruses derived from recombination events of distinct PERV genomes. Recently, human tropic replication competent (HTRC) PERV genomes obtaining hybrid sequences have been observed. Here, we carried out the complete polymorphism pattern analysis of the to date published full length PERV $\gamma 1$ clones as well as of the complete envelope (*env*) gene sequences. Several recombined full length clones and a high number of different recombination patterns in the *env* gene were identified.

Introduction

Xenotransplantation of genetically modified pig tissues aims to compensate for the shortage of human donor organs. Cross-species transmission of pathogens will be a major obstacle. Use of specific-pathogen-free (SPF) animals focuses the potential infectious risk to porcine endogenous retroviruses (PERV). Endogenous retroviruses (ERV) are copies of exogenous retroviral genomes integrated into the germ line of the host and have been found in multiple copy number in all mammals. Intact proviruses harbour the genes *gag*, *pro/pol* and *env* enclosed by long terminal repeats (LTR) at both ends. Most ERV are defective due to deleterious mutations. Production and cross-species infection of functional PERV have been observed in *in vivo* experiments. In addition, PERV have been shown to infect human cells *in vitro*.

PERV are classified into the retroviral β (B- or D-type) and γ (C-type) genera. All known human tropic infectious PERV have been assigned to the PERV γ 1 family consisting of the subfamilies A, B and C. Examination of porcine cell lines and pig breeds resulted in the detection of about 50 PERV γ 1 sequences including several intact copies. PERV γ 1A, B and C are highly homologous in their *gag* and *pro/pol* retroviral genes, whereas significant differences in the envelope (*env*) gene explain their different host tropism. Recently, chimeric PERV γ 1 sequences have been observed (Klymiuk et al., 2002; Lee et al., 2002; Oldmixon et al., 2002; Wilson et al., 2000).

To assign the proviral genomic sequences to the different host tropism, and to evaluate the potential infectious risk of recombinant clones in xenotransplantation, we analysed full length PERV γ 1 genomes as well as complete PERV γ 1 *env* gene sequences.

Results

Full length PERV γ 1 genomes and complete PERV γ 1 *env* gene sequences were identified in the GenBank DNA database by BLAST search and subsequently used in the study. Comparative sequence analysis was done by using ClustalW, MacClade (<http://phylogeny.arizona.edu/macclade/macclade.html>) and SeqApp (<http://ftp.bio.indiana.edu/soft/molbio/seqapp/>). Complete polymorphism pattern analysis was carried out by the alignment of the full length PERV γ 1 *gag*, *pro/pol* and *env* genes. Phylogenetic trees of the respective genome fragments were created by the PHYLIP package (<http://evolution.genetics.washington.edu/phylip.html>).

For the comparative analysis, 18 full length PERV γ 1 nucleotide sequences harbouring the complete *gag*, *pro/pol* and *env* genes were taken from GenBank. Having remained unconsidered two highly polymorphic clones, we obtained 972 nucleotide positions (14% of the complete sequence) in the sequences where more than one clone showed a polymorphism. 904 of them representing 84% of the polymorphic nucleotides, were found to be involved in the definition of three distinct subfamilies. The three patterns were assigned to PERV γ 1A, B and C which were defined by their different host tropism. The subsequent comparison of the polymorphic nucleotide patterns revealed the appearance of recombination events in individual sequences. Four obvious recombination sites were observed in the alignment. Separate phylogenetic analyses were carried out for the five fragments between the four recombination sites by the most parsimony method and strictly confirmed the classification of the clones.

In total, six recombinant proviruses (GenBank accession number A66552, A66553, AF038601, AF435966, AJ133817, AY099323) were found. All six recombinant proviruses were classified to PERV γ 1B both in the 5' and the 3' end, whereas the intermediate sequences were of PERV γ 1A. The recombinant PERV γ 1A fragments included the partial *pro/pol* gene (A66552, A66553) as well as the 3' end of *pro/pol* and the major part of the *env* gene (AF038601, AJ133817, AY099323) resulting in the γ 1A host tropism for the replication competent clones AJ133817 and AY099323. AF435966 harbouring multiple nucleotide polymorphisms in the *gag* and *pro/pol* genes was classified to the recombined clones AF038601, AJ133817 and AY099323 with the 5' end of the intermediate γ 1A fragment located in the *gag* gene (Klymiuk et al., 2003).

As the *env* gene is crucial for retroviral host tropism and, therefore, determines which PERV are capable of infecting human cells, in the further study we focused on recombination events of this gene. In total, we screened 82 complete PERV γ 1 *env* genes which have been submitted to GenBank. The *env* genes of the 18 γ 1 full length sequences described above were included. 58 fragments harboured an ORF. Designation of the *env* sequences to PERV γ 1A, B and C was carried out by comparison to AF417223, Y12239 and AF038600, respectively, which showed maximal sequence diversity in the nucleotide polymorphism patterns. 38 *env* sequences (46%) were classified completely to one of the three original subfamilies, whereas 44 (54%) were hybrid sequences. 57% (n=25) of the hybrid sequences showed an ORF. The hybrid sequences were classified to 15 distinct recombination patterns. Three retroviruses with hybrid sequences in the receptor binding domain (RBD) (AF417227, AF417228, AF417229) have been shown to be human tropic replication competent (HTRC) (Oldmixon et al., 2002), however it is not clear if the recombination has influenced the host tropism.

Five *env* genes (AF296168, AJ288586, AJ288587, AJ288590, AJ288591) showed sequence fragments with differences to the known PERV γ 1 subfamilies. These *env* sequences were suggested to be derived from recombinations with not yet known retroviral genomes (Klymiuk et al., 2003).

Conclusion

Having carried out the polymorphism pattern comparison, here we assigned the proviral nucleotide sequences to the different host tropism which has been previously described for the PERV γ 1 proviruses. Recombination events were found in full length PERV γ 1 sequences derived from *in vitro* studies with PK15 cells as well as in the genome of different breeds. In addition, the PERV γ 1 *env*

sequences of the three subfamilies A, B and C were defined showing maximal sequence diversity in the polymorphism patterns. The chimeric *env* sequences

containing fragments with low identity to PERV $\gamma 1$ A, B and C indicated the potential of not yet known retroviral genomes to get involved in recombination events with unknown consequences for the host tropism and the pathogenicity of the recombinant PERV $\gamma 1$ proviruses. Recombinational patch repair resulting in new retroviral genomes has been previously described in defective retroviral genomes. Although this has not yet been determined for mutant PERV $\gamma 1$ sequences, the potential infectious risk can not be ruled out for defective PERV $\gamma 1$ loci.

References

- Klymiuk N, Müller M, Brem G, Aigner B (2002) J Virol 76, 11738-43.
Klymiuk N, Müller M, Brem G, Aigner B (2003) J Gen Virol 84, 2729-34.
Lee JH, Webb GC, Allen RD, Moran C (2002) J Virol 76, 5548-56.
Oldmixon BA, Wood JC, Ericsson TA, Wilson CA, White-Scharf ME, Andersson G,
Greenstein JL, Schuurman HJ, Patience C (2002) J Virol 76, 3045-8.
Wilson CA, Wong S, Vanbrocklin M, Federspiel MJ (2000) J Virol 74, 49-56.

Corresponding author:

Bernhard Aigner
Lehrstuhl für Molekulare Tierzucht und Biotechnologie
Moorversuchsgut
Hackerstr. 27
D-85764 Oberschleißheim
E-mail: b.aigner@gen.vetmed.uni-muenchen.de

Investigation of the efficacy of rodent microbiological monitoring methods in a ventilated cage rack system

Susan R Compton¹, Felix Homberger², Judy MacArthur Clark³, & Frank X Paturzo¹.

¹Section of Comparative Medicine, Yale University School of Medicine, New Haven CT; ²Research Animal Resources Center, Weill Medical College of Cornell University and the Memorial Sloan-Kettering Cancer Center, New York NY;

³BioZone Inc, Carowinds Blvd., Fort Mill SC.

The use of individually ventilated caging (IVC) systems to house rodents is increasing rapidly and presents new challenges for effective microbiological monitoring. Since each cage is, theoretically at least, its own biocontainment zone, traditional methods such as exposure of sentinels to airborne infectious agents present in the room are inappropriate. Currently, soiled bedding sentinels are most commonly used to monitor mice housed in IVC systems, but this method is labour intensive and efficacy varies depending on the infectious agent being detected.

A method which exploits the characteristics of IVC systems by sampling exhaust air has recently been developed but the efficacy has not been systematically investigated. In an effort to aid laboratory animal personnel in making informed decisions on the most sensitive, specific and economical methods for microbiological monitoring of rodents housed in IVC systems, the efficacy of exhaust air monitoring using sentinels exposed to exhaust air (the BioScreen™ system) and filters placed in the exhaust air stream of the IVC rack were both compared with that of soiled bedding and contact sentinel monitoring.

Groups of 12 Swiss Webster mice were infected with mouse hepatitis virus (MHV), mouse parvovirus (MPV), murine rotavirus (EDIM), Sendai virus (SV), or *Helicobacter* and were monitored in an IVC rack, first for 12 weeks operated at positive pressure relative to the room and then for a further 12 weeks at negative

air pressure. The agents were chosen because they are common in contemporary mouse colonies and they vary in their infectivity, duration of infection, environmental stability and size.

The study was designed to also determine the time periods over which different infectious agents may be active and detectable by the different sentinel monitoring systems. It was hypothesized that nucleic acids would be present longer than infectious organisms and this was also investigated by comparing data from the BioScreen™ system with exhaust filter data. Furthermore, evidence presented suggests that the soiled bedding sentinel method may be less effective in IVC systems compared with static micro-isolator systems, due possibly to dilution and desiccation effects.

Given the speed of PCR-based assays to detect infectious agent nucleic acids, testing filters which have been exposed to the exhaust air from the IVC system was considered to be potentially very useful in an infectious agent outbreak to rapidly determine the location and distribution of the agent in the laboratory animal colony, and when the agent has been successfully eradicated. The labile nature of nucleic acids and the turnover of infectious agents on filters have been postulated as a possible drawback of using PCR-based detection of infectious agents on filters as a routine monitoring method. The labile nature of MHV, MPV, EDIM, SV and *Helicobacter* deposited on filters placed on the inner surface of the exhaust air port of the IVC rack was therefore tested.

The results of this study are intended to aid laboratory animal personnel in making informed decisions on applicable methods to use in routine microbiological monitoring of rodents housed in a comparable IVC system.

Optimization of the detection of *Helicobacter* spp. using PCR

K. Jacobsen¹, E. Mahabir¹, M. Brielmeier¹, P. Wilhelm¹, K. Seidel², J. Schmidt¹

¹Department of Comparative Medicine, GSF - National Research Centre for Environment and Health, 85764 Neuherberg, Germany, ²Institute of Medical Microbiology, Immunology and Hygiene, Technical University Munich, 81675 Munich, Germany

Introduction

Infection of laboratory mice with *Helicobacter hepaticus* (*H. hepaticus*) and its influence on animal experiments were reported for the first time in 1994. Since then, many other murine *Helicobacter* strains were characterized and classified. However, their influence on animal-based research is not yet cleared. In the amended recommendations for health monitoring of laboratory animals, FELASA recommends examination of *Helicobacter* spp. at least once per year. *Helicobacter* infections can be detected using different methods including ELISA (enzyme-linked immunosorbent assay), culture, histology and PCR (polymerase chain reaction), which differ in sensitivity and specificity. Generally, *Helicobacter* diagnostic is performed using the PCR. Various factors including PCR inhibitors, degradation of the sample DNA and storage of the sample DNA result in a lack of reproducibility of positive results or false-negative results are obtained. As such, it is often difficult to determine the *Helicobacter* status of a mouse colony.

Materials and Methods

To optimize the diagnostic method for *Helicobacter* spp., a "nested" PCR with two PCR steps was established. In the first step, the universal sequence of the bacterial 16S rRNA gene was amplified. In the second step, a *Helicobacter* genus-specific product was generated with the primers published by Riley et al.¹. The sensitivity and reproducibility of the "nested" PCR and the *Helicobacter* genus-specific PCR ("single step" PCR) was compared.

Results and Conclusion

The "nested" PCR was 10 times more sensitive than the "single step" PCR. In contrast to the sample DNA, the PCR product of the first reaction can be stored longer and can therefore be used for repeated analysis. The importance of the application of the "nested" PCR compared to a "single step" PCR for monitoring *Helicobacter* in a mouse colony with respect to sensitivity and reproducibility is demonstrated using an example.

Taken together, the present data show that the nested PCR can be used to optimize detection of *Helicobacter* spp. in laboratory animal facilities by increasing the sensitivity and reproducibility of the analysis.

Literature:

¹Riley, L.K., C.L. Franklin, R.R. Hook, Jr., and C. Besch-Williford. Identification of murine helicobacters by PCR and restriction enzyme analyses. *J Clin Microbiol* (1996) 34:942.

In utero infection of pseudopregnant mice recipients with Mouse Hepatitis Virus and Mouse Minute Virus

E. Mahabir, A. Mayer, J. Needham¹, J. Schmidt

Department of Comparative Medicine, GSF – National Research Centre for Environment and Health, D-85764 Neuherberg, Germany; ¹The Microbiology Laboratories, North Harrow, Middlesex, United Kingdom

Introduction

The technique of embryo transfer is commonly used to eliminate viral infections in colonies of laboratory mice. However, viruses may be re-introduced during embryo transfer via infected embryos and contaminated equipment and media. In order to minimize the risk of viral infection, embryos with an intact zona pellucida should be washed several times prior to transfer. Furthermore, it is important to minimize the volume of liquid in which embryos are transferred. In the present study, we determined the lowest virus dose sufficient to infect recipient mice by a route which mimics embryo transfer methodology. To this end, the immune response of pseudopregnant recipients was investigated following in utero infection with two of the most prevalent mouse pathogens in mouse facilities, Mouse Hepatitis Virus (MHV) and Mouse Minute Virus (MMV).

Materials and Methods

Seronegative, pseudopregnant 8 to 12-week old Swiss mice were inoculated in utero with varying doses of MHV-A59 and MMVp. For each dose, 4 mice were used. Control mice were sham-inoculated with 0.9% NaCl or transfer medium alone. Mice were kept in individually ventilated cages for the duration of the experiment. At sequential intervals post inoculation, sera were tested for the presence of antiviral antibodies using specific enzyme-linked immunosorbent assay (ELISA).

Results and Discussion

Within two to three weeks after inoculation, seroconversion occurred in recipients inoculated with virus-containing transfer medium. The lowest dose which induced seroconversion was 10^5 TCID₅₀/ml for MHV-A59 and 10^1

TCID₅₀/ml for MMVp. Controls were seronegative for the entire experimental period.

During embryo transfer, a maximum of 3 µl medium are inoculated into the uterus together with embryos transferred. The present data show that transfer medium containing virus with titers as shown above is sufficient for infection of the recipient.

This work was supported by the Gesellschaft für Versuchstierkunde, Society of Laboratory Animal Science (GV-SOLAS) and the National Genome Research Network, Germany.

Health monitoring of laboratory rodents: incidence and relevance of bacterial isolates from the trachea

M. Brielmeier, P. Wilhelm and J. Schmidt

Department of Comparative Medicine,
GSF – Research Centre for Environment and Health, D-85764 Neuherberg

Introduction:

Regular standardised health monitoring is of elementary relevance for the knowledge of the hygienic status of laboratory rodent colonies. On the one hand, examination of animals should cover all important organ systems and detect all relevant infectious agents. On the other hand, they should be labour-effective and provide an optimal cost-benefit relation. In 1994 and 2002, FELASA published recommendations for the health monitoring of rodent and rabbit colonies. These comprise a list of agents to be monitored, organ systems to be examined as well as test methods to be applied. For the examination of the respiratory tract, cultivation of samples taken from nasopharynx and trachea was recommended.

In the Animal Facility of the GSF Research Centre the bacteriological status of the respiratory tract of rodents is generally assessed by investigation of specimens taken from nasopharynx, trachea and lung. Detailed analyses, however, of our test results showed either absence of bacterial growth in specimens isolated from the trachea or redundant information obtained from the tracheal specimens when compared with those obtained from nasopharynx or lung in many instances. To evaluate the relevance of data obtained from trachea specimens, we compared the data from two years of health monitoring of the bacterial spectrum of the trachea with that of nasopharynx and lung.

Materials und Methods:

Examinations were carried out in specimens from 966 mice, 38 rats and 18 hamsters, kept in different areas of the GSF Animal Facility 1) in open cages with wire bar lids, 2) in filter top cages, 3) in individually ventilated cages (IVC) and 4) in Bioscreen cages in an IVC rack. Further differences included type of husbandry, barrier system and hygienic status according to FELASA recommendations. Among these, 973 were taken from sentinels and 49 from

random samples. The results of bacteriological examinations of samples taken from nasopharynx, trachea and lung were compared. Differences were determined using Fishers exact test.

Results:

From all samples taken from the 3 species, bacterial colonies were not isolated from the trachea in 640 out of 1022 (63%) animals. With respect to the 966 samples taken from mice, bacteria were not isolated from the trachea of 169 out of 216 (78%) animals kept in open cages, of 226 out of 403 (56%) animals kept in filter-topped cages, of 133 out of 215 (62%) animals kept in cages of a standard IVC system, and 75 out of 132 (57%) animals kept in cages of an IVC-BioScreen™ system. From one animal, bacteria were not isolated in either trachea, nasopharynx, or lung.

In 81 out of 966 (8%) mouse-derived specimens bacterial colonies were isolated from the trachea, which were different from those detected either in the nasopharynx or in the lungs. In these instances 8 out of 216 (4%) specimens were derived from mice kept in open cages, 34 out of 403 (8%) specimens were derived from mice kept in filter-topped cages, 23 out of 215 (11%) specimens were derived from mice kept in cages of a standard IVC system and 14 out of 132 (11%) specimens were derived from mice kept in cages of a BioScreen™-IVC system. The data are summarized in the Table.

Health monitoring of laboratory rodents: incidence and relevance of bacterial isolates from the trachea

Table

Bacterial growth in tracheal specimens during health monitoring of mice

Group No.	Holding system	Absence of bacteria in tracheal specimens*	Additional comparison
	nasopharynx and lung**		
1	Open cage with wire bar lid	169/216 (78%)	8/216 (4%)
2	Filter top cage	226/403 (56%)	34/403 (8%)
3	Individually ventilated cage (IVC)	133/215 (62%)	23/215 (11%)
4	Bioscreen cage in an IVC rack	75/132 (57%)	14/132 (11%)
Total		603/966 (63%)	81/966 (8%)

*Differences between groups 1/2: $p < 0.05$. **Differences between groups 1/3: $p < 0.01$, between groups 1/2 and groups 1/4: $p < 0.05$.

Conclusion:

During routine health monitoring of rodents kept in 4 different holding systems bacteria were not isolated from the trachea in an average of 63% of the overall specimens of the respiratory tract. In mice this figure varies from 56% to 78% depending on the holding system in which the mice were kept. In an average of 8.5% of the specimens taken from the animals of the different holding systems additional bacteria were isolated from the trachea as compared with those obtained during simultaneous examinations from nasopharynx and lung. From these data we conclude that examination of the trachea during routine health monitoring of laboratory rodents appears not to be justified in view of a critical cost-benefit analysis.

Changes in differential haemogram after infusion of mean and low molecular weight hydroxyethyl starch (HES) in rats

M. Wagenblast, A. Theisen, Ch. Tandi, H. Forester

Institute of Experimental Anaesthesiology, J. W. Goethe-University Hospital Frankfurt(M)

Introduction: Volume effect is achieved by use of colloidal volume substitutes like hydroxyethyl starch (HES) and represented by a decreasing value of haematocrit. Leukocyte concentration should be influenced by this effect in the same way. However, other effects of HES on leukocytes like intracellular storage and functional interference are discussed. Aim of this study was to figure out if changes in haemogram are not only caused by haemodilutional effects. Two different, commonly used HES-preparations were compared. Erythrocytes and leukocytes were measured by flow cytometrie.

Materials and methods: 8 Wistar WU-Rats (300-350 g) in each trial group were infused. Each 18 ml of 6% mean molecular weight, medium substituted HES 200/0,5 and of 6% low molecular weight, low substituted HES 130/0,4 (Haessteril® and Voluven®, both Fresenius Kabi, Bad Homburg, Germany) were administered within 3 hours via central venous catheter. Blood was taken pre-infusion, immediately post-infusion 2, 4, 6, 24 and 48 hours post-infusion by orbital puncture. A haemogram was determined using Cell-Dyn 3500R (Abbott). For statistical calculation, data were firstly tested for standardised normal distribution by Shapiro-Wilk-Test. In case of standardised normal distribution, two sample t-Test was used. In case of absence of standardised normal distribution, Wilcoxon-Mann-Whitney-U-Test was preferred. Level of significance was defined as 5%. Described changes in results are statistically significant to the extend that nothing else is mentioned.

Results: For Haematocrit (Htc) and quantity of red blood cells (RBC) a correlation was found ($r > 0,98$) after infusion of HES. MCV (mean corpuscular

volume) didn't change significantly. For this reason RBC showed volume effect comparable to Htc. RBC's were utilised for quantitative comparison of blood cells. RBC decreased for a short time post-infusion. However, RBC increased already 2 h (HES 130/0,4) respectively 4 h (HES 200/0,5) above the initial value. On the following days, RBC values were persistently lower than initial value. Comparing RBC with white blood cells (WBC) coefficients of correlation (r) ranged between 0,22 and - 0,64. 24 h and 48 h post-infusion WBC were increased after administration of HES 200/0,5. After administration of HES 130/0,4 WBC were not increased, 6 h post-infusion they were even decreased (s. Figure 1). The number of neutrophils increased after infusion of both HES solutions. Number of Lymphocytes decreased until 6 h (HES 200/0,5) respectively 24h (HES 130/0,4) post-infusion, in the following time quantity increased in relation to initial value (s. Figure 2). Quantity of monocytes increased 3,8 to 6,4-times after infusion of HES 200/0,5 in comparison to the initial value (s. Figure 3). In contrast, increase of monocytes was not significant after infusion of HES 130/0,4. Quantity of basophils and eosinophils didn't increase until 24 h (HES 200/0,5) respectively 48 h (HES 130/0,4) post infusion.

Discussion: As shown by the missing correlation, changes in white blood cell count are not only explainable by haemodilutional effects. On the other hand, some changes can be explained by influences of narcosis and surgical procedure. However, it is known that in the first line monocytes absorb HES in association with storage. Up to now, it was unknown that the quantity of monocytes increases directly post-infusion in contrary to the haemodilutional effect of the administered solution. This effect was less pronounced after infusion of HES 130/0,4 than after infusion of HES 200/0,5.

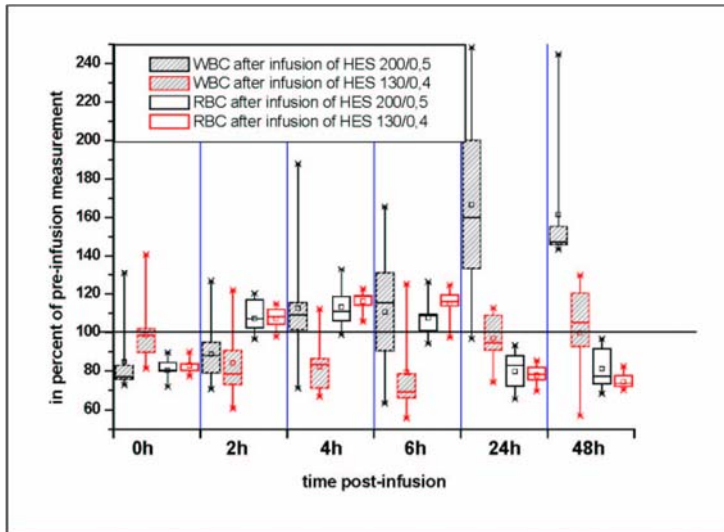


Figure 1:
Comparison of RBC and WBC after infusion of two different HES preparations

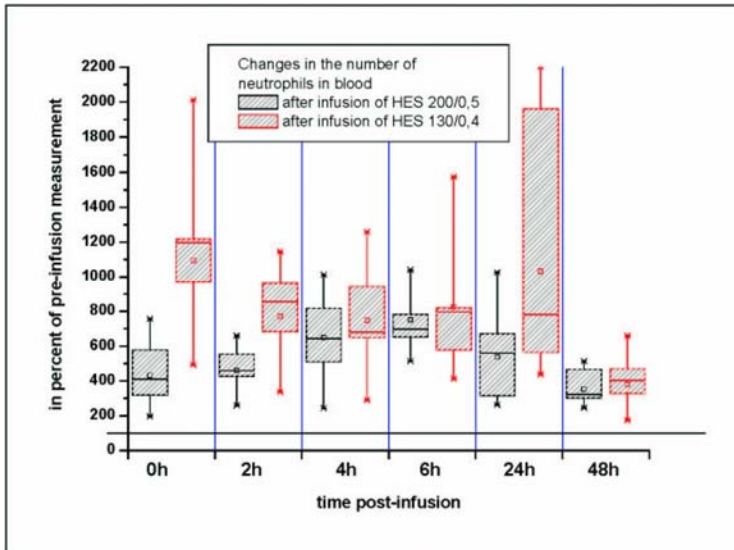


Figure 2:
Changes in the number of neutrophils after infusion of two different HES preparations

Changes in differential haemogram after infusion of mean and low molecular weight hydroxyethyl starch (HES) in rats

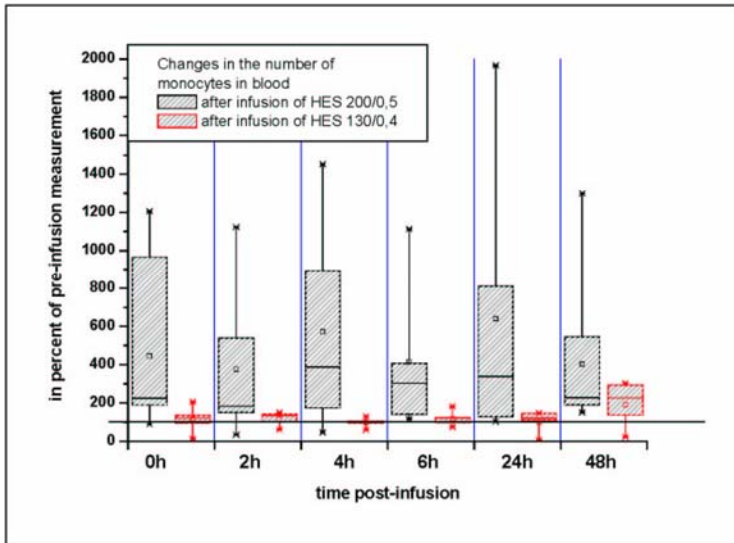


Figure 3:
Changes in the number of monocytes after infusion of two different HES preparations

Does inhalation anesthesia act beneficial in preventing distress from tail biopsy in laboratory mice?

M. Arras, A. Rettich, B. Seifert, T. Rüllicke

University of Zurich, Institute of Laboratory Animal Science, Central Biological Laboratory, Sternwartstrasse 6, CH-8091 Zurich, Switzerland

Tail biopsy (clipping the tail tip) is a frequently used procedure to obtain cells for genotyping genetically modified mice. Although used routinely, there is discrepancy whether this is an amputation and therefore is mandatory to be carried out under anesthesia or if it could be done in the conscious animal without any pain relief. Therefore, we investigated the influence of tail biopsy on mice's well-being by use of the body weight curve and telemetrically measured heart rate, body core temperature and locomotor activity during and for 4 days after cutting the tail tip without anesthesia and under anesthesia (uncontrolled vaporization in an anesthetic chamber) with either diethylether (ether) or methoxyflurane (MOF). Anesthesia was characterized by the time course for induction, immobilization, surgical tolerance and recovery and by blood gases and acid-base equilibria in arterial blood. For assessment of the irritant action of ether on mucous membranes the behavior of the mice during induction of anesthesia was documented.

As results we found considerable acute respiratory acidosis in both anesthetics. Duration of surgical tolerance (average: ether 28 sec, MOF 35 sec) was similar under standardized conditions (after removing the mouse from the anesthetic atmosphere) but induction and recovery were markedly prolonged under MOF: completing the procedure needs 207 sec with ether and 785 sec with MOF. The stress induced significant (Student's paired T Test, $p < 0.01$) increase of heart rate, that occurred for one hour after tail biopsy was inhibited by ether but remained after MOF for up to 4 hours. Furthermore, BT increased significantly after MOF for 3 hours and decreased significantly in the first night after anesthesia. A significant increase of locomotor activity was found only after MOF. Seventeen out of 30 mice showed nictation and nose scratching when exposed to ether and nine mice exhibited panic-like behavior and escape trials during induction with

Does inhalation anesthesia act beneficial in preventing distress from tail biopsy in laboratory mice?

MOF. Two mice died from ether anesthesia. Body weight remained unchanged after all interventions.

Summarized, our measurements give no hints, that tail biopsy in conscious mice caused major pain or distress. Anesthetizing mice with ether or MOF induced aversive behaviors and aberrations in physiology that persisted for up to 12 hours and implied, that mice have suffered more from anesthesia than from cutting the tail tip.

We conclude, that it is reasonable to take tail biopsies in laboratory mice without anesthesia.

Animal Experimentation: A Comparison of the Attitude of the German and the British Population

C. Exner (1, 2) and G. Heldmaier (1)

- (1) Dept. of Biology – Animal Physiology, University of Marburg, Germany
- (2) Advisory Committee on Animal Experiments of the German Science Foundation (DFG), Germany

Summary:

A controversial discussion about the necessity of animal experimentation for scientific progress is taking place in Germany as well as in Great Britain. At the same time, the media frequently draw a negative picture of biomedical research using animals. However, the opinion of the population on this topic has not been well researched. The main objective of the study described here was to investigate the general public's view of animal experiments. This examination was designed to address the following questions: current level of public knowledge about animals in research, current concern about this topic, the values influencing attitudes and assumptions, and the difference in people's response to arguments and information.

In general, questions of animal rights and the regulations for animal protection were discussed very emotionally. People being interviewed showed a lack of knowledge about the legal requirements for performing animal experiments. However, the prevailing tenor is that people are concerned because experiments may harm the animals. One of the main results of this study was the finding that both the opinion polls and the focus groups endorse animal experiments for medical purposes. In particular, if people were informed about the research goals, 71-75% of interviewees found animal experiments for biomedical research acceptable with some limitations, while 10-11% supported animal-based research on principle (EMNID '85). For the testing of pharmaceuticals, people accepted or even postulated animal testing models (more than 75%; EMNID '85, '86, '89).

In contrast to Germany, 2/3 of Britons disagreed that scientists should be allowed to conduct experiments on live animals. In both countries, the target groups and the experts criticised the lack of information flow in mainstream biomedical science with regard to the use of animals in research. In Germany, the public believed information coming from universities to be more credible than that coming from the pharmaceutical industry. The Britons trust animal welfare organisations more than either educational institutions or the pharmaceutical industry. The attitude of the German and the British population toward animal experiments is actually more positive than how it is described by the media. Sound information about the necessity of animal experiments for biomedical research is needed and it could influence the opinion of the public.

In Great Britain and Germany, the historical development of court decisions with regard to animal experimentation can be traced back for centuries. The existence of many animal welfare organisations and the presence of the subject of protection of animal rights in the media make it safe to assume that the population has significant interest in this topic and similar issues (1). It is important for the biomedical sciences to know what the position of the general population is with regard to questions involving animal experimentation for research purposes.

In order to present a clear picture, there were nine major quantitative studies conducted in Germany during the 80s and 90s, which were compared in a meta-analysis by independent polling institutes (UMBRA, Landau; ZUMA, Mannheim; 2). This analysis was accompanied by a so-called qualitative study, in which laypeople and experts were asked for their opinion on animal experiments (Sinus Sociovision GmbH, Heidelberg; 3). At the same time, MORIS (Market & Opinion Research International) carried out two similar studies (1999, 2002; 4-6) on behalf of *New Scientist* and the Medical Research Council in Great Britain. Here, too, the goal was to determine the motives behind public opinions on animal experimentation are and how these opinions are formed.

Both the quantitative studies and the direct survey made it clear that the topic of animal experimentation is an emotionally charged question in both countries. In UK, as many as 67% of those surveyed were fundamentally interested in this topic. Mainly newspaper articles and television coverage stimulate this interest. In Germany, discourse about this subject has been more or less avoided. In the 80s, about 30% had no concerns and 44 – 50% had few concerns with regard to animal experiments (EMNID). Both countries have in common that there is a

great deal of uncertainty with regard to the legal ramifications of animal experimentation. The survey of the German focus groups made it clear that respondents were not aware of the underlying legal circumstances for such experiments nor of the requirements involved in how the animals are housed and treated. In the EMNID surveys (1985 and 1986), about 50% of the respondents were not able to define their opinion on whether regulations for animal experiments should be changed within the framework of the German Animal Protection Act.

In Great Britain, more than 80% of the respondents admitted that they did not know the legal provisions regarding animal experimentation. At the same time, the Britons had little confidence in the competence of the public agencies involved—at least in 1999—and most were convinced that duplicated experiments were being carried out. In the 2002 survey, the negative attitude toward the reliability of the research was significantly revised and the interviewees evaluated the way that scientists handled the laboratory animals much more positively.

Regarding the question of whether using animals for research purposes is justifiable, the two countries differed substantially. The attitude of the Britons was considerably more negative than that of the Germans. In Great Britain, 64% of the interviewees opposed the use of animals unless there is a clear reason for the experiment. In Germany as well, having a specific reason for the experiment contributed significantly to a positive attitude on the part of respondents. Depending on the survey, the ratio of supporters is at over 70% (EMNID '85, '86) and at 50% (GFM GETAS '93) (7).

In both countries, animal experimentation within the purview of human or veterinary medicine was accepted to a substantially higher degree than for other sectors, such as quality assurance or testing for sensitivities for cosmetics. This makes it safe to assume that the desire for credible medical oversight is very high. Both countries have in common the desire for additional research and sponsorship of so-called alternative methods.

The current information deficit contributes to the general feeling of uncertainty when forming opinions on animal experimentation. In Great Britain, 65% of the interviewees admit the need for additional information about animal experiments for research purposes before they can form a final opinion about this topic. The lifestyle of the respondents, as well as the degree to which they were directly affected by illness in their immediate social environment, but also their gender

and their age were factors that influenced their opinions.

Regarding the question of who is perceived as a reliable source of information for animal experiments for research purposes, the two countries differed. In Germany, universities and other publicly sponsored research facilities enjoyed a good reputation, while the Britons had greater confidence in veterinarians and animal rights organisations as sources of information.

Literature:

- (1) Brunner P. (1995):Tierschutz in Deutschland und im Vereinigten Königreich; Diss. med. vet. München
- (2) Andritzky M. (1998): Pro und Kontra Tierversuche, einer Metaanalyse; durchgeführt von UMBRA Umfragen Beratung Analysen; Landau; im Auftrage von DFG und MPG
- (3) Anonym (1999): Summary zur Studie Tierexperimente; durchgeführt von Sinus Sociovision Heidelberg; im Auftrag von DFG und MPG
- (4) Anonym (1999): Attitudes towards experimentation on live animals; a quantitative survey among the general public; research study conducted for New Scientist by MORI
- (5) Anonym (1999):Animals in medicine and science; general public research conducted for the Medical Research Council by MORI
- (6) Anonym (2002):The use of animals in medical research conducted for the coalition for medical progress by MORI
- (7) Exner C., Heldmaier G. (2003): Die Einstellung der Bevölkerung zu Tierversuchen in der Forschung - ein Vergleich zwischen Großbritannien und Deutschland; Der Tierschutzbeauftragte 1/03; 39-42

Corresponding author

Dr Cornelia Exner

Dept of Biology, University of Marburg

Karl von Frisch Str. 6

35043 Marburg

exner@staff.uni-marburg.de

WOKW rats: an excellent animal model for the complete metabolic syndrome

Ingrid Klötting and Nora Klötting

Department of Laboratory Animal Science, Medical Faculty, University of Greifswald, Karlsburg, Germany

There is no doubt that along with profound changes in lifestyle, the modern society has brought an increased incidence of cardiovascular disease (CVD). About 17 million people throughout the world die every year from CVD according to the World Health Organisation. The metabolic syndrome including obesity, dyslipidemia, glucose intolerance or hyperglycemia, and hypertension appears to be a major, if not the main underlying problem of CV mortality (1).

Facets of the metabolic syndrome can also be observed in laboratory rats having been bred under an affluent environment for more than 200 generations. Comparing metabolic traits between males of 7 well-known inbred rat strains (BB/OK, BN/Crl, DA/K, F344/Crl, LEW/K, WKY/Crl, SHR/Mol), the Wistar Ottawa Karlsburg W (RT1^u) rat strain (WOKW) and progeny of wild rats (F2) captured in the northern part of Germany, it is clearly demonstrated that most traits studied are significantly elevated in inbred strains (cf. Fig.). Six out of 8 inbred rat strains were significantly heavier and characterised by significantly higher body mass index (BMI) than wild rats indicating an increase of fat deposit in these inbred strains. Serum insulin was significantly increased in 5 out of 8 whereas serum triglycerides were significantly higher in 2 out of 8 inbred rat strains compared with wild rats. In contrast, serum total cholesterol was significantly increased in all inbred strains compared with wild rat progeny. Comparing values of all inbred strains studied WOKW rats developed most metabolic alterations (2-4). A cross-sectional comparative study showed that WOKW rat begins to manifest the signs of the metabolic syndrome between 8 and 10 weeks of age (5). A longitudinal study of WOKW and disease-resistant DA rats up to an age of 17 months indicated that the facets of the metabolic syndrome were obviously pronounced in the course of lifetime (6). WOKW rats were characterised by increasing blood pressure, serum triglycerides and total cholesterol, BMI and serum leptin, impaired glucose tolerance, insulin resistance, proteinuria and impaired creatinine clearance. Especially the total protein excretion, which dramatically increased with age, similarly to blood pressure and serum lipids could be a hint proposing that WOKW rats have also a high risk of developing cardiovascular disease. This assumption is supported by studies in human, which have clearly

shown that already microalbuminuria is a strong predictor of cardiovascular morbidity and mortality in patients with impaired glucose tolerance and hypertension (7). Therefore, the dramatically increased proteinuria with age may suggest that WOKW rats also develop CVD. An assumption supported by our observation that about 30 per cent of WOKW rats at higher age (> 20 months) developed black tail ends diagnosed as *Gangraena sicca*. In addition, 20 per cent of WOKW rats died without macroscopical features and 80 per cent of WOKW rats must be killed because of their worse state of health. Examination of these rats showed marked alterations of liver and kidneys.

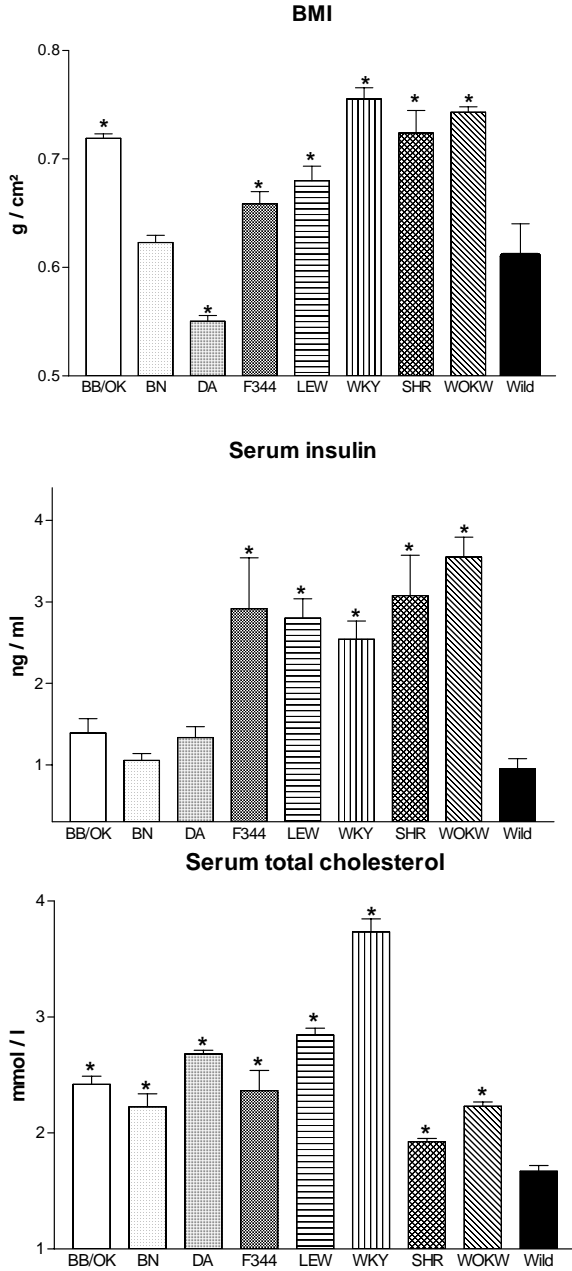
Genetic studies using (WOKW x DA)F₂ hybrid population clearly demonstrated that the metabolic syndrome in WOKW rats is under polygenic control. Male- or female-specific quantitative trait loci (QTLs) were mapped for body weight, body mass index, adiposity index and serum insulin on chromosomes 1 and 5, serum triglycerides on chromosomes 4, 7, 11 and 16, serum total and high density lipoprotein cholesterol on chromosomes 3, 4, 5, 10 and 17, serum leptin on chromosomes 8 and 16 as well as blood glucose and glucose tolerance on chromosomes 3, 4 and 17. QTLs for both, males and females were only found for body weight on chromosome 1 and for serum total cholesterol on chromosome 3 and 10. These findings clearly demonstrated that facets of the metabolic syndrome in WOKW rats are under polygenic control (8,9).

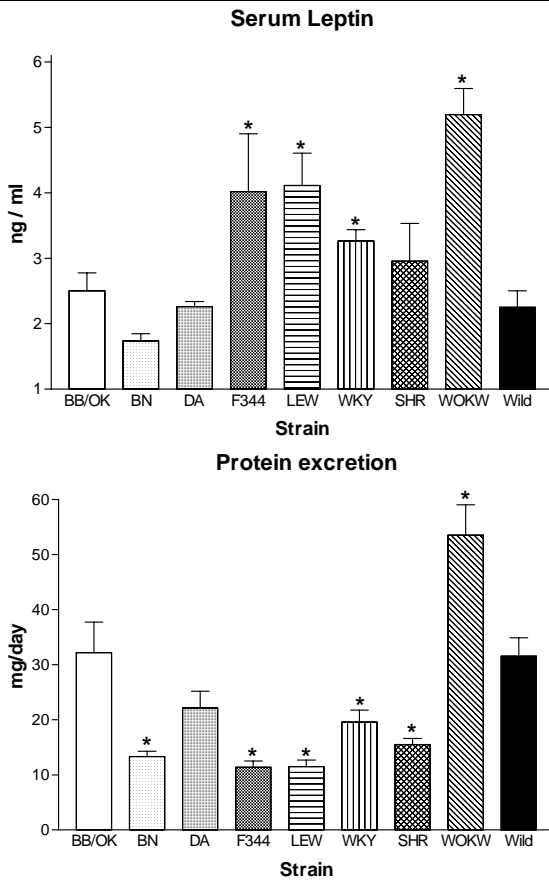
In accordance with the WHO proposal for components of the metabolic syndrome, the WOKW rat doubtlessly develops a complete metabolic syndrome characterised by increasing blood pressure (>160 mmHg), serum triglycerides (>4.5 mmol/l), BMI (> 0.9 g/cm²) and proteinuria (>300mg/day). Considering all phenotypic findings described until now and the fact that the metabolic syndrome in WOKW rats is polygenetically determined (2-5; 7-9) the WOKW rat is an excellent and unique animal model to study the pathophysiology of the facets of the syndrome. WOKW rat will not only help in advance our understanding of the syndrome but also assist the development and testing of new therapeutic strategies reducing the burden of the syndrome in human.

References

- 1 Ramos F, Baglivo HP, Ramirez AJ, Sanchez R. The metabolic syndrome and related cardiovascular risk. *Curr Hypertens Rep* 3, 2001,100-106.
- 2 van den Brandt J, Kovacs P, Klötting I. Blood pressure, heart rate and motor activity in 6 inbred rat strains and wild rats (*Rattus norvegicus*): A comparative study. *Exp Anim* 48, 1999, 235-240.
- 3 van den Brandt J, Kovacs P, Klötting I. Metabolic variability among disease resistant inbred rat strains and in comparison with wild rats (*Rattus norvegicus*). *Clin Exp Pharmacol Physiol* 27, 2000, 793-795.
- 4 van den Brandt J, Kovacs P, Klötting I. Metabolic features in disease-resistant as well as in hypertensive SHR and newly established obese Wistar Ottawa Karlsburg inbred rats. *Int J Obesity* 24, 2000, 1618-1616.
- 5 van den Brandt J, Kovacs P, Klötting I. Features of the metabolic syndrome in the spontaneously hypertriglyceridemic Wistar Ottawa Karlsburg W (RT haplotype) rat. *Metabolism* 49, 2000, 1140-1144.
- 6 Isomaa B, Almgren P, Tuomi T, Forsen B, Lahti K, Nissen M, Taskinen M, Groop L. Cardiovascular morbidity and mortality associated with the metabolic syndrome. *Diabetes Care* 24, 2001, 683-689.
- 7 van den Brandt J, Kovacs P, Klötting I. Metabolic syndrome and ageing in Wistar Ottawa Karlsburg W rats. *Int J Obesity* 26, 2002, 1-4.
- 8 Kovacs P, van den Brandt J, Klötting I. Genetic dissection of the syndrome X in the rat. *Biochem Biophys Res Commun* 269, 2000, 600-605.
- 9 Klötting I, Kovacs P, van den Brandt J. Sex-specific and sex-independent quantitative trait loci for facets of the metabolic syndrome. *Biochem Biophys Res Commun* 284, 2001, 150-156.

Figure 1: Body mass index (BMI), serum insulin, triglycerides and total cholesterol in males of 8 inbred rat strains compared with progeny of wild rats (Wild) at an age of 12 weeks





12 males per strain were studied. Data are given as mean \pm SD. * Significantly different from wild rats.

The proinflammatory cytokine interferon- γ induces chronic active myocarditis and cardiomyopathy in transgenic mice

S. Ott*, J. Löhler&, K. Yamamura# und K. Reifenberg§

Tierforschungszentrum, Universität Ulm(*); Heinrich Pette Institut, Hamburg(&), Institute of Molecular Embryology and Genetics, Kumamoto (#) und Zentrale Versuchstiereinrichtung, Mainz (§)

Dilated cardiomyopathy (DCM) causes a significant world-wide health problem since it represents a major cause of severe heart failure in young people and is the commonest indication for heart transplantation. Pathogenesis of this heart disease is poorly understood. It has been hypothesized that many cases of DCM represent a long term consequence of viral myocarditis. In the last years an interesting pathogenetic mechanism was developed of how progression from viral myocarditis to DCM may occur. It was speculated that viral infection of the heart musculature may not directly lead to cardiomyopathy but may trigger a chronic autoimmune reaction directed against cardiac structures culminating in the development of DCM. This theory was supported by a multitude of characteristic traits which could frequently be observed in patients with myocarditis / DCM and which are typical for autoimmune diseases. These autoimmune features include familial aggregation, association -albeit weak- with certain HLA molecules, abnormal expression of HLA class II on cardiac endothelium, and detection of organ-specific autoantibodies.

The suggested autoimmune mechanism of the transition from myocarditis to DCM received considerable support from experimental studies with laboratory animals. Susceptible mice can easily be infected with cardiotropic viruses such as coxsackievirus or encephalomyocarditis virus. These experimental infections of rodents clearly have demonstrated that the immunologic reactions elicited by cardiotropic viruses not always lead to viral clearance and healing of the cardiac injuries. Alternatively, inadequate immune reactions could be observed resulting in either viral persistence or autoimmunity. Very importantly, it was found that murine myocarditis could

also be triggering by mere immunization with cardiac myosin. The persistent cardiac immune or autoimmune reactions, triggered by infection of mice with cardiotropic virus, had the potential of inducing long-term tissue destruction leading to dilated cardiomyopathy.

Proinflammatory cytokines play an important role in the development of chronic inflammatory diseases and, thus, are likely candidates to be involved in the putative progression of human myocarditis to cardiomyopathy. The role of the proinflammatory cytokine interferon- γ (IFN γ) in the development of chronic myocarditis and cardiomyopathy is unclear. At early phases of virus-induced or immunization-mediated murine myocarditis IFN γ was shown to exhibit a protective function. However, at later stages of coxsackievirus induced murine myocarditis, IFN γ was found to exert additional detrimental effects on heart disease.

The aim of the present study was to investigate the role of IFN γ in the development of chronic myocarditis and the potential transition process of myocarditis to cardiomyopathy. To this aim we used the murine strain SAP-IFN γ which constitutively expresses IFN γ in the liver and develops chronic active hepatitis. Hepatic IFN γ synthesis of the SAP-IFN γ mice is such intensive that the cytokine can be detected in the serum of transgenic mice by birth. Permanent IFN γ serum expression of SAP-IFN γ mice enabled us to investigate whether this cytokine may induce pathologic processes in the murine heart.

To our surprise, we found that the SAP-IFN γ mice spontaneously develop chronic active myocarditis and cardiomyopathy. The first morphological alterations in the myocardium of SAP-IFN γ transgenic mice indicating the onset of chronic myocarditis and cardiomyopathy were represented by scattered cardiomyocytes with a homogeneous hypereosinophilic cytoplasm and condensed hyperchromatic nuclei. In close spatial association with decaying cardiomyocytes a few phagocytically active macrophages and single lymphocytes can be recognized. Alternatively, necrotic cardiomyocytes showed a globular/floccular degeneration of the sarcoplasm in combination with cytoplasmic vacuolization. With progression of the disease process the myocytolyses which were predominantly located in the subepicardial ventricular myocardium and in the muscular septum became more apparent together with a loose, interstitial mononuclear infiltrate. At this stage of the disease process the tissue got an edematous appearance. During the more advanced stages, the interstitial and perivascular connective tissue was moderately increased and the walls of the ventricular branches of the coronary blood vessels were thickened and occasionally calcified.

The proinflammatory cytokine interferon- γ induces chronic active myocarditis and cardiomyopathy in transgenic mice

Continuous destruction of cardiomyocytes evoked in a portion of the mutant mice a focal, compensatory, and transient hypertrophic change of the cardiac muscle tissue as evidenced by the appearance of hypertrophic cardiomyocytes with typical nuclear signs such as enlargement and hyperchromasia but ultimately resulted in the atrophy of the heart musculature, morphologically characterized by rarefaction and considerable variation in the diameters of the cardiac muscle fibers. In the final stage, the outcome of SAP-IFN γ transgenic mice suffering from chronic cardiomyopathy and myocarditis was fatal and the cause of death could be determined by global heart failure which morphologically was best documented by the appearance of typical alterations of the liver namely, centrilobular, perivenular dilation of sinusoids caused by venous congestion, atrophy of hepatocytic trabecules and centrilobular fatty change of hepatocytes.

Our data indicate that the proinflammatory cytokine IFN γ is able to induce chronic active myocarditis and cardiomyopathy in the *in vivo* model of transgenic mice. The pathogenic mechanism mediated by IFN γ is characterized by a high degree of tissue specificity, since other organs in particular smooth and cross striated muscle cells did not exhibit comparable alterations. In the future we will try to further analyze the mechanism underlying the development of myocarditis and cardiomyopathy in SAP-IFN γ transgenic mice.

Genetics of the Metabolic Syndrome in NZO Mice

R. Kluge, M. Grothe, S. Scherneck, K. Schmolz, K. Giesen, L. Plum, H.G. Joost

German Institute of Human Nutrition, Potsdam-Rehbrücke

Introduction

The so-called ‘metabolic syndrome’ represents one of the most important risk factors for cardiovascular diseases in humans. It is a complex of interacting single traits, e.g. obesity, insulin resistance, high blood pressure and diabetes. The phenotype is known to be significantly influenced by the genetic background. However, most of the underlying genes are still unknown as well as the mode of interactions between the responsible genes and the environment. Applying the mouse model described below we want to contribute to the knowledge of the genetic basis of this important and complex syndrome. The mouse strain NZO (New Zealand obese) exhibits a polygenic complex of obesity, insulin resistance and diabetes resembling the human syndrome. Thus, it seems to be a good model for identification of the genes responsible for aberrations of body weight and fattening regulation. In addition, NZO mice have been used to characterize the interaction between obesity and diabetes (diabesity). Establishing a backcross of NZO with lean SJL mice (resistant to enhanced dietary fat) we were able to identify several chromosomal segments containing QTL (quantitative trait loci) which seem to affect traits of the metabolic syndrome. It could be shown that the fat content of diet significantly enhanced these effects. Furthermore, recombinant congenic inbred strains (Demant and Hart, 1986) are in progress harbouring different segments of the QTL. By this breeding method a fine mapping of genes seems possible in addition to sequencing and candidate gene search.

Materials and methods

NZO/H1Bom and SJL/NBom inbred mice were originally obtained from Bomholtgard (Taconic), Ry, Denmark. With female SJL and male NZO an F1 generation was set up which was backcrossed to NZO using inbred females and F1 males. After weaning with 3 weeks of age two types of diets were provided to the backcross mice. One group received a standard maintaining diet with 4% of crude fat and 50.5% carbohydrates, the other group was fed with a diet of 17% of fat (sunflower oil) and 46.8% carbohydrates (C 1057). Both diets were from Altromin (Lage, Germany). Food and water were given ad lib. After weaning, the

mice were kept as full sib groups separated according to sex in Macrolon cages (type III) in a temperature controlled room (21 ± 1 °C; $55 \pm 5\%$ relative humidity) with a 12 hrs light-dark cycle and lights on at 6:00 a.m. Animals were killed at an age of 22 weeks in isoflurane anaesthesia collecting blood by heart puncture and subsequent cervical dislocation.

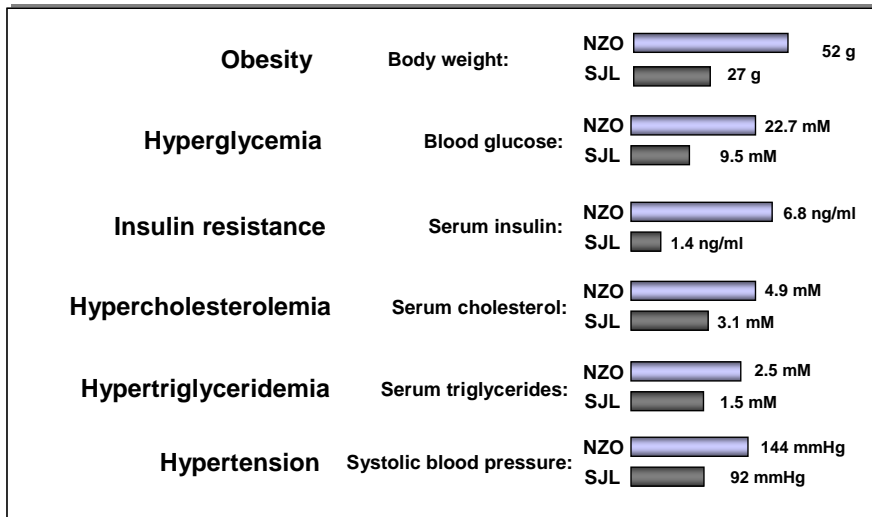


Fig. 1 Characters of the metabolic syndrome compared between male obese NZO and lean SJL mice

Body weight and body composition were measured once a week during the whole observation period up to 22 weeks. Body length was measured once after bleeding the anaesthetized mice fixing the animals on millimetre scale paper. The body mass index (BMI) could thus be calculated to include the relation body weight to body length ($BMI = \text{body weight [g]} / \text{body length [cm]}^2$). The development of body fat and muscle was observed using nuclear magnetic resonance tomography (Minispec Bruker, USA). The weekly blood glucose was obtained by glucose sticks (Glucometer ELITE, Bayer, Germany). Serum cholesterol and triglyceride concentrations were measured by an auto-analyser (Johnson & Johnson, Neckargemünd, Germany). Insulin values were obtained from serum by radioimmunoassay (Amersham-Pharmacia, Freiburg, Germany) with anti-rat insulin antiserum and ^{125}I -labelled rat insulin as tracer. Free and bound radioactivity was separated with an anti-IgG antibody.

DNA was prepared from mouse tail tips with a DNA isolation kit (InViTek, Berlin, Germany) based on a salt precipitation method. In an initial genome wide scan 109 polymorphic microsatellite markers were genotyped applying PCR.

A QTL analysis was done using the program Mapmaker/QTL 1.1 (Lincoln et al, 1992) after construction of the genetic map with Mapmaker/EXP 3.0 (Lincoln et al, 1992a).

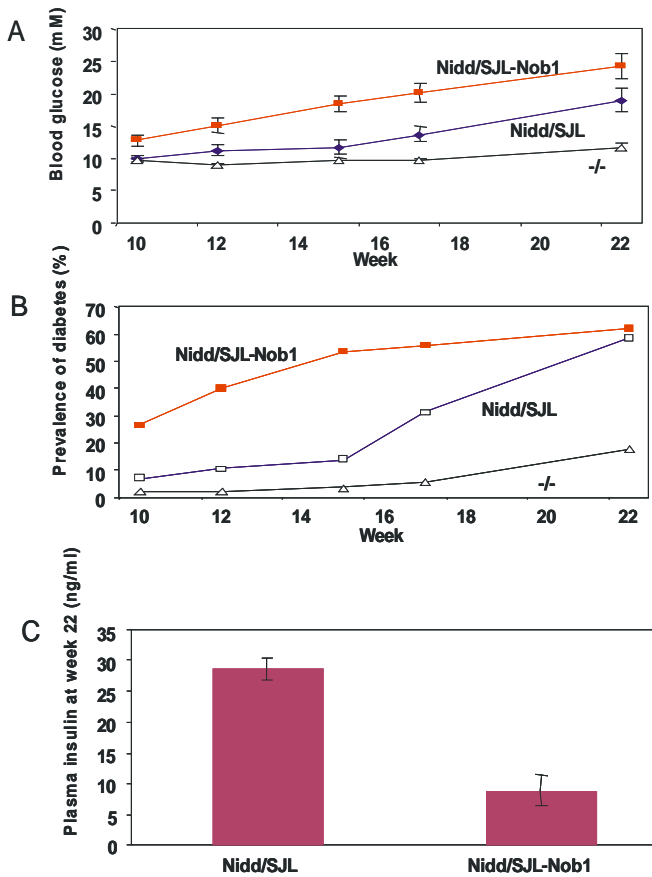


Fig. 2 Hyperglycaemia and hypoinsulinaemia in male backcross *Nidd/SJL* carriers

Results and discussion

In the backcross with NZO, a total of 199 male mice were raised on the high fat diet. At week 17, 30.5% of them exhibited severe hyperglycaemia (blood glucose > 16 mmol/l) and at week 22, 44% were diabetic. Body weights of diabetic and non-diabetic animals developed differently: being identical at week 4 (means: 13.6 vs. 13.1 g), the body weights of diabetic animals were significantly higher at later ages: at week 10, the difference was 4.3 g and at week 14 5.7 g. In addition, there was a significant difference in the serum insulin level at week 10, which was 13.1 ng/ml in diabetic mice compared to 5.4 ng/ml in non-diabetics. However, at

week 22 the levels of both groups were comparable, indicating that the pancreas could not longer compensate for the severe hyperglycaemia at this time (mean blood sugar 26.8 vs. 10.1 mmol/l). Fig. 1 shows the characters of the metabolic syndrome compared between the NZO and the lean SJL strain.

The QTL analysis revealed several chromosomal regions showing a linkage disequilibrium with characters of diabetes and body fattening. The three most important will be described here.

On chromosome 4 with a maximum between the markers D4Mit278 and D4Mit203 a region was identified which was strongly correlated (LOD score > 10) with the onset and time course of diabetes and islet cell loss, as well as resulting consequences as hypoinsulinaemia (Fig. 2) and loss of body weight (Plum et al., 2002). This QTL was obviously contributed by the lean SJL strain since animals were affected which were heterozygous at the relevant markers whereas the mice homozygous NZO type became diabetic much later (Fig. 2A). The effect of the aberrant *Nidd/SJL* allele is only visible in mice with an early high body weight (BW > 45 g in week 12). In these animals the variant accounts for more than 70% of the diabetes prevalence.

On chromosome 5 at D5Mit392 the genome scan revealed the existence of a QTL, which was called *Nob1*, originating from NZO and responsible for characters of body fattening (LOD scores 3.8). Its effects could be only assured applying the high fat diet (Kluge et al., 2000). More important than the separate effects is the interaction between *Nob1* and *Nidd/SJL* which results in a markedly enhanced diabetes prevalence and an accelerated time course of diabetes (Fig. 3). Distal to *Nob1* a susceptibility locus for hypercholesterolaemia was identified also on chromosome 5 (Giesen et al., 2003). The maximum LOD score for this QTL called *Chol1/NZO* was 14.5 in the backcross population. Plasma cholesterol levels were significantly elevated in both genders homozygous for *Chol1/NZO*. The allele showed no association with body weight, serum insulin, or hyperglycaemia. The high fat diet increased the serum cholesterol levels but did not alter the absolute effect of this QTL (mean values and SEM of males fed on standard diet vs. males on high fat diet: 4.2 ± 0.7 vs. 4.9 ± 1.1 mmol).

For fine mapping of the responsible QTL regions and subsequent gene identification several approaches are in progress now. In addition to sequencing of possibly relevant genes of the peak regions and expression analysis of candidate genes recombinant congenic mouse strains (RCS) are established for *Nidd/SJL* and *Nob1*. Recombinant genotypes of the QTL segments are fixed by inbreeding after a limited number of backcrosses to reduce the background

variation. *Nidd/SJL* components are transferred to C57BL/6 whereas *Nob1* recombinants are crossed to the closest relative of NZO, the non diabetic NZB

strain. Preliminary results of the RCS show the successful breeding transfer of the different QTL elements contributing significantly to the precise fine mapping of

the relevant gene regions. However, it also became obvious that 10 – 15 RCS are required to be really successful. The definite number depends on the size of the QTL, its effects, and the influence of the background. These characters also affect the number of animals which is required within each RCS. That may vary between 50 – 100 mice.

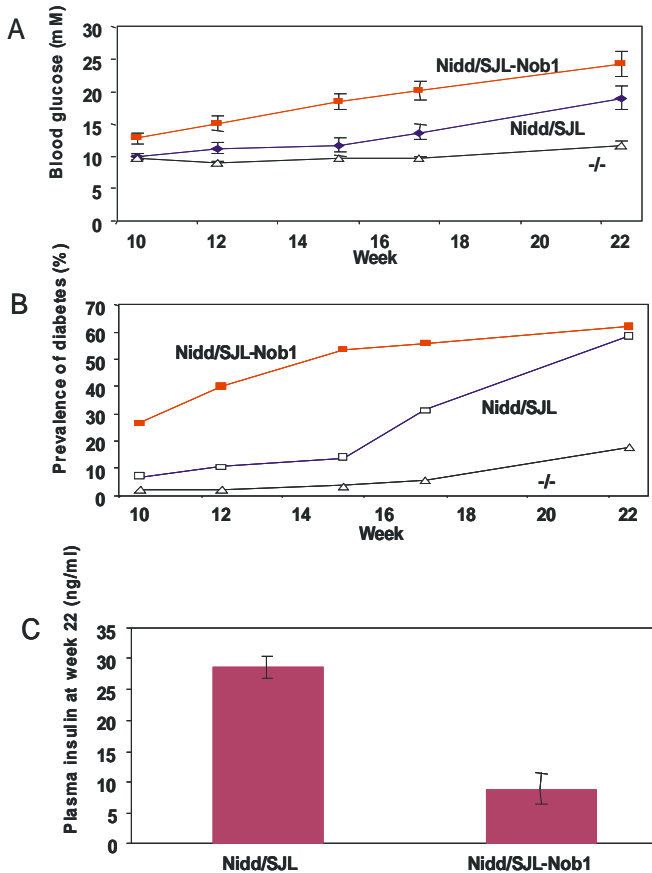


Fig. 3 Interaction between *Nidd/SJL* and *NOB1* alleles in blood glucose, diabetes prevalence and plasma insulin

References:

- Demant, P and AAM Hart (1986): Recombinant congenic strains – a new tool for analysing genetic traits determined by more than one gene. *Immunogenetics* 24: 416 – 422.
- Giesen K, L Plum, R Kluge, J Ortlepp, HG Joost (2003): Diet dependent obesity and hypercholesterolemia in the New Zealand obese mouse: identification of a quantitative trait locus for elevated serum cholesterol on the distal mouse chromosome 5. *Biochem Biophys Res Comm* 304: 812 – 817.
- Kluge R, L Plum, G Bahrenberg, K Giesen, JR Ortlepp, HG Joost (2000): Two quantitative trait loci for obesity and insulin resistance (Nob1, Nob2) in New Zealand obese (NZO) mice and their interaction with the leptin receptor allele (*Lepr*^{A720T/T1044I}) of NZO. *Diabetologia* 43: 1565 - 1572.
- Lincoln S, Daly M, Lander E (1992): Mapping genes controlling quantitative traits with Mapmaker/QTL 1.1. Whitehead Institute Technical Report, 2nd ed.
- Lincoln S, Daly M, Lander E (1992a): Constructing genetic maps with Mapmaker/EXP 3.0. Whitehead Institute Technical Report, 3rd ed.
- Plum L, K Giesen, R Kluge, E Junger, K Linnartz, A Schürmann, W Becker, HG Joost (2002): Characterization of the mouse diabetes susceptibility locus Nidd/SJL: islet cell destruction, interaction with the obesity QTL Nob1, and effect of dietary fat. *Diabetologia* 45: 823 - 830.

Differences of pathogenicity of *Pasteurella pneumotropica* biotypes

H. Meyer, S. Ott

Tierforschungszentrum, Universität Ulm

Pasteurella pneumotropica, a gram-negative opportunistic pathogen, is often present in conventional as well as barrier maintained colonies of mice, rats, hamster and guinea pig. The bacterium is detected in urogenital tract, oral cavity, pharynx and conjunctivitis with different prevalence. Its role as primary pathogenic bacterium is uncertain. Yet, it is an important opportunistic or secondary causative organism of conjunctivitis, otitis, uterine infection, dacryoadenitis, panophthalmitis and abscesses of the bulbourethral glands.

Pasteurella pneumotropica (P.p) is isolated by routine monitoring of animals from one of our facilities as well as in examinations of sick animals. These animal facility is a simple dry barrier, that means only fresh coats and overshoes are worn. Users may enter freely this area. Newly arrived animals are imported into the facility if a hygiene declaration is provided or our own examinations permit this act.

P.p is found in rodents in two easily distinguishable biotypes. We use biochemical features as well as molecular biological methods of differentiation like PCR with genus and species specific primers. Both biotypes are easily differentiated by digestion of the PCR products with restriction enzymes. We prefer Taq I because both biotypes could easily differentiated by the digestion pattern of the PCR products obtained by this restriction enzyme.

Significant differences were observed in the ratio of both biotypes when the bacteria were isolated from different sources of the animal facility. One hundred twenty-two P.p. isolates were detected in routine examinations of 460 animals during the last three years. Out of these isolates 70% belong to the biotype Jawetz and 30% belong to the biotype Heyl. Also in other animals that we examined for other reasons like tumors, leukemia, nephritis, *Pneumocystis carinii* infection etc, we detected 60% of biotype Jawetz and 40% of biotype Heyl. Thus, we obtained a similar distribution of biotypes in both cases. However, a reversed distribution of both biotypes was obtained when P.p. was isolated in

pure culture from organs of infected animals (sepsis, pneumonia, uterine infection, etc). In these cases, 69% biotype Heyl and 31% biotype Jawetz were identified.

Abscess formation are the most important disease caused by P.p. In these cases, Heyl was the predominant biotype. In addition, we found only the biotype Heyl in orbital abscesses that are typical of P.p infections. This finding is remarkable because we determined in conjunctivitis a twofold surplus of biotype Jawetz over biotype Heyl.

Alterations are observed by bacteriological investigations of colonies during the last three years. In routine examinations and bacteriological investigations of sick animals, we found similar ratios of biotype Jawetz to biotype Heyl but increasing numbers of P.p.: in 2000 (17%:12%), in 2001 (24%:22%) and in 2002 (36%:25%), respectively. The *Pasteurella* isolates from sick animals increased significantly up to 34% during the year 2003.

Biotype Jawetz occurred increasingly in routine examinations during the last years. This biotype was also frequently found in sick animals. A significant alteration, however, is observed in 2003. Until now 75% of the isolates from sick animals belong to biotype Heyl.

More abscesses were observed during the last few years as well as P.p cases. Abscesses caused by distinct bacteria remained constant. This is also true for abscesses of biotype Jawetz. Thus, the increasing number of abscesses in animals is due to the increasing number of cases caused by biotype Heyl. This fact is illustrated by the following example.

In 2001 no case of orbital abscess was monitored in our rodent population. The first orbital abscesses were detected in 2002. This number of cases increased dramatically during this year. All of the cases were caused by biotype Heyl and most of them were observed by a single transgenic mouse strain. A special correlation becomes obvious when these orbital abscesses were analyzed on a time scale.

In March 2002 the new line was settle in the animal facility. The first animal with orbital abscess was detected in June 2002, a second one in September 2002. Thereafter an increasing number of cases were observed: In January 5 mice and in February 2 additional ones. During March two mice of another line fall ill next door to the original room. Also in May, June, and July additional animals with

orbital abscesses were found.

Discussion: The prevalence of biotype Heyl with orbital infections are well known. Artwohl et. al (2000) found exclusively orbital abscesses caused by this biotype in a transgenic line with immune defect. Two possibilities might be discussed for the sudden increase of these special infections.

The newly settled animal line was tested positive for P.p. before it was put into the animal facility. We were able to determine both P-biotypes in these animals. Therefore, these animals could kept together only with the P.p. contaminated colony. It might be possible that a new Past. strain was introduced. This is in accordance with the observed abscesses in the orbita, which was diagnosed in this line for a long while ago. The description of the transgenic features does not indicate any immunodeficiency of the animals.

It might be possible that the observed P. strain is a new one with special virulence. This idea is supported by the fact that orbital infections occurred also in other mouse lines, which were kept in other rooms. Two of these mice belong to a line with known immunodeficiencies, while another mouse belongs to a line without any known immunodeficiency.

P.p is routinely isolated from this part of the animal facility. Orbital infections have not been observed until 2002, although several tribes with diverse immunodeficiencies were reared in this animal colony. For this reason, an infection of the new line by the ordinary P.-strain seems unlikely.

Thus, we will investigate a possible virulence factor and we will analyze for possible immunodeficiencies in cooperation with the user of that particular mouse strain.

Health monitoring results obtained from mice and rats from commercial breeders

Werner Nicklas

Microbiological Diagnostic, German Cancer Research Centre, Heidelberg

Health reports are an essential prerequisite to evaluate the infectious status of an animal population. They represent an important management aid and are the basis for many fundamental decisions. While it is sometimes difficult to get results of comprehensive health monitoring from experimental colonies, health reports indicating careful testing are supplied by commercial breeders.

We occasionally check mice and rats from commercial breeders to evaluate their status. We usually order 5 animals of a certain strain at an age of 10 weeks or older (or ex-breeders) from a specific breeding unit. Immediately upon receipt, animals are transferred to our diagnostic laboratory in the transportation boxes. For capacity reasons, only 3 animals of a shipment are submitted to complete health monitoring including necropsy, bacteriology, serology, parasitology, and PCR testing. The remaining 2 animals are tested only by serology. In detail, animals are bled from the retroorbital sinus under anaesthesia with CO₂ and subsequently euthanised by CO₂. Samples from the fur and skin scrapings are tested for ectoparasites under the binocular and by microscopy at a low magnification. Monitoring for endoparasites is conducted by cellophane tape, flotation of faecal pellets, and by microscopy of wet mounts of intestinal contents (duodenum and caecum). Samples from various locations [nasal cavity, nasopharynx, trachea, lungs, kidney, uterus, vagina (or prepuce in males), duodenum and caecum] are streaked on several non-selective and selective media for bacterial culture. PCR is regularly conducted from caecal contents to detect *Helicobacter* sp. and from lungs of immunodeficient animals to monitor for *Pneumocystis carinii*. Additional samples are taken and monitored (including histopathology) if lesions or abnormalities are observed. Serologic monitoring is conducted by ELISA, IFA and HI for viruses as suggested in the FELASA recommendations (2002) and additionally for several bacterial antigens. Positive or questionable serological results are confirmed by one or more confirmatory methods and by at least one external laboratory. From January 2001 until September 2003, altogether 320 mice and 120 rats from 14 different breeding units were tested.

Our results confirmed in most cases the data given on health reports from the commercial breeders. In the majority of breeding units, agents were not detected for which monitoring is recommended by FELASA, or, agents for which a population was declared positive in the breeder's health report (e.g., *Helicobacter*), were also detected in our laboratory.

In general, agreement was very good between the breeder's health report and our results for serology. Antibodies to viral pathogens or *Mycoplasma (M.) pulmonis* and *M. arthritis* were not found. However, we found antibodies to *Clostridium piliforme* in 1 of 5 rat breeding units by IFA and by a commercial ELISA, and our results were also confirmed by two external laboratories. However, we never observed clinical signs in these animals and could not detect the agent by PCR in serologically positive animals nor in nude rats which had been used as sentinels. Parasitological testing revealed intestinal flagellates in two units and entamoebae in one unit although these units were declared negative in the breeder's health report. Other parasites were not detected.

Bacterial culture more frequently led to contradictory results. *Bordetella bronchiseptica* was isolated from the lungs and the trachea of a nude rat. *Pseudomonas aeruginosa* was repeatedly found in animals from 3 breeding units. Beta-haemolytic *Streptococci (Sc.)* serogroup G (*Sc. dysgalactiae* subsp. *equisimilis*) were repeatedly cultured from nude rats. *Streptococci* serogroup B (*Sc. agalactiae*) were cultured from various organs of immunodeficient and immunocompetent mice and rats purchased from several breeding units including isolators.

Sc. pneumoniae was repeatedly found in nasal cavities of rats from 1 breeding unit during a period of 6 months. The diagnosis was confirmed by the National Reference Centre for *Streptococci*, and the isolates were typed as serotype 14. In the same breeding unit all rats that were cultured between October 2002 and September 2003 were positive for *Pasteurella pneumotropica*. Rats in this breeding unit were positive for a number of opportunistic pathogens such as *Helicobacter*, *Pneumocystis carinii*, *Pasteurella pneumotropica*, *Pseudomonas aeruginosa*, *Sc. pneumoniae*, and *Haemophilus parainfluenzae*. *Haemophilus sp.* was found in the majority of rat breeding units and was also isolated from mice, primarily from the lungs and the trachea. These bacteria are not cultured by the majority of diagnostic laboratories although it is suggested by FELASA that mice and rats are monitored for all *Pasteurellaceae*.

In some cases negative results for unwanted agents were confirmed. However, finding of a large variety of different *Enterobacteriaceae* and environmental

organism such as Bacilli or Acinetobacter in nod-scid mice are unexpected as such animals are bred in isolators. Presence of such a diversity of bacteria should be considered an indicator of insufficient hygiene procedures or management failures.

Our results show that agreement between results from our laboratory and the information given on health reports was very good for serology and PCR testing. Both are easy to standardise and lead to objective results if appropriate methods are applied. Serum samples or DNA can easily be shipped to other laboratories for retesting or confirmation. We also found little disagreement in parasitology although two different protozoans were found that were not mentioned in health reports. However, the large variety of opportunistic bacterial pathogens was unexpected in animals purchased from commercial breeders. Compared to routine health monitoring that was conducted by the breeder we tested much smaller numbers of animals but frequently found agents for which animals were declared negative in the health report. Unwanted agents were also found in immunodeficient mice and rats bred in isolators. In contrast to serology and PCR, bacterial culture is frequently considered less important. In addition, bacteriology requires whole animals, is expensive, time consuming, and the results are dependent on various factors such as the media used, organs cultured, culture conditions, incubation periods, and the methods used for bacterial identification. In general, bacterial culture is more difficult to standardise, and there is a higher likelihood of variation in the results compared to serology or PCR.

It is not clear if the agents were not detected in the breeders' laboratories or if they are considered unimportant and are therefore not mentioned. The agents found in animals upon receipt from the breeder are of low pathogenicity, and there is very little published evidence of impact of these agents on research results. They may be acceptable in a breeding population, but they occasionally cause severe problems in a research facility. In experimental units, immunocompetent and immunodeficient animals may be housed together. They may receive immunosuppressive treatment such as drugs or irradiation and are sometimes housed for longer periods of time which may lead to exacerbation of microorganisms with a low pathogenicity. It would, therefore, be desirable that breeders supply information on the presence or absence of microorganisms in a breeding population even if they are classified as secondary or weak pathogens by the breeder.

References

FELASA recommendations for the health monitoring of rodent and rabbit colonies in breeding and experimental units (2002). *Lab. Anim.* 36, 20-42.

Address: Dr. Werner Nicklas, DipECLAM
Microbiological Diagnostic German Cancer Research Centre
Im Neuenheimer Feld 280 69120 Heidelberg

The sheep as a chronic animal model for the long-term test of left ventricular assist device

C Ballat, H. Alekuzei, K. Steinke, J. Schmitto, H. Doerge, F Schoendube

Thoracic and Cardiovascular Surgery, Georg August University Goettingen

Sheep are comparable to the human being with their size and weight as well as the heart-circuit-physiology and are used as experimental animals because of their calm behaviour (postoperative care) in case of chronic experiments. Within a clinical certification test over 7 days a left ventricular assist device was implanted into sheep.

Methods and results: First the animals were premedicated with xylazin and ketamin i.m., intubated and mechanically ventilated. A stomach tube was placed. Anesthesia was maintained by fentanyl i.v. and isofluran. One catheter was placed in the left carotid artery and another in the left jugular vein. Both were led subcutaneously to the withers and there through the skin to be connected to the monitoring system for intra- and postoperative continuous blood pressure measurement and blood gas analysis and for volume substitution and systemic anticoagulation. After lateral thoracotomy a heparin-bolus (5000 IE/animal) was given for anticoagulation. The aorta and the left atrium were cannulated and further 5000 IE heparin were applied to each cannula. The cannulas were connected with the pump and the pump was started. After insertion of a thoracic drainage and wound closure the animals were placed into a special cage in which they awoke and also were monitored in the following days. Place to lying and standing was available to the animals sufficiently while turning around of the animal was being prevented by an adjustable sidewall. The further monitoring occurred by regular control of the general condition and the blood values as well as a video camera which decreased the stress of the animals. The sheep received a cephalosporin as an antibiotic over a period of 5 days. A sufficient analgesia is necessary in order to minimize postoperative pain causing respiratory depression as well as improve the general condition and food intake. Buprenorphin, carprofen or flunixin-meglumin for at least 3 days was given to the animals, if required also longer. The anticoagulation was maintained by continuous infusion of a heparin-solution (100 IE heparin/ml saline) under control of the ACT (Activated Clotting Time). Some animals received additionally acetylsalicylic acid once daily. As only few dates to the coagulation system and different information

on the anticoagulation of the sheep are available in the literature, adaptations were carried out in the experimental process in the target values of anticoagulation, the anticoagulants used and their dosage, to minimize haemorrhagic complications on the one hand and blood clotting on the other hand.

Conclusion: The sheep is suitable for the test of left ventricular assist device as a chronic animal model. Further investigations concerning height and application kind of the anticoagulation need to be done to achieve a firm anticoagulation also for a longer time.

Reconstitution of immunodeficient mice

Beuter, C., Stauffer, U., Kwiatkowski, H., Joswig, N., Mossmann, H.

Max-Planck Institute for Immunobiology, Freiburg, Germany

The breeding and maintaining of immunodeficient mice is often hampered by the weak constitution of the breeders, even in an SPF-area. Because of their incapability to overcome infections with more or less ubiquitous microorganisms, also the experimental results are very likely to be inconsistent. Therefore, the aim should be to have these lines in a germfree/gnotobiotic status. Because this procedure is very time-consuming, problems may arise in the meantime to keep these strains alive and to expand the stocks for the transfer. Special breeding regiments and the application of antibiotics may be helpful, but in our hands the best method was the reconstitution with immunocompetent cells. In the experiments to be described, various ways of reconstitution were tested, especially in the *RAG- γ c strain being devoid of B-, T-, and Nk-cells. To prevent graft versus host reaction, F1 hybrids with the wildtype-strain were used as donors for spleen, lymph node and bone marrow cells. From the various populations, 5×10^6 to 2×10^7 cells were injected intraperitoneally or intravenously. After 6 weeks, the distribution of the infected cells or their progeny was analyzed by *FACS in various organs. In preliminary experiments, the resistance to an infection with *Trypanosoma cruzi* was evaluated. In addition to these detailed examinations, we had the strong impression, that reconstituted breeders represent an improved constitution and an augmented reproductive potential. This was an enormous help for the transfer into the appropriate hygienic status.

*Abbreviations: RAG: rearrangement antigen (knock-out), FACS: immunofluorescent-activated cell sorting.

Key words: Immunodeficient mouse strains, reconstitution, RAG- γ c

4 Major candidate genes for experimental IBD identified by microarray analysis in combination with quantitative trait locus (QTL) mapping data in IL-10-deficient mice

André Bleich, Medical¹, Jörg Lauber², Jan Buer², Hans Hedrich¹, Michael Mähler¹

¹ Medical School Hannover, Hannover, Germany; ² German Research Centre for Biotechnology, Braunschweig, Germany

Background & Aim: Interleukin-10-deficient (*Il10*^{tm1Cgn}) mice serve as a model for human inflammatory bowel disease (IBD). The severity of colitis depends on the genetic background strain carrying the disrupted *Il10* gene: C3H/HeJBir-*Il10*^{tm1Cgn} mice develop severe colitis, while C57BL/6J-*Il10*^{tm1Cgn} mice are colitis-resistant. Two previous studies reported 10 QTLs associated with colitis susceptibility in these strains. The aim of this study was to identify candidate genes within the QTL intervals, which likely contribute to colitis susceptibility. Therefore, we analyzed gene expression patterns in colonic tissue of both strains and combined the results with previous QTL mapping data. **Methods:** Microarray analyses were performed by using Affymetrix GeneChip technology. Total RNA was isolated from colonic tissue of 4-week-old C3H/HeJBir- and C57BL/6J-*Il10*^{tm1Cgn} mice (before onset of colitis) as well as C3H/HeJBir and C57BL/6J wildtype mice. In each of the four groups, RNA extracted from five colons was pooled. Expression was filtered using the following threshold values: signal difference >40, change fold >2.0, change p-values >0.99 and <0.01 respectively; for some genes change fold was >1.5, signal difference >200 and change p values >0.99 and <0.01. **Results:** 651 genes were differentially expressed between colitis-susceptible C3H/HeJBir-*Il10*^{tm1Cgn} and colitis-resistant C57BL/6J-*Il10*^{tm1Cgn} mice, 134 of them were located within the 10 QTL intervals. 42 of these 134 genes represent attractive candidate genes because of their known role in immune and defense responses. Expression of the 42 candidate genes was compared in all four groups of mice (both wt and both IL10 KO strains). Four of these genes (*Pla2a*, *Gbp1*, *Cd14*, *Vdr*) showed more prominent expression levels in the IL10 KO mice than in the WT mice and were considered to be the major candidate genes. **Conclusion:** Using a combination of QTL analysis with microarrays, we were able

4 Major candidate genes for experimental IBD identified by microarray analysis in combination with quantitative trait locus

to identify 42 likely candidate genes, and 4 major candidate genes which may contribute to colitis susceptibility in the *I110^{mlCgn}* mouse model. Expression differences of the candidate genes have to be confirmed by realtime PCR before conducting sequence analyses and functional assays to determine their relevance to colitis susceptibility.

Health problems in South African Clawed Frogs (*Xenopus laevis*): Pathological, microbiological, and parasitological findings

Ines Bolle & Gero Hilken

Central Animal Laboratory, University of Duisburg-Essen Medical School,
Hufelandstraße 55, 45122 Essen

Xenopus frogs are used to obtain oocytes in our facility. They are kept in aquaria (73 cm x 57 cm x 25 cm) with a water level of 7 cm and 7 litre water per frog. The water is changed daily, the water temperature is adjusted to 21°C. Frogs are offered in turn bovine heard, *Xenopus*-pellets (Provimi Kliba AG) and earthworms. Animals are obtained as captive bred frogs from German, American, and South African breeders. 241 autopsies were performed when animals were moribund or died spontaneously (223 females, 18 males).

The pathology showed that all frogs were wild caught or that captive bred animals have contacted wild caught clawed frogs. The causes of diseases and death could be assigned to five different categories:

- a) Bacterial infections (34,1%): Septicaemia, oedema, and red-leg-disease caused by infections with *Aeromonas hydrophila*, *Citrobacter freundii*-complex, *Enterobacter* sp., and *Actinobacter* sp.;
- b) Organ alteration (29,1%): Hyperplasia of the liver, spleen, and the kidney, fatty liver, neoplasms of the liver or spleen, intestinal invaginations;
- c) Parasites (4,5%): Nematoda: *Capillaria xenopodis* (skin), *Spinicauda* sp., Cestoda: *Cephalochlamys namaquensis* (rectum), Protozoa: *Nyctotherrus xenopodis*, *Balantidium* sp., *Protoopalina* sp., *Typhlonectes* sp., *Trichomonas* sp.(intestinum);
- d) Injuries caused by husbandry or shipment (2,6%): Abrasions, dehydration, inflammation after transponder implantation;
- e) Autolysis or unclear cases of death (29,7%).

The reason of bacterial infections might come from purchased animals themselves or from the earthworms which were fed to the animals. All investigated frogs were infested with several parasites, however, the lethal cause of these parasites occurred only in 2.5%. The cestod *C. namaquensis* was introduced in our facility by frogs from South Africa, where this parasite could be found in the natural habitat of the clawed frogs. Dead bodies of the animals often become autolytic due to the aquatic environment. Some unclear reasons of death can possibly

Health problems in South African Clawed Frogs (*Xenopus laevis*): Pathological, microbiological and parasitological findings

trace back to a Chytridiomycosis (*Batrachochytridium dendrobatidis*) or to viral infections. At the same time the death of hundreds of frogs was also reported from other German animal facilities, although all animals were treated by antibiotics.

Buying only captive bred *Xenopus* frogs is highly recommended. Strict hygienic conditions are important, such as regular cleaning of the aquaria, strict separation of the animal groups, using individual material, e. g. dip net, for every aquarium, disinfections of the material after using.

The influence of changed cage structuring on fighting and basic physiological parameters of the Athymic Nude-nu/nu mouse

T. Bürge and L. Fozard

Novartis Institutes for Biomedical Research, Basel, Switzerland

Introduction

Social conflict is common in group housed laboratory mice. Bite wounds of various severity in male cage mates result from repeated fighting. Other consequences of agonistic behaviour may result in changes of physiological and immunological parameters. The occurrence of bite wounds in male social groups often forces the researcher to separate (all) animals of a group and/or euthanise injured animals.

It is well known that the extent of aggressive behaviour differs between mouse strains and that environmental enrichment may modulate the incidence and severity of fighting.

Athymic nude mice are commonly used in Oncology Research. Continuous backcrosses of animals with the original nude mutation to various inbred and outbred lines led to different nude strains which are commercially available nowadays. We have noted a difference in aggressive behaviour between males of the strains used at our institution; according to our experience the BALB/c nude the least, the SWISS nude the most and the Athymic nu-nude are the intermediate agonistic males of the 3 nude strains. Partly because of this, male mice of the more aggressive strains are not been used extensively by researchers.

The objective of this study was to investigate whether environmental enrichment by cage structuring with a mouse shelter may lead to reduced inter-male aggression as measured by the incidence and severity of bite wounds in the HsdNpa:Athymic nude mouse in our Oncology Research housing setup, Macrolon Type III cage, max. 8 - 10 mice per cage. Preference of shelter use, weight development and incidence of bite wounds were measured weekly over a period of 24 weeks, and terminal observations were made following week 26. For comparison of inter-sex differences and effect of the mouse shelter on female mice, this gender was also included in the study.

The influence of changed cage structuring on fighting and basic physiological parameters of the Athymic Nude- nu/nu mouse

It was thought that a beneficial outcome regarding social conflicts and other findings may lead to more frequent use of male HsdNpa:Athymic nude mice in experimental research and contribute to the 3R's through: 1.) reduced fighting and injury (stress) and 2.) avoidance of elimination of „unused“ male mice in the breeding colonies.

Materials and Methods

Study animals:

Animal species/strain:	Mouse; HsdNpa:Athymic Nude-nu/nu. (fig. 1)
Animal hygiene:	SPF
Supplier: (internal breeding).	Novartis Institutes for Biomedical Research
Number of animals:	240
Gender:	120 females, 120 males, 20 days old at study begin.
Cage enrichment: a shelter .	6 cages per gender with Kleenex paper towels and 6 cages per gender with Kleenex paper towels without a shelter (“conventional housing”).



Fig. 1: HsdNpa:Athymic Nude-nu/nu mouse

Husbandry

Housing type:	Optimised Housing Conditions (OHC).
Housing cages:	Type III, macrolon with filter tops (Tecniplast, I-Buggugiate).
Room temperature:	24 +/- 2°C (Digital-Thermometer / Hygrometer Model: TFA). The temperature within the cage below the filter tops is approx. 1.5 - 2°C higher than in the room.
Room humidity:	Minimum 45% before room cleaning (Digital-Thermometer / Hygrometer Model: TFA). The relative humidity within the cage is approx. 10-20% higher than in the room.

Photoperiod:	12 hours light / 12 hours dark (6h00-18h00), with a dimming period of about 30minutes in morning and evening.
Diet:	Kliba 3304, autoclaved, ad libitum (Provimi Kliba AG, CH-Kaiseraugst).
Drinking water:	Tap water, sterile filtered in 700ml bottles. Water change twice a week.
Bedding:	Approx. 200g dust-free, autoclaved wood chips (Scierie des Eplatures, CH-La Chaux de Fonds, Switzerland).
Basic enrichment:	Kleenex paper handkerchiefs (Kimberly-Clark Corporation).
Cage change:	Twice a week, on Mondays and Wednesdays.
Change of shelter:	At every 3rd to 5th cage change, depending on dirtiness of the device.

Terminal investigations

Haematology:	Bleeding from the retro-bulbar plexus in terminal isofluorane anaesthesia followed by cervical dislocation. Blood analysis (Advia 120 [®] , Bayer AG).
Necropsy:	Complete necropsy and organ investigation. Weighing of spleen and adrenals.

Selection of the shelter (fig. 3)

Many attractive shelter types for mice are available on the market. Therefore we decided not to produce an new type but to evaluate the “One” for best use in this study. The following criteria were defined for the selection:

- Acceptable size to receive 10 mice or possibility to combine two shelters into one.
- Easy to use.
- Resistant to gnawing and destruction.
- Autoclavable.
- Darkness for the animals within the shelter but still transparent for observation by the human eye (transparent red colour).
- Openings to the side and the upper surface of the shelter.

The influence of changed cage structuring on fighting and basic physiological parameters of the Athymic Nude- nu/nu mouse

□

- Possibility to use a (horizontal) roof of the shelter as exercise area.
- Proven references available about the shelter (previous studies).
- Commercial availability

Based on those criteria, the Tecniplast Mouse House™ (“Mouse House”, Fig. 2) was selected for use in this study. In order to accept all mice in the cage, two Mouse Houses were stuck together to form a “double” Mouse House (Fig. 3), and a direct opening between the two Mouse Houses was formed.



Fig. 2: The Mouse House™ by Tecniplast



Fig. 3: „double“ Mouse House with connection in between the two mouse houses

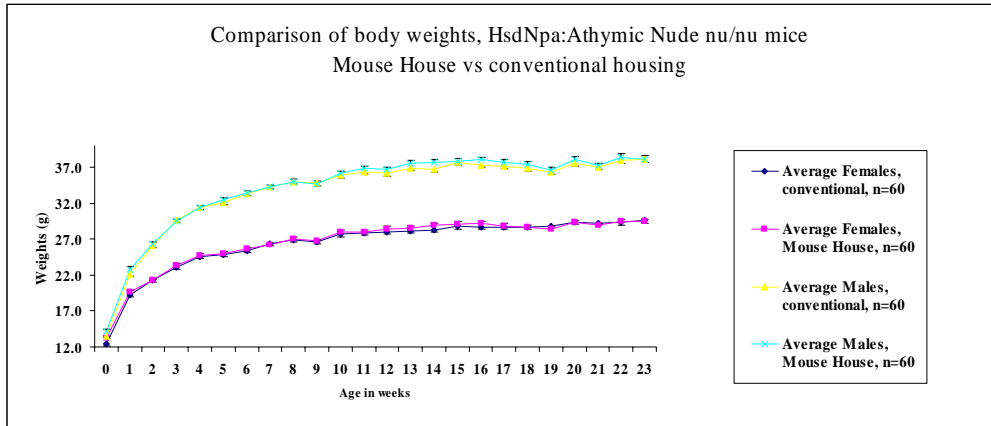
Study duration / Recording and analysis

The study was conducted for 24 weeks and terminal investigations made after 26 weeks. All in-vivo findings were recorded on-line or entered manually onto the institutions EDP system and comparisons of groups were analysed statistically.

Results

Body weight development

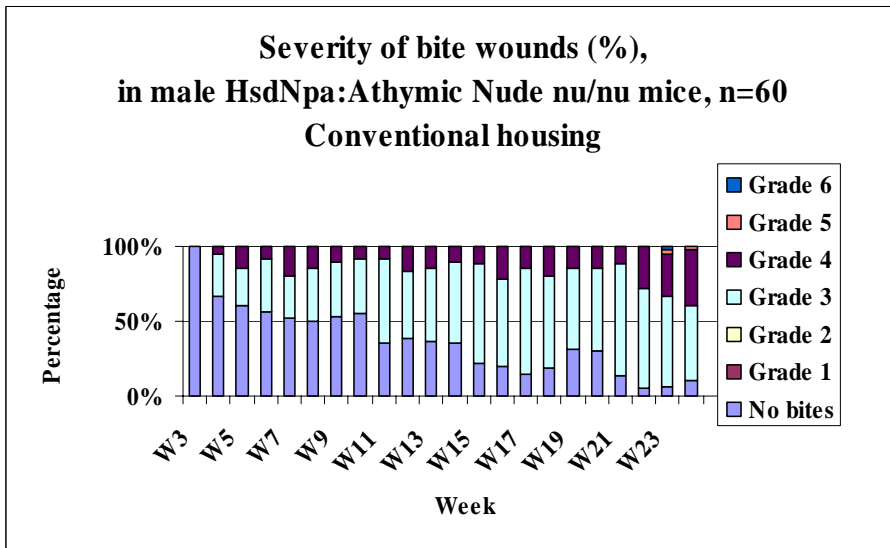
During the whole observation period, no statistically significant difference in mean body weight was noted in either genders (see graph on the right). In addition, no statistically significant decrease or increase of intra-group weight variation was noted in the groups with the Mouse House.



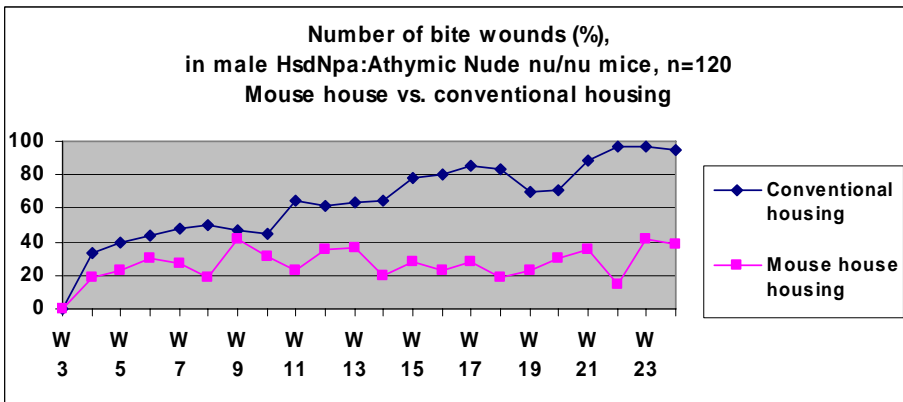
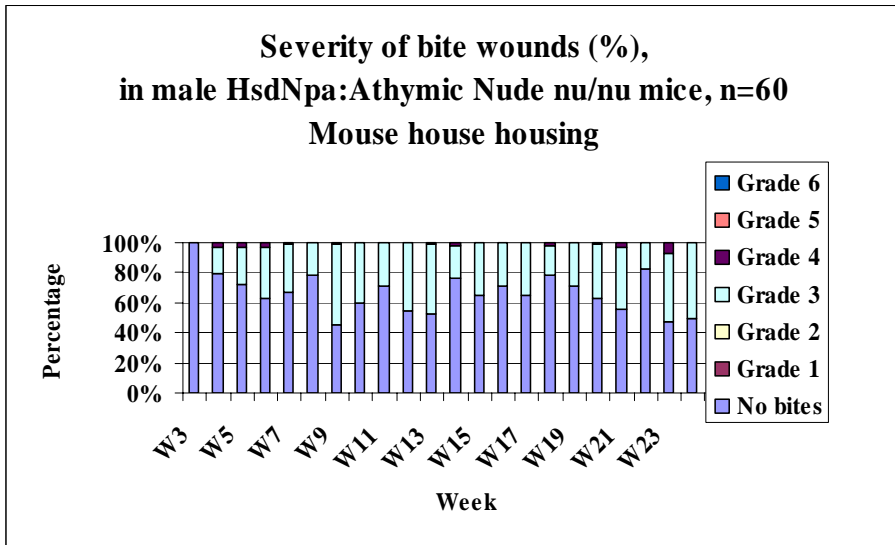
Bite wounds

Appearance of bite wounds in male mice was observed from one week after study begin onwards, in both groups. In contrast to a growing incidence and severity of bite wounds in the conventional group, incidence and severity in male animals with the Mouse House remained low during the whole study duration (see graphs on the right and below).

There was no difference between the female groups.



The influence of changed cage structuring on fighting and basic physiological parameters of the Athymic Nude- nu/nu mouse



Use of the Mouse House

In both genders, the Mouse House was actively used for exercising and climbing and also preferentially selected as a nesting and sleeping place (data not shown).

Haematology

For the haematology, the difference between the white blood cell counts (WBC) and red blood cell counts (RBC) in males was not statistically significant whereas the difference between the neutrophil percentages and the lymphocyte percentages was.

In contrast, the WBC, RBC, neutrophil and lymphocytes differences in the female animals were statistically significant.

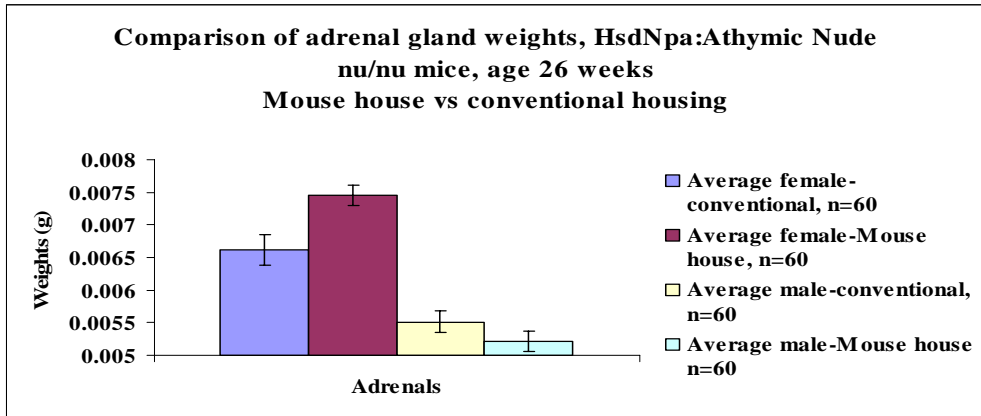
	WBC ($\times 10^9$ cells/L)	NEUT (%)	LYM (%)	RBC ($\times 10^{12}$ cells/L)
Average female-Mouse house, n=60	8.96	16.3	77.4	9.05
Standard deviation	2.77	0.45	5.88	7.20
Average female-conventional, n=60	7.66	19.0	74.3	8.81
Standard deviation	3.36	5.82	7.22	0.51

	WBC ($\times 10^9$ cells/L)	NEUT (%)	LYM (%)	RBC ($\times 10^{12}$ cells/L)
Average male-Mouse house n=60	5.23	24.2	67.5	8.45
Standard deviation	2.99	9.00	11.58	0.49
Average male-conventional, n=60	5.13	30.2	60.6	8.47
Standard deviation	2.23	11.49	12.84	0.66

Adrenal weights

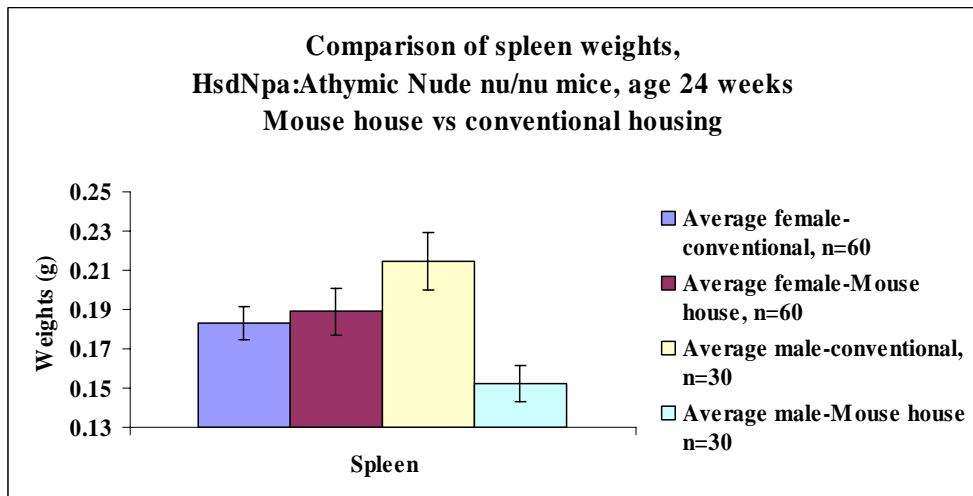
A significant difference was measured in the female mouse adrenal glands (Mouse House > conventional). No significant difference was noted in the male mice (see graph below).

The influence of changed cage structuring on fighting and basic physiological parameters of the Athymic Nude- nu/nu mouse



Spleen weights

Male mice showed a significant difference in spleen weights (conventional > Mouse House). No difference was found in the other gender (see graph below).



Conclusion

The study indicated, as interpreted from incidence and severity of bite wounds, that the introduction of the Mouse House reduced aggressive interactions between male HsdNpa:Athymic nude-nu mice. This finding shows that male mice of this strain can be kept longer in social groups thanks to this specified environmental enrichment.

The Mouse House did not influence the growth of either male or female animals and was actively used by the animals.

As the spleen and blood are involved in the immunological response, the increased size of the first and the differences in parameters of the latter in conventionally housed male animals were regarded as being related to the bite wounds.

The increased adrenal size and changes in blood parameters in female animals with the Mouse House were statistically significant and require further investigation.

From this study it was concluded that the insertion of the Mouse House has beneficial effects in socially housed male HsdNpa:Athymic nude-nu mice in this housing setup. This result may lead to an increase of use of males of this strain in research.

Further studies are planned to investigate the modulation of the Mouse House effects in other housing setups and other strains commonly used in *in-vivo* research.

References

Developing and testing a novel cage insert, the “Mouse House”, designed to enrich the lives of laboratory mice without adversely affecting the science. D. Key, A. Hewett, August 2002. *Animal Technology and Welfare*. P. 55-64.
<http://www.tecniplast.it>

Genetical characterization of the LEW/*Ztm-ci2* (circling2) and the BH.7A/*Ztm-ci3* (circling3) rats as animal models for syndromic deafness (USH1) respectively lateralization of brain function and hyperlocomotion

W.T. Chwalisz, D. Wedekind, H.J. Hedrich

Medical School Hannover, Hannover, Germany

Both, the LEW/*Ztm-ci2* and the BH.7A/*Ztm-ci3* rat, carry spontaneous mutations, which cause lateralized circling behavior and locomotor hyperactivity. The *ci2* phenotype is also characterized by ataxia and opisthotonus.

Previous studies have shown a neurochemical lateralization within the dopaminergic system of the basal ganglia in both rats and a morphological lateralization of dopaminergic neurons in the BH.7A/*Ztm-ci3* rat. In addition, functional and histological analyses of the inner ear of the LEW/*Ztm-ci2* rat revealed degenerations concerning the hair cells of the cochlea and the vestibular apparatus leading to profound deafness and vestibular dysfunction.

Using breeding experiments it was shown that both mutations are genetically transmitted as autosomal recessive traits. Furthermore, a classical complementation analysis (cis-trans test) clearly indicated that both circling mutations affect different loci.

In this study genetic analyses were performed in order to identify the chromosomal localization bearing the *ci2* and the *ci3* mutation and to present functional candidate genes. Using anonymous microsatellite markers two backcross populations ((LEW/*Ztm-ci2* x BN/*Ztm*)F1 x LEW/*Ztm-ci2*;

(BN/Ztm xBH.7A/Ztm-*ci3*)F1 x BH.7A/Ztm-*ci3*) were analyzed, which were previously phenotyped by behavioral testing. The incidence of circling behavior in both populations was nearly 50 %, indicating that the *ci2* as well as the *ci3* phenotype are caused by a defect in a single locus. These linkage analyses mapped the *ci2* mutation to rat chromosome 10 (RNO10) and the *ci3* mutation to RNO11.

A gene-linked marker for *Myo15* was designed and the position of this gene in the rat genome described for the first time within the non-recombinant interval of the core region of association on RNO10. Thus *Myo15*, which codes for an unconventional myosin (Myosin XV) that is expressed in the hair cells of the inner ear, can be regarded as a candidate gene for the *ci2* phenotype. This is based on the fact, that mutations in the homologue genes of human and mouse are known to cause profound deafness and vestibular dysfunction due to sensorineural degenerations of the inner ear. Further on, mutations in human *MYO7A*, a gene that encodes for a myosin with significant structural similarities to Myosin XV, are known to cause “Usher Syndrome” 1B, which is characterized by sensorineural hearing loss, vestibular dysfunction and a progressive retinal degeneration.

Because of the hind, that a mutation in a gene encoding for an unconventional myosin might be responsible for the *ci2* phenotype, GOCKELN et al. (2003) performed functional and histological analysis of the retina of LEW/Ztm-*ci2* rats. This analysis revealed that LEW-*ci2* rats display a progressive retinopathy as described for the “Usher Syndrome” in Human. In this study behavioral testing of the (LEW/Ztm-*ci2* x BN/Ztm)F1 x LEW/Ztm-*ci2* backcross population indicated that affected individuals of this backcross also display a loss of retinal function.

A physical map of the non-recombinant interval on RNO10 was generated, which describes the position of *Kcnj12* to this part of the rat genome. This gene, which codes for an inwardly rectifying potassium channel, can also be regarded as a candidate gene for the deafblind LEW/Ztm-*ci2* rat as these types of channels are known to play an important role for the physiology of both the retina and the inner ear.

The „UCSC Genome Bioinformatics“ database describes the chromosomal position of *Drd3* within the core region of association with the *ci3* phenotype on RNO11. This gene codes for the dopamine D3 receptor and can be regarded as a

functional candidate for the phenotype of the BH.7A/*Ztm-ci3* rat, which seems to be related to a lateralization of the dopaminergic system of the basal ganglia. PCR-amplification of the seven exons of *Drd3* was performed in this study using genomic DNA of a BH.7A/*Ztm-ci3* rat and a rat from the background strain. No differences in the length of the PCR-products could be detected indicating that this gene is not affected by deletions. This result does not exclude that a single point mutation within the sequence of *Drd3* might be responsible for the phenotype of the BH.7A/*Ztm-ci3* rat.

Induced Intracerebral Haemorrhage in Rats: Comparison of the Validity of Computertomography (CT) and Magnetresonanztomographie (MRI)

V. Elste

Roche Vitamins Ltd., Human Nutrition and Health, Basel, Switzerland

Background: Stroke symptoms are caused in 10 to 15 % by intracerebral haemorrhage. It is often not possible to differentiate intracerebral haemorrhage from cerebral ischemia by clinical examination. The therapeutic decision between thrombolysis or conservative therapy is comprised by the etiology. To exclude intracerebral haemorrhage as the cause of clinical symptoms, a CT is usually performed. However, CT can not detect the whole extent of cerebral ischemia within the first hours. Instead MRI with diffusion and perfusion weighted sequences is capable to detect early ischemia within the therapeutic relevant first hours. If special MR sequences are as least as sensitive as CT for the detection of intracerebral haemorrhage, CT is not further necessary in the management of patients with stroke symptoms. The aim of our study was a direct comparison of the sensitivity of CT and MRI to detect acute intracerebral haemorrhage. The model of induced intracerebral haemorrhage in rats (1) was used to be able to compare different clinical diagnostic technique and histological examination.

Materials and Methods: In eight anaesthetised male Wistar rats intracerebral haemorrhage was induced by the infusion of collagenase (1). Immediately after surgery, the animals were scanned by MRI and CT. All MRI studies were performed on a 1.5 T clinical whole body MR imager (THE EDGE, Picker, Cleveland, USA). Routine brain imaging with proton density- and T2-weighted imaging was continued. Subsequently T1-, diffusion-, T2*-weighted and FLAIR sequences were performed. The CT examinations were carried out on a PQ 2000 CT (Picker, Cleveland, USA) scanner. After the imaging protocol the rats were killed during the anaesthesia. Fixed brains were cut and stained with hemalaun and eosin .

Induced Intracerebral Haemorrhage in Rats: Comparison of the Validity of Computertomography (CT) and Magnetresonanztomographie (MRI)

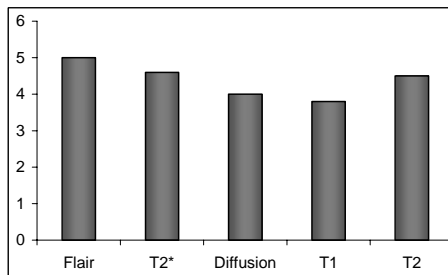


Figure 1: Visibility of different MR-Sequences 60 min. after induction of intracerebrale induced haemorrhage (1=not visible to 5=clearly visible).

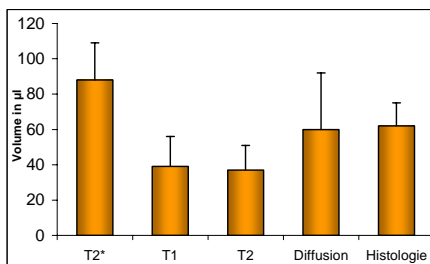


Figure 2: Volume of haemorrhage, determined with different MR-Sequences 60 min. after induction of intracerebral haemorrhage, compared with the histological determined volume.

Results: In all animals, intracerebral hemorrhage was present in T2*-weighted gradient echo and diffusion weighted MR images 1 hour after infusion of collagenase. In T2*-weighted MRI intracerebral haemorrhage was visible as an area of marked hypointensity, in diffusion weighted MRI, the hypointensity was less pronounced, but clearly visible. T2- and proton density weighted images were positive in 7/8 rats. In these sequences the bleeding presented as a hyperintense area with mass effect. In one animal the intracerebral hemorrhage was less than 2 mm in diameter and not clearly visible in PD and T2-weighted images. T1 weighted images revealed signal changes in 4/8 rats, and FLAIR sequence was positive in 6/8 rats. In CT intracerebral hemorrhage was only visible in 3/8 rats. Histology revealed an acute intracerebral hematoma in all animals.

Conclusions: In this animal model, T2*- and diffusion weighted magnetic resonance imaging all well as FLAIR-sequences proved to be the most sensitive imaging modality in the detection of acute intracerebral haemorrhage and is by far more sensitive than CT. The diffusion weighted MRI is an important technique to diagnose acute cerebral ischemia. It is very helpful to detect less perfused areas very early after closing of vessels. This region is shown as a hyperintense area. In our experimental model the haematoma was shown as a hypointense area, so contrarily to the acute intracerebral ischemia. This means, that an acute intracerebral haemorrhage can be distinguished very quickly from an

acute intracerebral ischemia. At a collagenase induced haemorrhage (1) the blood appears in the acute phase in T1-, PD- and T2- weighted sequences hyperintense

because of the higher liquid concentration of blood particles. But in the acute phase this is often difficult to differentiate from the normal brain tissue. Often

only the expanding effect is detectable. Because of this an optimised MR-protocol to detect an early cerebral ischemia also should include diffusion- and T2*-weighted MRI sequences (2).

The possibility to be able to test different techniques at a “patient” and to be able to compare these directly with histological examinations support the development of new diagnostic procedures. So this animal model was able to improve the differentiation between early cerebral ischemia and acute intracerebral hemorrhage.

Key Words: Cerebrovascular diseases - intracerebral haemorrhage - magnetic resonance imaging - rats

References: (1) Rosenberg GA, et al., Collagenase induced intracerebral hemorrhage in rats. *Stroke* 21:801-807

(2) S. Kuhn, W. Reith, B. Ertl-Wagner, V. Elste, K. Sartor; *Radiologe*, 1999, 39:855-859, Vergleich der Wertigkeit der Computertomographie und der MRT in der Diagnostik der akuten intrazerebralen Blutung

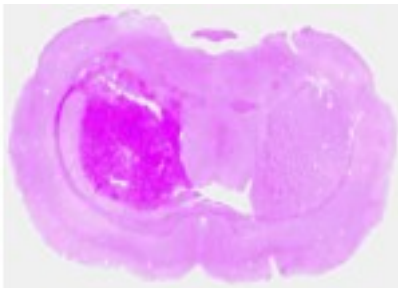


Figure 3:
Corresponding histological preparation (Hemalaun-Eosin-Staining).

Induced Intracerebral Haemorrhage in Rats: Comparison of the Validity of
Computertomography (CT) and Magnetresonanztomographie (MRI)

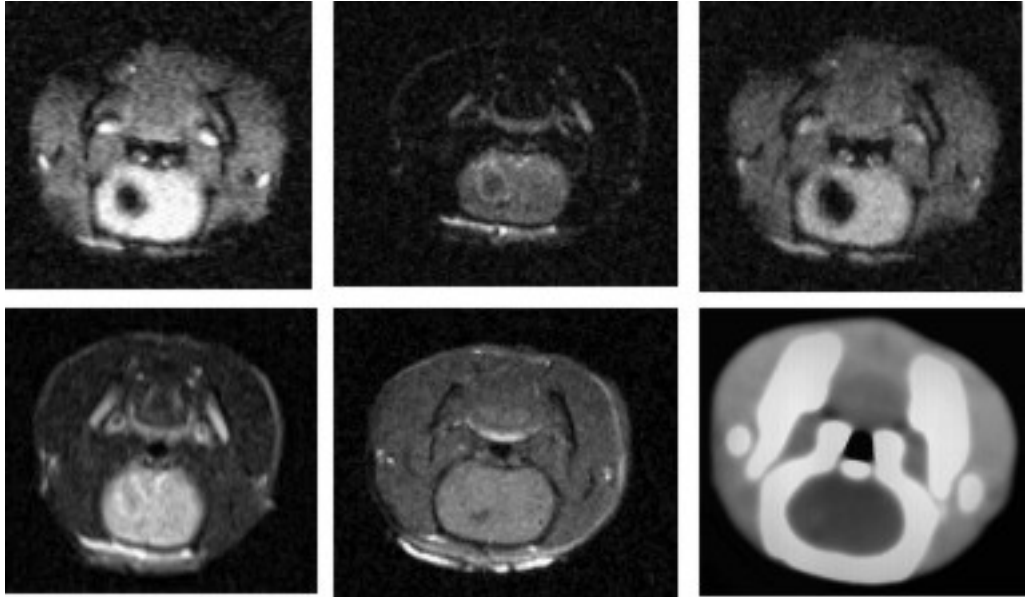


Figure 4 a-f: The intracerebral haemorrhage is clearly seen in the different MR-images 60 min after induction. (a=Flair, b=Diffusion, c=T2*, d= T2, e=T1); At the CT-image the haemorrhage is seen as a slight hyperintense area (f=CT).

PyRAT- Python based relational animal tracking – a new web-based solution for animal facility management

J. Helppi¹, J. Oegema² & J. Duperon²

¹Max Planck Institute of Molecular Cell Biology and Genetics (MPI-CBG), Dresden, Germany and ²Scionics Computer Innovation GmbH, Dresden, Germany

Managing work flow, administrative, and research information is a challenge faced by every animal facility. Many of the software packages available are difficult to learn, configure, and use and often come with a significant per-client cost. PyRAT was designed from the beginning to manage the basic animal related information flow in an easy and transparent way using a web interface. PyRAT's development model was unique in that its design was directly based on day-to-day interactions with the animal facility management, animal caretakers, and scientists using the MPI-CBG Animal Facility.

PyRAT is constructed in a modular and easily extendible way allowing facilities to request their own special feature set. The base package includes the tracking of: id-numbers, cage cards, locations, strains and mutations, weanings, pedigrees, detailed animal history, age, owner and project information, budgeting, and the export and import of animals. In addition the base package has a complete work request management system that allows users to submit work requests without phone or e-mail, allows administrators to assign work requests and exchange information, tracks incident status and priority, and many other functions. Data from PyRAT can be exported and analyzed using its report generation tool, and summaries and budgeting information can be easily extracted.

PyRAT keeps an internal user database that allows the administrator to create new users and control their access level. Users can be granted permission to simply view the data, administrate certain groups or projects, modify animal information (animal caretakers), or administrate the entire database.

The dorsal skinfold chamber as useful model for the investigation of microcirculation and angiogenesis

Markus Heuser, Gerhard Zöller, Rolf H. Ringert, Bernhard Hemmerlein

Department of Urology, Georg-August-University, Gottingen, Germany.

Introduction: The dorsal skinfold chamber in rodents has been often used for the assessment of angiogenesis and microcirculation of freely implanted benign or malign tissue onto the striated skin muscle. By means of this technique the formation of new vessels and the perfusion in the implanted tissue is easily visualized and quantified by means of intravital microscopy and image analysis systems.

Material and methods: Using an example of an oncologic study regarding the angiogenesis in renal cell carcinoma the process of tumor implantation and the angiogenic potency of the chamber is demonstrated. Multicellular tumor spheroids of A-498 carcinoma cells are implanted into the chambers. Intravital fluorescence microscopy is repeatedly used to visualize angiogenesis in the same animal for up to 14 days. In detail, the microvessel density and parameters of tumor perfusion (e.g. red blood cell velocity) are assessed by means of a digital image analysis system. The model offers the opportunity to investigate the influence of antiangiogenic drugs on the angiogenesis in renal cell carcinoma. Our group has studied the effects of a Gastrin Releasing Peptide receptor blockade on angiogenesis in renal cell carcinoma.

Results and conclusions: In our opinion, the dorsal skinfold chamber model is a feasible and animal sparing model. Furthermore, this model is very helpful for the assessment of angiogenesis and microcirculation in freely implanted tissue especially in combination with molecular biology.

Spontaneous tumours in a colony of *Cynomolgus* monkeys (*Macaca fascicularis*) observed during a 10-year period (1992-2002), with a survey of the literature

J.Kaspareit, S.Friderichs-Gromoll, E.Buse, G.Habermann and F. Vogel

Department of Pathology, Covance Laboratories, Münster, Germany

A lot of information is available in the scientific literature about the tumour incidences and tumour types of common used laboratory animal species like rat, mouse and hamster. For laboratory dogs countless reports on the tumours of dogs kept as pet animals exist. In contrast to that situation there are only few reports about tumours of the different primate species (especially those used in toxicological studies). Especially for cynomolgus monkeys only nineteen reports on neoplasms could be found in the literature between 1970 and 2003. They included: pituitary adenomas (2,12), squamous cell carcinomas (3,14), basal cell carcinoma (19), hepatocellular carcinomas (4), intestinal adenocarcinomas (5), choriocarcinoma/teratoma (6), lymphoma/lymphosarcoma (1,7,9,11), astrocytoma (8), ameloblastic odontoma (10), malignant nephroblastoma (12), renal carcinoma (15), olfactory neuroblastoma (17), papilliferous cystadenoma of the skin (16) and duodenal carcinoid (18). Some of these reports describe findings in zoo animals, that were kept until the end of their natural life-span and therefore reached an age where the incidence of neoplasia increases. Since primates that die in zoos rarely are examined as intensely as primates in toxicological studies, data from this source cannot be considered to be representative for a primate species. In contrast, a wide spectrum of organs (including even small organs like pituitary gland and parathyroid gland) is examined after terminal sacrifice of a toxicological study. However, these animals seldom reach the end of the first decade of their life-span resulting in low tumour incidences.

A total of 14 tumours was observed between 1992 – 2002 in the Covance primate colony. Animals were experimental animals that were used in studies or stock animals. Five tumours were already detected at necropsy, the rest at histopathological examination. The neoplasms found belonged to the pulmonary,

endocrine, haematopoietic (Fig. 1) and genital system (Fig.2). Details are presented in Table 1. The age of the animals ranged between 2 years and 2

months and 7 years and 3 months. Seven males and five females were affected by neoplasms. Although the observation period was short, a slight prevalence of endocrine tumours (thyroid, adrenal gland) was observed in our colony. However, for precise information on incidence and tumour spectrum of cynomolgus monkeys the examination of a larger number of aged animals of this species is necessary.

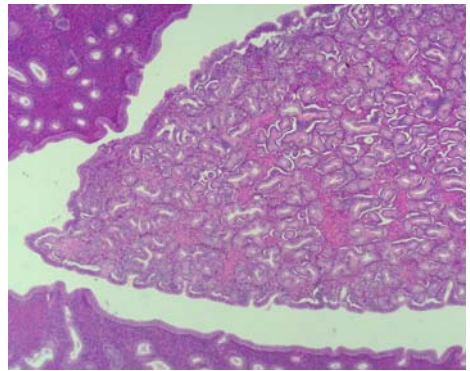
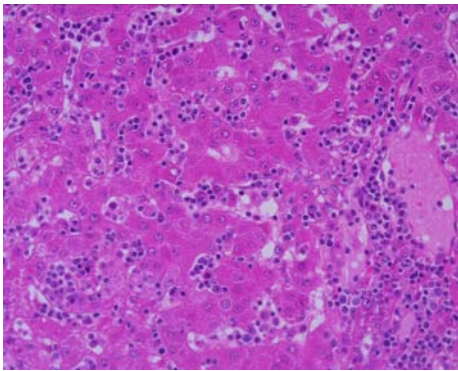


Fig.1.: Lymphosarcoma invading the liver. H.E., x 150. Fig.2.: Uterine polyp in the lumen of an uterus. H.E., x 150.

Tumour type	Organ	Sex	Age (y/m)	Experimental group
Bronchial papilloma	Lung	M	6y 7m	High dose
Cartilagenous hamartoma	Lung	M	2y 2m	High dose
Squamous carcinoma	Lung	M	7y 3m	Control
Cortical adenoma	Adrenal gland	M	6y 4m	Control
Cortical adenoma	Adrenal gland	M	4y 11m	High dose
Cortical adenoma	Adrenal gland	M	6y 5m	High dose
Cortical adenoma	Adrenal gland	F	5y 10m	High dose
Follicular adenoma	Thyroid	M	4y 10m	Control
C-cell carcinoma	Thyroid	M	?	Control
Lymphosarcoma	Subcutis (leg)	F	?	Stock
Lymphosarcoma	Liver/Diaphragm/Abdominal cavity	F	3y 2m	Stock
Adenoma	Seminal vesicle	M	?	Control
Teratoma	Ovary	F	7y 2m	Control
Polyp	Uterus	F	6y	High dose

Tab.1: Spontaneous tumours observed in Cynomolgus Monkeys (*Macaca fascicularis*) during a 10-year period (1992-2002)

References

1. Paramastri YA et al.: Vet Pathol 2002, 39 (3), 399-402.
2. Daviau JS and Trupkiewicz JG: Contemp Top Lab Anim Sci 2001, 40 (5), 57-9.
3. Nakamura S et al.: Exp Anim 2000, 49 (3), 225-8.
4. Reindel JF et al.: Vet Pathol 2000, 47 (6), 656-62.
5. Valverde CR et al.: Comp Med 2000, 50 (5), 540-4.
6. Toyosava K et al.: Vet Pathol 2000, 37 (2), 186-8.
7. Anderson WI et al.: J Med Primatol 1994, 23 (1), 56-7.
8. Yanai T et al.: Vet Pathol 1992, 29 (6), 569-71.
9. Jayo MJ et al.: Lab Anim Sci 1988, 38 (6), 722-6.
10. Davis JA et al.: Lab Anim Sci 1988, 38 (3), 312-5.
11. Jaax NK et al.: Lab AnimSci 1988, 38 (2), 198-200.
12. Tsuchitani M and Narama I: Vet Pathol 1984, 21 (4), 444-7.
13. Bennet BT et al.: Lab Anim Sci 1982, 32 (4), 403-4.
14. Morin at al.: Lab Anim Sci 1980, 30 (1), 110-2.
15. Kommineni C et al.: Vet Pathol 1978, 15 (4), 569-70.
16. Kim JC and Palazzo MC: J Med Primatol 1978, 7 (3), 189-91.
17. Correa P et al.: J Med Primatol 1975, 4 (1), 51-61.
18. Lau DT and Spinelli JS: Lab Anim Care 1970, 20 (6), 1145-8.
19. Gonzalez Navarro BO et al.: Lab Animal 3(1), 22-25.

Mycobacterium marinum infection in *Xenopus laevis* – a case study

Sarah Kimmina

Dept. of Laboratory Animal Science, University of Goettingen, Goettingen, Germany

Mycobacterium marinum belongs to the group of atypical mycobacteria, which are common in aquatic animals.

As they are a cause of zoonotic infection, they form a serious risk for people working with infected animals. Often the potentially developing skin infections are overlooked in the beginning, and are not recognized by the treating physicians. Furthermore this disease asks for a long term antibiotic treatment to get under control.

Herein we describe an infection with mycobacteria in a group of lab animal *xenopus laevis* and *xenopus tropicalis*.

The microbiological agent was histologically detectable by a Ziehl-Neelsen-staining of lung, kidney, spleen, gut, ovary and liver. At the same time a cultivation of the agent was done, and then a partial sequencing of genome was performed.

We evaluated the dissection of 100 frogs, whereas a verification of *mycobacterium marinum* succeeded only in animals, that had been obviously ill anyway. There hasn't been any typical sign of the illness, the animals showed symptoms as ascites, edema of the subcutis, anaemia, mycosis, sudden death, anorexia and apathy.

Strikingly there had been no typical macroscopic granuloma nodules. Often the animals suffered from bleedings in the small and large intestine, and had huge atelectatic areas in the lungs. Microbiologically *aeromonas* spp. and *erwinia* spp. could be detected commonly.

It remains unclear whether there is a chronic infection in this unit, which occasionally leads to a manifestation of the disease, only in case of additional stress or to which extent the pathogenic potential of any such primary infection has to be evaluated.

Determination of circadian rhythm of body temperature in laboratory mice and rats by rectal probe

M. Klein¹, T. Tillmann¹, P. P. Tsai², H. Hackbarth², C. Dasenbrock¹

¹Fraunhofer Institute of Toxicology and Experimental Medicine, Hannover, Germany

²Center for Animal Welfare, Hannover Veterinary School, Germany

Background: Body temperature is regulated not only homeostatically, but also undergoes regular daily fluctuations. Therefore, it is important that the time point of measurement be taken into consideration when determining body temperature values. In this study, rectal body temperature of laboratory mice and rats was determined using a digital thermometer. Over a period of four weeks, measurements were done on four time points per day.

Materials and Methods: 40 B6C3F1/Crl mice, 40 Wistar WU (Crl: WU), and 40 Fischer (F344/Crl) rats (each group 20 ♂/20 ♀), 5 weeks of age at delivery, were purchased from Charles River Deutschland, Sulzfeld, Germany. After one week acclimatization to the standard laboratory conditions (room temperature 22 ± 2 °C, relative humidity 55 ± 15 %, air change rate 10-15 times/h, 12:12 h light/dark cycle, 7 p.m. to 7 a.m. light off), animals were accustomed to the handling and temperature measurements during a 14-day training period. The care of the laboratory animals and all temperature measurements were performed by a single person. Rats were removed from their cages by their chests and slightly restrained on the observer's arm for rectal temperature measurement. Mice were taken from their cages by their tails. For body temperature measurement, the animals were held by their tail and their forepaws rested on the observer's chest. On six different days (days 1, 2, 5, 7, 14, 27) over a period of four weeks, rectal body temperature was measured at defined daily time points (6 a.m., 12 a.m., 6 p.m., 12 p.m.) using a digital thermometer of 0.1 °C accuracy (MD 3060, Beckmann und Egle, Kernertal, Germany) and a flexible measurement probe (MD 3024). Between measurements, the probe was lubricated with vaseline. The probe was inserted 1.5 cm into the rectum of mice and 5 cm into the rectum of rats.

Determination of circadian rhythm of body temperature in laboratory mice and rats by rectal probe

Results: The mean measurement time of the digital thermometer was 5 ± 1 sec. in mice and 8 ± 2 sec. in rats. By measuring the temperature at four different time points per day, a circadian rhythm of rectal body temperature could be confirmed in both species. The low values of the circadian rhythm of body temperature were measured during the light phase (7 a.m. – 7 p.m.) and the high values during the dark phase (7 p.m. – 7 a.m.).

Conclusion: Habituation to handling and rectal body temperature measurement as well as a thermometer with a very short measurement time and a standardized insertion of the temperature probe are necessary to get reliable temperature values. Furthermore the stress-induced hyperthermia, even induced by a slight disturbance (i.e., animal caretaking, previous measurements), and its time dependent temperature decrease to “baseline” values (normothermia), should be taken into consideration when selecting the different measurement time points. If these requirements are met, temperature values measured by rectal probe are comparable with telemetrically recorded values.

Key Words: Laboratory mice and rats, rectal body temperature measurement, circadian rhythm

Subcutaneously implanted transponders/microchips – a new minimally invasive method of body temperature measurement?

M. Klein¹, T. Tillmann¹, P. P. Tsai², H. Hackbarth², C. Dasenbrock¹

¹Fraunhofer Institute of Toxicology and Experimental Medicine, Hannover, Germany

²Center for Animal Welfare, Hannover Veterinary School, Germany

Background: It is well known that animal restraint, which is necessary for rectal temperature determination, is associated with stress-induced hyperthermia especially in mice. Therefore, the practicability and reliability of subcutaneously implanted microchips for body temperature measurement (IPPT-200, PLEXX, The Netherlands) was investigated in mice and rats.

Materials and Methods: 40 B6C3F1/Crl mice, 40 Wistar WU (Crl: WU), and 40 Fischer (F344/Crl) rats (each group 20 ♂/20 ♀) were housed under standard laboratory conditions (room temperature 22 ± 2 °C, relative humidity 55 ± 15 %, air change rate 10-15 times/h, 12:12 h light/dark cycle, 7 p.m. – 7 a.m. light off). The transponders, preloaded in the lumen of sterile needles, were implanted subcutaneously in the dorsolateral back of the animals without any anesthesia, using the especially designed insertion device. These injections were carried out 14 days prior to the start of the temperature measurements. Over a period of four weeks, subcutaneous body temperature measurement via s.c. implanted transponders/microchips was compared to rectal body temperature determination using a digital thermometer.

Results: The transponders were implanted subcutaneously without any complications, anesthesia was not required. The animals were only restrained manually. The reading distance between the scanner and the microchip was 1 cm or less. In most cases, the scanner had to touch the animal's skin directly above the transponder to obtain a temperature value. Both rectal and subcutaneous body temperature measurements required handling of the animals. On average, the subcutaneous body temperature of mice was 0.6-0.8 °C lower and that of rats 0.9-1.0 °C lower than the rectal body temperature. Temperatures measured by the transponder were displayed on the reader within 1 sec in mice and 3 ± 2 sec in rats. During the six weeks observation period, 8 % of the implanted transponders

Subcutaneously implanted transponders/microchips – a new minimally invasive method of body temperature measurement?

(mice: 6 transponders, rats: 4 transponders) were lost by the animals and found in their fur or in the softwood bedding of the cages. These losses occurred mostly during the first two weeks after implantation, but also during the remaining four weeks.

Conclusion: Compared to rectal body temperature measurement, the microchip implant system has the similar disadvantage of having to handle the animals. Therefore, radiotelemetry remains the only method for continuous observation of body temperature in undisturbed laboratory animals over a long period.

Key Words: Laboratory mice and rats, body temperature measurement, transponders/microchips

The polydactyly luxate syndrome of the rat: Morphological and genetical findings

C. Krüger¹, D. Büttner¹, H. Böhme² & K. Militzer¹

¹ Central Animal Laboratory (ZTL), University Clinic of Essen, Hufelandstraße 55, D-45122 Essen; ² Leibniz Institute for Neurobiology, Brennekestr. 6, 39118 D-Magdeburg

The polydactyly luxate syndrome (PLS) of the rat represents hereditary malformations of the distal limbs with highly variable characteristics. We examined Shoe:Wist rats coming from the Leibniz Institute for Neurobiology in Magdeburg which we have continued to breed at the ZTL as inbred strain since 2001. The rats are kept under standard conditions.

For morphological diagnosis, animals were euthanised and examined macroscopically and using X-rays (Siemens Gigantos Optimac, Mamoray HD X-ray cassettes, and Agfa HDR X-ray films). Afterwards they were dissected.

In order to clarify the heredity of PLS, Shoe:Wist rats were crossbred with LEW/Crl rats. Further reciprocal backcrosses of the F1 with LEW/Crl rats and Shoe:Wist rats were carried out.

Morphological changes exclusively were observed in the zeugopode and autopode of the hind limbs, where the changes always occur on both of the extremities with different intensity. Most frequently, changes occur on phalangeal, metatarsal, and on tarsal bones. The simplest form of the changes is a triphalangy of the first toe. Duplicate toes occur in particular for the second and third toe and may result in 6 to 8 toes per foot. The affected toes can be soft tissue, osseous, or even fully triphalangeal developed, partly with fusions in the metatarsal area. In the tarsus, bone fusions and missing Os tarsale primum and Os tarsi tibiale are predominant. Possible changes on the zeugopode are the thickening of the fibula with separation from the tibia as well as shortenings and deformities of both bones. Also, their distal parts of the epiphysis and diaphysis may miss and thus cause luxation of the tarsocrural joint. The patella can vary in shape and size and may also be luxated.

The F1 (n = 25) of the crossbreeding did not show any morphological changes. The reciprocal backcrosses of the F1-hybrids with Shoe:Wist rats resulted in 219 animals. 110 of them showed PLS-characteristic changes. The offsprings of the reciprocal backcrosses with LEW/Crl rats (n=144) did not show any changes.

The polydactyly luxate syndrome of the rat: Morphological and genetical findings

The conclusion of these results is that PLS is inherited recessively. There are no indications that the transmission is gender-specific.

The polydactyly luxate syndrome of the Shoe:Wist rat largely corresponds to the preaxial polydactyly of humans. Consequently, this rat strain is a particularly suitable animal model for further morphological and genetical studies.

Detection of MHV and MMV in mice: Comparison of a viral plaque assay with the MAP-test and PCR

E. Mahabir¹, K. Jacobsen¹, D. Peters², J. Needham³, J. Schmidt¹

¹Department of Comparative Medicine, ²Institute of Experimental Genetics, GSF - National Research Centre for Environment and Health, D-85764 Neuherberg, Germany

³The Microbiology Laboratories, North Harrow, Middlesex, United Kingdom

Introduction

To efficiently monitor the health status of laboratory mice and to screen biological materials for unwanted murine viral agents, it is important to apply sensitive and reliable diagnostic methods to detect such pathogens. In this study, the sensitivity and reproducibility of three different diagnostic methods for mouse hepatitis virus (MHV-A59) and mouse minute virus (MMVp): viral plaque assay, mouse antibody production test (MAP) and polymerase chain reaction (PCR) was investigated.

Material and methods

For each method, serial tenfold dilutions of 10^9 to 10^{-1} TCID₅₀/ml MHV-A59 and 10^4 to 10^{-6} TCID₅₀/ml MMVp were made. L929 and A9 cells were seeded in 96-well plates for plaque assay of MHV-A59 and MMVp, respectively. For plaque assay, 12-fold wells were infected with 100 μ l virus suspension and the appearance of a cytopathic effect (CPE) was determined. The MAP tests were performed by inoculating six to eight week-old, male, specific pathogen free outbred Swiss mice (4 mice per dilution) with MHV-A59 and MMVp by intraperitoneal (450 μ l) and intranasal (50 μ l) application. Serological analysis for MHV-A59 and MMVp specific antibodies was performed using enzyme linked immunosorbent assay (ELISA) 14 and 28 days post inoculation (p. i.) and for MMVp specific antibodies also 49 day p. i. The MHV RT-PCR was performed using primers published by Taylor and Copley (1994) while the MMV PCR was performed using primers from Bootz and Sieber (2002). For each virus, five replications were performed.

Results

MHV-A59: For detection of MHV-A59, the MAP test (10^{-1} TCID₅₀/ml) was more sensitive than the plaque assay (10^0 TCID₅₀/ml) and the RT-PCR (10^3

Detection of MHV and MMV in mice: Comparison of a viral plaque assay with the MAP-test and PCR

TCID₅₀/ml). The results of the MAP test (10^{-1} TCID₅₀/ml) were more reproducible than the plaque assay (10^2 TCID₅₀/ml) and the RT-PCR (10^3 TCID₅₀/ml).

MMVp: The plaque assay (10^0 TCID₅₀/ml) was equally sensitive to the MAP test (10^0 TCID₅₀/ml), the PCR (10^{-6} TCID₅₀/ml) being the most sensitive method. The MAP test showed that all 4 mice from the group receiving 10^{-2} TCID₅₀/ml had produced anti-MMVp antibodies not by day 28 but by day 49 p.i. The results of the PCR (10^{-5} TCID₅₀/ml) were more reproducible than those of the MAP test (10^4 TCID₅₀/ml) and the plaque assay (10^2 TCID₅₀/ml).

Discussion

Our results indicate that viruses cannot be detected using only one method. The most sensitive method has to be determined for each virus. The results of a plaque assay depend on the permissive cell line used. The PCR is influenced by the PCR conditions and the quality of the DNA/RNA. Both methods contribute to animal welfare since no animals are used. The success of the MAP test depends on the immune competence of the mice and their susceptibility to the viruses. Furthermore, the present study showed that the results of the MAP tests for MMVp detection depend on the time to antibody production after infection.

Individually Ventilated Cages and Open Cages with or without environmental enrichment: a comparative study on body weight, major organs weight and blood parameters in Hsd:ICR(CD-1)[®] mice

Gianpaolo Milite

DVM, M.Sc. Manager Technical Services and Training Tecniplast Gazzada, Italy

The large diffusion of IVC cages and the use of inserts for the environmental enrichment of mice, are two major changes occurred in husbandry of this species and in the technology used as equipment in modern animal facilities. Many attempts to verify possible influences due to highly ventilated cages and/or inserts were made in terms of standard performances: breeding, growth curve, behaviour. The aim of this study was to evaluate possible influences on the growth curve, main organs weight, haematological and chimico-clinical parameters in Hsd:ICR(CD-1)[→] mice maintained in IVC or Open Cages either with or without the environmental enrichment named Mouse House. Two hundred and forty Hsd:ICR(CD-1)[→] male mice were randomly distributed 5 to cage to the four groups and weighed. They were then weighed on a weekly basis and at the age of 23 weeks 50% of the mice from each group were culled with CO₂, weighed and the main organs removed.

The remaining 50% of mice were anaesthetised and blood samples taken from the abdominal aorta for haematological and chimico-clinical analysis.

No evidence of statistically significant differences were found for the body weight, haematological and chimico-clinical parameters and organs weight at 23 weeks of age. The mean combined weight of the adrenal glands from animals of the groups with the Mouse House was lower than the counterpart without the insert. Furthermore, a level 14% higher of HDL in the blood of the mice housed in IVC with the Mouse House vs. those in the Open Cages was detected. In conclusion, no differences and influence on the parameters under investigation were found after 20 weeks of study due to the caging system, the Mouse House being or not in the cages and the combination of the two parameters.

Investigations on the effect of inhalative formaldehyde exposure on the open field behavior in rats

K.-U. Möritz*, F. A. Malek**, and J. Fanghänel**

*Peter Holtz Research Center for Pharmacology and Experimental Therapeutics, Ernst Moritz Arndt University, Friedrich-Loeffler-Street 23 d, D-17487 Greifswald, Germany, and

** Department of Anatomy, Ernst Moritz Arndt University, Friedrich-Loeffler-Street 23 c, D-17487 Greifswald, Germany

In the present study, we investigated the effect of inhalative formaldehyde exposure on the locomotor and explorative behavior in rats. Adult male and female LEW.1A rats were exposed to different formaldehyde concentrations (0, 0.1, 0.5, or 5 ppm, respectively) by inhalation for 10 consecutive days (2 hours per day). On day 10 (two hours after the last exposure), the locomotor and explorative behavior of the rats was determined using an open field test. Formaldehyde-exposed male and female rats crossed a significantly decreased number of floor squares than controls. Formaldehyde-exposed males exhibited reduced frequencies of floor sniffing, rearing, wall climbing, and defecation. The females exposed to 0.1 ppm formaldehyde showed a significant increase in rearing and grooming.

Our results demonstrate that a repeated inhalative exposure to the used formaldehyde concentrations causes behavioral alterations in male and female rats and that these are dose- and gender-dependent. The observed formaldehyde-mediated behavioral changes are suggested to be mainly attributable to the neurotoxic characteristics of the substance. However, formaldehyde-induced irritation of the respiratory and sensory systems can not be ruled out to be responsible, even when in part, for the observed deviations in the explorative behavior of the experimental rats.

TierBase: A program for computer-assisted management of an animal breeding and experimentation facility

P. Nielsen und H. Mossmann

Max-Planck-Institut fuer Immunbiologie, Stuebeweg 51, 79108 Freiburg

Due to the dramatic increase in the generation of genetically manipulated animal lines, as well as to the increasing need to document animal breeding and experimentation, a computer-based management of such information has obvious advantages. TierBase is a database which can greatly improve many aspects of managing the breeding and animal experimentation of genetically modified animal strains at research and commercial breeding facilities.

TierBase organizes information for various topics such as animal lines and colonies, users, animal ethics projects, breeding results etc. in an easily accessible form. Particular attention has been given to provide a user friendly interface. Its' multi-user capability, support for Windows® and Macintosh® operating systems and integrated online-help all contribute to an improved collaboration between animal technicians, breeding administrators, animal ethics officers and scientists.

Colony and Line Data: TierBase stores animal colony information such as the owner, responsible scientists and animal technicians, location of animals, etc. In addition, extensive line information can be stored including mutant loci, screening protocols, phenotypic and anatomical changes, lethality, special breeding requirements, etc. Access to each colony can be specified for each individual user. In this way, it is very easy to keep an overview of which colonies are held in the facility and who is responsible for them.

Job Management: Animal use is registered by creating different types of jobs such as animal orders, elimination, start mating, cryoconservation, tissue order and many more. These jobs are processed by the breeding facility and represent a history of the services provided. Each user can see the status of their jobs at all times. It is also possible to use the jobs to create invoices for customer billing.

Animal Ethics: Projects registered with the governmental authorities for working with animals are stored including the project leaders, approved treatments, registered co-workers, animal quotas etc.

TierBase: A program for computer-assisted management of an animal breeding and experimentation facility

Breeding Analysis: TierBase can store a complete breeding history of a colony. This makes it possible to answer questions about breeding productivity, litter size, genotypic frequencies resulting from the matings, geneology, etc. It also makes it possible to know at all times which animals are in current matings and which are available for experimentation.

TierBase is designed to be easy to use. Based on the experiences at numerous breeding facilities, it has proven to be very valuable in several ways. It can stimulate an efficient communication between scientists and the breeding facility. Scientists have immediate access to information such as which colonies they are responsible for, which ethics projects they have and how many animals are available. Animal technicians have an overview of jobs that need to be processed, the breeding productivity for each mating and which lines belong to whom. Animal ethics officers can see which animals were used for which purpose and can easily create project reports for submission to the governmental authorities. The use of TierBase can lead to a more efficient management and use of the breeding facility and experimental animal lines.

(Windows® is a registered trademark of Microsoft Corp.
Macintosh® is a registered trademark of Apple Computer Inc.)

Neuropathological results in laboratory mice

S. Ott, H. Meyer, N. Gerstmayr, G. Spindler

Institut of laboratory animal science, department diagnostik, university of ulm

Diseases of the brain are not common in laboratory mice. From 1 802 animals from our laboratory animal facility, which have been killed because of illness in the last 3 years, 19 showed signs of brain damage, mostly hydrocephalie (13), 4 had tumours (2 glioma, 2 lymphoma) and 2 purulent encephalitis.

The encephalitis cases were caused by *staphylococcus xylosus* in genetically modified immunodefficient mice. Both animals showed severe distress. The brains were soft and pale. In the histological slide there can bee seen an broad granulocyte infiltration and, at it`s border, macrophages with incorpotated bacteriae. *S. xylosus* was isolated in oure culture from blood and barin.

The incidence of hydrocephali depends on the genetically background. But in small breeding stocks, it may be impossible, to erradicate the disease. The only possibility is, to train the staff for killing the affected animals immediatelly after weaning.

S. xylosus is part of the normal flora of the mouse skin, and it was not expected to cause a health problem even in these immunodeficient mice. Today in many laboratory animal facilities more than 90% of the mice are genetically modified. It is a callenge for the diagnostic departments to find unexpected results of these modifications.

Pasteurella pneumotropica – Pathology of Virulent Biotypes

S. Ott, H. Meyer, J. Brodbeck, P. Nusser, G. Spindler

Institute of Laboratory Animal Science, Department of Diagnostics, University of Ulm

Pasteurella pneumotropica is a common germ in laboratory animal colonies. In highly frequented areas it is difficult to keep out. This may be the reason for the wide acceptance of *pasteurella* contamination, although it is known that *pasteurella* can be a pathogen. Actually the pathogenity can be fatal and represents a considerable problem in breeding and experimentation.

In our experimental facility of approximately 15,000 laboratory mice, *pasteurella pneumotropica* is responsible for 50% of all bacterial infections (tab. 1). We found severe inflammations and abscesses, in particular of the orbits and of the eye (fig. 1), caused mainly by *pasteurella pneumotropica* biotype Heyl. This biotype can also be isolated from purulent metritis (fig. 2) and from fetuses that died *in utero*. Frequently it is isolated from purulent dermatitis and subcutaneous abscesses and, less often, from purulent pneumoniae. Septicaemia is possible, with infection of various organs such as the heart (fig. 3). In a mouse with severe immunodeficiency (RAG backcross) we found biotype Jawetz in blood and brain.

The pathogenity of *pasteurella pneumotropica* is broadly underestimated. Pasteurella-free laboratory mice should be preferred for animal experimentation. Bioremediation using embryo transfer is easy and should be conducted at least for immunodeficient mice and breeding colonies.

In microbiological diagnostics it is important to distinguish between the different biotypes of *pasteurella pneumotropica*, due to their variations in pathogenicity.

New mouse models derived from the Munich ENU mouse mutagenesis project for iron metabolism research

B. Rathkolb (1), M. Klempt (1), M. Mohr (1), D. Soewarto (2), S. Hoffmann (2), S. Wagner (2), M. Hrabé de Angelis (2), E. Wolf (1), B. Aigner (1)

1 Institute of Molekular Animal Breeding and Biotechnology, Genecentre, LMU, Feodor-Lynen-Str. 25, 81377 München, 2 Institute of Experimental Genetics, GSF Research Centre, Ingolstädter Landstr. 1, 85764 Neuherberg

Iron is necessary for many metabolic processes, such as oxigen transport and DNA synthesis. It is the capability of iron to accept or donate electrons, that makes it an essential element but also causes cytotoxicity. Therefore the body and tissue iron content is balanced in narrow ranges by regulatory mechanisms, which are only in part unraveled. Several inherited disorders of iron metabolism, like hemochromatosis or hyperferritinemia, are known in humans and animals, but the pathogenesis of many such diseases remains to be elucidated. Some of these disorders are associated with neurological symptoms and it has been shown, that iron plays a crucial role in myelin formation and the development of the neuronal dendritic tree. Therefore, iron homeostasis is critical for normal brain function, especially in learning and memory. Also in complex neurodegenerative disorders like Parkinson`s or Alzheimer`s disease changes of iron homeostasis were found that are likely to contribute to the pathogenesis of these diseases.

A substantial part of what we know today about the regulation of iron metabolism is based on investigations on mouse models, such as the hypotransferrinemic mouse ($\text{Trf}^{\text{hpx/hpx}}$) or the transferrin receptor knockout mouse ($\text{TrfR}^{-/-}$). However, many details of the regulation of iron homeostasis are still unclear.

Within the Munich ENU mouse mutagenesis project several new mutant mouse line have been established by the clinical chemical and hematological screen showing different forms of inherited changes in iron metabolism, including iron deficiency syndroms as well as disorders of iron distribution and storage. A detailed phenotypic and genetic analysis of these mouse mutants will add new details to our current knowledge in this field.

New mouse models derived from the Munich NEU mouse mutagenesis project for iron metabolism research

We have just started to further characterize some of these mouse lines. The mouse line FER001 for example exhibits extremely high plasma ferritin levels without major changes of the red blood cell count and pathology. The mutation maps to a region, where no gene associated with iron metabolism is known. Another extremely interesting line is MVD019, a mouse line with dominantly inherited microcytic anemia. The increased ferritin levels and reduced transferrin saturation in plasma samples of heterozygous mutants belonging to this line, suggest a defect of iron transport or distribution.

Effects of soy-containing rat chow on estrogen receptive organs

G. Rimoldi, J. Chistoffel, D. Seidlova-Wuttke, W. Wuttke

Frauenklinik, Abt. Klinische und Experimentelle Endokrinologie. Uniklinikum Göttingen

There is ample evidence that soy contains isoflavones, primarily genistein, daidzein, formononetin and equol, all of which have more or less pronounced estrogenic actions. Soy is the major constituent of rat chow and it is therefore possible that the therein contained isoflavones may exert chronic estrogenic actions, which may mask or modify the effects of experimental treatments in a variety of estrogen regulated organs. Estrogen regulated organs are numerous since almost every cell of the body expresses the estrogen receptor α ($ER\alpha$), the $ER\beta$ or even both. Therefore we tested the effects of pelleted rat food containing soy as a protein source, which includes the above-mentioned isoflavones or potato proteins. Adult female rats were kept under both food sources and mated. After weaning the offspring were kept under soy containing and soy free food until three month of age when they were ovariectomized (ovx). Three months after ovx both animal groups were sacrificed and a number of organs collected and weighed. From these organs mRNA was extracted for quantitative real time RT-PCR for a number of estrogen regulated genes.

Most prominent estrogen-like regulated effects of the soy containing food were observed in the uteri, which had almost double the size of the uteri of the animals kept under soy free potato protein enriched food. Addition of estradiol to the pelleted food resulted in a seven-fold increase of uterine weight. Both, soy and estradiol had also a significant effect on gene expression of the progesterone receptor in the vagina, while no estrogenic effect of soy was observed in the heart, of which the weight was significantly stimulated by the estradiol treatment. All other measured organs like the pituitary and adrenal glands, the kidney and the urinary bladder were not affected by either treatment.

These results indicate that food supplemented with soy as a protein source may exert estrogenic effects in some but not all organs and this may confound any other possible treatment with test substances.

Enrichment in the housing of laboratory dogs

L. Schmid, D. Döring-Schätzl, M. H. Erhard

Institute for Animal Welfare, Animal Behaviour and Animal Hygiene Ludwig-Maximilians-University Munich, Schwere-Reiter-Str. 9, 80797 München

Background: Housing Enrichment for laboratory dogs was rarely brought up as a topic in literature so far. In some animal holding facilities dogs were offered a raised platform, to enlarge the usable space on different levels. Since contact to care staff and to other dogs is of great importance to most laboratory dogs, different raised platforms were tested, from which the animals had a larger field of vision. The question was, to what extent the dogs would make use of this form of enrichment.

Material and methods: Male Beagles ($n = 8$) at an age of approx. 11 months were held in groups of two in indoor kennels. The part of the box next to the centre aisle was equipped with a resting board ($186 \times 50 \text{ cm}^2$) at a height of approx. 40 cm. The animals could only see a very limited part of the aisle where most staff usually worked. Also observing dogs in other boxes was barely possible.

In a first experimental setup a raised platform ($90 \times 60 \text{ cm}^2$) at a height of 110 cm was offered additionally to the resting board. This enabled the dogs to see parts of the neighbouring boxes. The platform could be reached by a ramp. In order to prevent the animals from falling down, the platform was surrounded on three sides by lattice. In a second experimental setup, the resting board was replaced by a raised platform, so that the animals could see parts of the neighbouring boxes and a large area of the centre aisle. Before the two experimental periods, the animals received an acclimatization period of two weeks. During a preliminary period and the experimental periods the dogs were filmed one day per week from 7 a.m. to 5 p.m.. The behaviour of the individual animals was evaluated on basis of the videotapes using a computer program. The method used was the “focal animal sampling” with “continuous recording”. Significances were determined with the help of the t-test.

Results: The resting board in the preliminary period was used 40 % (± 15 %) of the observed time by each animal. In the first experimental setup each dog used the resting board 21 % ($\pm 17\%$) and the raised platform 20 % ($\pm 12\%$), so that each animal spent 41 % ($\pm 15\%$) on a raised area. In the second experimental setup the platform was used 73 % (± 9 %) of the observed time. This shows a significantly ($p < 0,0007$) longer use of a raised area compared to the preliminary period or to the first experimental setup.

Discussion: The study shows, that a raised platform was well accepted by the animals. However, the acceptance of the raised area depended on the enlargement of the field of vision. A raised platform or a resting board, which offers dogs the possibility to observe other dogs and to observe activities outside their boxes was frequently used by the animals and represents a good form of enrichment.

Keywords: Enrichment, dog, laboratory animals, behaviour, platform, focal animal sampling

The Effect of Hyperventilation on Cognitive Performance, Motor Function and Lesion Volume After Controlled Cortical Impact in the Rat

E. Eberspächer, M. Blobner, S. Ruf, K. Engelhard, B. Eckel, C. Werner

Klinik für Anaesthesiologie, Klinikum rechts der Isar, Technische Universität München

Introduction: This study investigates the effects of post-traumatic hyperventilation on neurocognitive and motor function as well as lesion volume in rats subjected to focal traumatic brain injury (controlled cortical impact, CCI).

Methods: Following institutional animal care committee approval 20 male Sprague-Dawley rats (369±15 g) were trained using a battery of cognitive and behavioural tests (modified hole-board¹, beam walk, beam balance, neurologic score) for a period of 10 days. After completion of training and evaluation of baseline parameters rats were anesthetized with 1.0-1.5 Vol% halothane in O₂/N₂O (FiO₂=0.33), intubated, and mechanically ventilated for surgical preparation. After skull trepanation controlled cortical impact was induced using a pneumatic pistol (Ø 5 mm, 1.75 mm depth, 200 ms, 4 m/sec). Animals were then randomly assigned to two groups of four hours post-traumatic ventilation with halothane (0.8-1.0 Vol%): group 1 normoventilation (n=10; PaCO₂=38-42 mmHg); group 2 hyperventilation (n=10; PaCO₂=28-32 mmHg). During the entire study, brain temperature and mean arterial blood pressure were kept constant at physiologic levels. Upon recovery post-traumatic performance in the above mentioned behavioural tests was re-evaluated for 20 days. The rats were then decapitated in deep anesthesia, their brains frozen and cut in 10 µm sections to evaluate lesion volume after kresylviolet and hematoxylin/eosin staining.

Statistics: Two-way ANOVA (p<0.05), mean ± standard deviation.

Results: Hyperventilated animals developed a significant deficit in declarative memory (hole-board test) on day 1 and 2 after trauma. This was associated with a decreased neurological score between days 1 and 3 compared to normoventilated animals with a decrease only on day 1. Both groups showed deficits in the beam walk and beam balance test compared to baseline values. In these tests

hyperventilated animals performed three-times worse compared to their normoventilated controls. In each test performance returned to baseline levels at latest on day 6. On day 20 after injury, lesion volume was significantly larger with hyperventilation ($69.7 \pm 13.0 \text{ mm}^3$) compared to normoventilation ($48.3 \pm 15.6 \text{ mm}^3$). There were no differences between groups with respect to walking, climbing, grooming, consciousness, nutrition-uptake, and anxiety related behaviour.

Discussion: Sustained post-traumatic hyperventilation transiently impairs hippocampus-dependant declarative memory, as well as motor and neurocognitive function. Likewise, and in contrast to normoventilation, hyperventilation enhances long-term histological damage. These data suggest that hypocapnic vasoconstriction caused by hyperventilation reduces the perfusion in peritraumatic tissue (penumbra) rather than redistributing cerebral blood flow in favor of ischemic territories (inverse steal effect).

References:

1. Ohl F et al. 2001 Behav Res Methods Instrum Comput 33: 392-397

Right ventricular pressure load in pigs

C. Sellin¹, H. Doerge¹, M. Coulibaly¹, C. Muehlfeld², C. Ballat¹, F.A. Schoendube¹

¹=Department of Thoracic and Cardiovascular Surgery, Robert-Koch-Straße 40, D-37075 Goettingen, Germany

²=Department of Anatomy, Division Electron Microscopy, Kreuzberggring 36, D-37075 Goettingen, Germany

Acute right ventricular pressure load (RVPL) is a frequent and severe clinical situation associated with pulmonary embolism and heart transplantation. An animal model for examination of the pathophysiology of acute RVPL is still lacking. Therefore, we aimed to establish such a model using pigs since the porcine coronary anatomy and cardiac output are similar to that of human beings. On this basis, hemodynamic and ultrastructural alterations representative of clinical events should be able to be elucidated.

The pigs were randomly sorted into a control or banding group. All procedures were performed under sterile conditions and constant veterinary control. After premedication with ketamine (10-15mg/kg i.m.), atropine (0.03mg/kg i.m.) and azaperone (4mg/kg i.m.), pentobarbital (5mg/kg i.v.) was injected for induction of anesthesia. The pigs were ventilated by endotracheal intubation with an air/oxygen mixture. During the protocol, anesthesia was maintained intravenously by ketamine (7-9mg/kg/h) and pentobarbital (6-9mg/kg/h), muscle relaxation by pancuronium (4mg). An electrocardiogram was recorded during the operation. Initially, the right internal carotid artery and the right internal jugular vein were exposed and catheterized to measure arterial blood pressure and central venous pressure. A Fogarty-catheter was placed in the right femoral artery to adjust systemic blood pressure. A sternotomy was performed, the pericardial sac was opened and the thymus was excised to gain access to the pulmonary trunc and the ascending aorta. Two pressure transducer-tip catheters were then placed in the pulmonary trunc and the right ventricle and were fixed with sutures. Furthermore, the right coronary artery and the proximal aorta were exposed and the blood flow was measured in both vessels. An epicardial vein was catheterized to investigate the cardiac consumption of oxygen. A pair of sonomicrometric piezoelectric crystals were placed in the right ventricular free wall to analyze the changes in longitudinal segment lengths. After a period of stabilization, in the banding group, the right ventricular pressure was increased

about 2.5 fold by constriction of the pulmonary trunc. The degree of constriction remained unchanged and arterial blood pressure, central venous pressure and heart rate were kept constant throughout the protocol. Right ventricular pressure, changes in longitudinal segment lengths and coronary blood flow were continuously documented. In both groups, myocardial biopsies were taken from the right ventricular free wall using a biopsy needle. Measurements were repeated after ten minutes, one, three and six hours in control and banding group. After right ventricular biopsies had been taken at six hours, the pigs were killed by an overdose of KCl.

Acute right ventricular pressure load caused a progressive loss in right ventricular function without limitation of oxygen supply. Mitochondrial ultrastructure was not changed in the banding group.

Thus, the present setup seems to be an appropriate animal model for examination of the pathophysiology in acute right heart failure.

Increased cancer risk in the B6C3F1 progeny of female mice exposed to X-rays before conception?

T. Tillmann, H. Ernst, C. Dasenbrock

Fraunhofer Institute of Toxicology and Experimental Medicine (ITEM),
Hannover, Germany

Background: Whether, and to what extent, preconceptual exposure to ionizing radiation has an impact on the tumor incidence and tumor spectrum in the progeny, especially if exposure was close to the time of conception, was to be investigated in an animal model. At the same time, it was to be clarified whether germ cell alteration in maternal animals after X-ray exposure increases the tumor risk in the offspring in case of exposure to immunomodulating or tumor-promoting agents later in life. Due to its still wide-spread use, cyclosporine A (CsA) was applied in this animal study. In addition to its immunosuppressive effects in humans and animals, CsA also promotes tumorigenesis. A possible combination of an immunomodulating and a tumor-promoting effect in the “preconceptually“ damaged descendants might be analyzed with this CsA treatment.

Methodology: Female mice (C57BL/6N) received X-ray irradiation (2 x 2 Gy with a 24-hour interval in between) and two weeks later were mated with untreated males (C3H/HeN). After weaning, the B6C3F1 descendants were subdivided into two groups: One was left untreated to observe the consequences of the preconceptual radiation exposure per se, the other was exposed to cyclosporine A (CsA, 150 mg/kg diet) for 6 months. All animals were maintained under standard laboratory conditions and analyzed for the occurrence of tumors. At the age of about 28 months, surviving mice were killed humanely by an overdose of CO₂. A complete necropsy was carried out on all animals, including those which died or had to be euthanized prematurely. All organs and tissues were fixed in formalin. In addition, individual organs or parts of these were snap-frozen in liquid nitrogen for future molecular analysis. The lungs, liver, spleen and any tissue with tumor-suspicious macroscopic findings were evaluated by light microscopy.

Results: Fertility as well as the lifetime of the maternal mice were significantly reduced by the X-ray irradiation (2 x 2 Gy) two weeks before conception, and their incidence of lung and liver tumors was significantly increased compared to non-irradiated maternals.

The F1-descendants of all groups revealed comparable body weights and mortality rates. A significantly increased incidence of lung and liver tumors in the sham-treated male descendants of irradiated mothers was detected, suggesting germ cell-mediated induction of these lesions.

The increased incidence of malignant lymphomas in the CsA-treated F1 females underlined the tumor-promoting effect of cyclosporine A in this specific model.

Keywords: Transgeneration carcinogenesis, X-ray irradiation, cyclosporine A, B6C3F1 mice

EEG monitoring of anaesthetic depth using Bispectral Index[®] (BIS[™]) measurement in large experimental surgery in swine

M. Wagenblast, H. Winklmaier and A. Theisen

Central Animal Care and Research Facilities, J.W.Goethe-University Hospital
Frankfurt(M)

Abstract (authors translation):

Introduction: It is indispensable to ensure sufficient depth of anaesthesia during long-lasting experimental surgical procedures, especially when neuromuscular blocking agents are being used. Blood pressure and heart frequency often provide inadequate information on anaesthetic depth. A suitable alternative in monitoring depth of anaesthesia is given by the electroencephalogram (EEG). Aim of this study was to investigate if commercially available equipment for EEG monitoring from human medicine could be used in laboratory swine.

Several systems are commercially available for the calculation of specific factors and indices representing depth of anaesthesia in addition to EEG pattern. Systems with increasing demand are calculating so-called Bispectral Index (BIS[™]) and suppression ratio (SR). Bispectral Index is based on spectral analysis of EEG data. It is defined as a nondimensional number between 0 and 100. SR represents the part of flat line EEG of the complete pattern.

Materials and methods: 6 german landrace pigs were monitored undergoing thoraco-cardial surgery with extracorporeal circulation. Anaesthetic agents and neuromuscular blocking agents (Propofol / Fentanyl / Pancuronium) were administered total-intravenously. Pigs were ventilated mechanically. EEG monitoring was performed using BIS Monitor 2000 XP (Aspect MS, Leiden, Netherlands). Target parameters were the course of Bispectral Index (BIS values) and the course of suppression ratio (SR values). Further parameters were: Arterial blood pressure, endexpiratorial CO₂, arterial blood gases, ECG.

Results: The self-adhesive electrode carrying four sensor elements obviously fitted with the proportions of the pig-forehead. Stable measurements were possible over a period of many hours. BIS values about 0 are correlating with high suppression ratio (ca. 100) representing flat line EEG. Reliable anaesthetic depth can be expected while BIS values are ranging between 0 and 60 according

to EEG pattern and the suppression ratio. Thus, the situation seems to be comparable to human patients.

Discussion: EEG monitoring of pig anaesthesia seems to be a practicable method. The different anatomic proportions don't require any kind of adaptation of the sensor. EEG pattern of anaesthetised swine obviously causes similar BIS values as in human beings, in principle. Validation of the system will be performed in further studies.

Introduction:

Monitoring of anaesthetic depth is mostly done on the basis of clinical criteria. In the 1920's Guedel had developed a scheme usable for ether-narcosis. Criteria like corneal reflex, spontaneous respiration and muscle tonus have been availed for validation. Currently, blood pressure and heart rate are used for monitoring of anaesthetic depth, either. However, the regulation of both depends on the age of the patient and on type of anesthesia. Another possibility for monitoring anaesthetic depth is monitoring EEG.

It is of great importance to warrant adequate anaesthesia in experimental animals, especially when neuromuscular blocking drugs (NMBI's) are involved (Drummond et al. 1996). Under usage of NMBI's it is possible that animals are conscious during surgery while they are unable to react.

EEG monitoring only observes the state of awareness. On the other hand, the status of relaxation and analgesia is not represented by EEG monitoring itself. Although EEG does not reveal anything about analgesia as a matter of principle, pain can cause impulses for waking up.

EEG monitoring is important for prevention of too light anaesthesia, which can be the reason for massive intraoperative stress. On the other hand, it is also useful to prevent too deep anaesthesia as well. Too deep anesthesia increasingly leads to haemodynamic impairments and delayed recovery. Anaesthetic drugs can be saved, too.

Disadvantage of EEG monitoring is the rather difficult interpretation of the EEG pattern. Development of Bispectral Index has simplified this significantly. Another disadvantage is that the equipment of human medicine is limited in utilisation on laboratory animals. For example the electrodes can't be placed in small animals like rodents with the standard sensor.

Basic principles of electroencephalography and monitoring of anaesthetic depth:

Principle of EEG is that electric potentials are measured. Primarily four different category groups of frequency are defined. EEG is divided in alpha (8-13 Hz)-, beta (> 13 Hz)-, theta (4-8 Hz)- and delta (0,5-4 Hz)-waves.

In the EEG of awake subjects predominantly alpha- and beta-waves can be seen. After sedation a so-called beta-activation with increasing frequency follows, particularly beta-waves can be found in the EEG pattern now. Lower frequencies occur with increasing anaesthetic depth. Theta- and at last particularly long delta-waves can be seen. Below a certain point suppression begins, which can only be interrupted by so-called bursts at any time. Absolute suppression with complete isoelectric EEG is reached at last.

EEG data of numerous patients were measured for development of BIS algorithm (Johansen and Sebel 2000). Data were analysed for the powerspectrum according to the classical form of EEG analysis, the Fourier analysis (Rampil 1998). The bispectral analysis was developed additionally by quantifying the correlation between all the frequencies within the signal (Sigl et al. 1994, Glass et al. 1997). Characteristics of both types of analysis which correlate best with clinical endpoints of anaesthesia have been combined for development of Bispectral Index. BIS is defined as an absolute number between 0 (absence of electrical brain activity) and 100 (wide awake). It is therefore relatively simple to interpret. At low BIS values, the degree of EEG suppression is the primary determinant of the BIS values (Bruhn et al. 2000). The BIS Index is a unique, clinically-validated parameter that allows to trend changes in the hypnotic state in human medicine (Glass et al. 1997, Iselin-Chaves et al. 1998, Kearsse et al. 1998).

EEG monitoring in swine:

Martin-Cancho et al. (2003) reported that BIS Monitor A1050™ was useful for predicting changes in anaesthetic depth in swine anaesthetised with clinical dosages of inhalant anaesthetics. The Bispectral Index Scale has also been used to document the hypnotic effect of etomidate and propofol in studies with pigs (Johnson, Egan, Kern et al. 2003, Johnson, Egan, Layman et al. 2003).

Aim of our study was to figure out if routine monitoring for supervision of anaesthetic depth in swine is suitable with the newly developed BIS Monitor 2000 XP. Suppression ratio (SR) was recorded in addition to Bispectral Index. SR indicates percentage of time that the EEG signal is in isoelectric state.

Intraoperative oxygen consumption was monitored as an additional reference parameter. This seems to be the only possible way to validate EEG monitoring in animals, because this parameter correlates with intraoperative stress-reactions, too.

The sensor-electrodes must be placed in only one hemisphere, as shown in Fig. 1. Firstly, the head must be shaved and defatted with alcohol to ensure good contact. In our experiments signal quality was always sufficient during

measurement. Only rare interfering EMG-activity was seen. Clinical reactions during narcosis in swine using BIS monitoring seem to have a close match with the BIS range guidelines validated for man (Johansen and Sebel 2000).

At isoelectric EEG the BIS range 0 was displayed, too. At values about 40 to 60 delta-waves appeared while intraoperative oxygen consumption didn't change at this level. This points on absence of stress at this BIS range and an adequate anaesthetic depth in swine. In individual cases, we found in these relatively young animals SR values of 10 associated with BIS values of more than 70. One single animal, not undergoing a final experiment, was beginning to recover at a BIS of 90 as it is the case in human patients.



Fig. 1
Premedicated (Ketamin/Xylazine) pig with
BIS – sensor attached

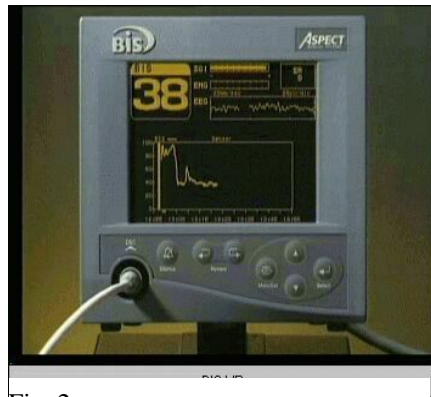


Fig. 2
BIS- Monitor in process

Conclusion:

Even with high BIS values up to about 60 no changes in oxygen consumption were recordable. Thus, it is presumable that no stress had occurred. At a BIS about 70 - 80 awareness can't be precluded. We suggest therefore to avoid BIS values above 60, but raw EEG and SR should always be considered. In human patients, SR of higher than 10 is said to be correlating with absence of awareness.

According to these findings, it is important to point out that not only the BIS number is to be considered. The BIS number eases interpretation of EEG, but it isn't able to substitute interpretation completely. The trend of BIS range must always be considered additionally to get relevant information on anaesthetic depth. Additional observance of EEG pattern and suppression ratio is also important for interpretation of the EEG.

Literature:

1. Bruhn J, Bouillon TW, Shafer SL (2000) Bispectral index (BIS) and burst suppression: Revealing part of the BIS algorithm. *Journal of Clinical Monitoring and Computing* 16, 593-6
2. Drummond JC, Todd MM, Saidman LJ (1996) Use of neuromuscular blocking drugs in scientific investigations involving animal subjects. The benefit of doubt goes to the animal. *Anaesthesiology* 85, 697-9
3. Glass PS, Bloom M, Kearse L, Rosow C, Sebel P, Manberg P (1997) Bispectral analysis measures sedation and memory effects of propofol, midazolam, isoflurane, and alfentanil in healthy volunteers. *Anaesthesiology* 86, 836-47
4. Iselin-Chaves IA, Flaishon R, Sebel PS, Howell S, Gan TJ, Sigl J, Ginsberg B, Glass PS (1998) The effect of the interaction of propofol and alfentanil on recall, loss of consciousness, and the Bispectral Index. *Anesthesia and analgesia* 87, 949-55
5. Johansen JW, Sebel PS (2000) Development and clinical application of electroencephalographic bispectrum monitoring. *Anaesthesiology* 93, 1336-44
6. Johnson KB, Egan TD, Layman J, Kern SE, White JL, McJames SW, Syroid N, Whiddon D, church T (2003) The influence of hemorrhagic shock on propofol. A pharmacokinetic and pharmacodynamic analysis. *Anesthesiology* 99, 409-20
7. Johnson KB, Egan TD, Kern SE, White JL, McJames SW (2003) The influence of hemorrhagic shock on etomidate: a pharmacokinetic and pharmacodynamic analysis. *Anesthesia and analgesia* 96, 1360-8
8. Kearse LA, Jr., Rosow C, Zaslavsky A, Connors P, Dershwitz M, Denman W. (1998) Bispectral analysis of the electroencephalogram predicts conscious processing of information during propofol sedation and hypnosis. *Anesthesiology* 88, 25-34
9. Martin-Cancho M F, Lima, JR, Luis L, Crisostomo V, Ezquerro LJ; Carrasco MS, Uson-Gargallo JU (2003) Bispectral index, spectral edge frequency 95%, and median frequency recorded for various concentrations of isoflurane and sevoflurane in pigs. *American Journal of Veterinary Research* 64, 866-73
10. Rampil IJ (1998) A primer for EEG signal processing in anesthesia. *Anesthesiology* 89, 980-1002
11. Sigl JC, Chamoun NG (1994) An introduction to bispectral analysis for the electroencephalogram. *Journal of Clinical Monitoring and Computing* 10, 392-404

Changes in differential haemogram after infusion of mean and low molecular weight hydroxyethyl starch (HES) in rats

M. Wagenblast, A. Theisen, Ch. Tandi, H. Foerster

Institute of Experimental Anaesthesiology, J. W. Goethe-University Hospital Frankfurt(M)

Introduction: Volume effect is achieved by use of colloidal volume substitutes like hydroxyethyl starch (HES) and represented by a decreasing value of haematocrit. Leukocyte concentration should be influenced by this effect in the same way. However, other effects of HES on leukocytes like intracellular storage and functional interference are discussed. Aim of this study was to figure out if changes in haemogram are not only caused by haemodilutional effects. Two different, commonly used HES-preparations were compared. Erythrocytes and leukocytes were measured by flow cytometrie.

Materials and methods: 8 Wistar WU-Rats (300-350 g) in each trial group were infused. Each 18 ml of 6% mean molecular weight, medium substituted HES 200/0,5 and of 6% low molecular weight, low substituted HES 130/0,4 (Haes-steril® and Voluven®, both Fresenius Kabi, Bad Homburg, Germany) were administered within 3 hours via central venous catheter. Blood was taken pre-infusion, immediately post-infusion 2, 4, 6, 24 and 48 hours post-infusion by orbital puncture. A haemogram was determined using Cell-Dyn 3500R (Abbott). For statistical calculation, data were firstly tested for standardised normal distribution by Shapiro-Wilk-Test. In case of standardised normal distribution, two sample t-Test was used. In case of absence of standardised normal distribution, Wilcoxon-Mann-Withney-U-Test was preferred. Level of significance was defined as 5%. Described changes in results are statistically significant to the extend that nothing else is mentioned.

Results: For Haematocrit (Htc) and quantity of red blood cells (RBC) a correlation was found ($r > 0,98$) after infusion of HES. MCV (mean corpuscular volume) didn't change significantly. For this reason RBC showed volume effect

comparable to Htc. RBC's were utilised for quantitative comparison of blood cells. RBC decreased for a short time post-infusion. However, RBC increased already 2 h (HES 130/0,4) respectively 4 h (HES 200/0,5) above the initial value. On the following days, RBC values were persistently lower than initial value. Comparing RBC with white blood cells (WBC) coefficients of correlation (r) ranged between 0,22 and $-0,64$. 24 h and 48 h post-infusion WBC were increased after administration of HES 200/0,5. After administration of HES 130/0,4 WBC were not increased, 6 h post-infusion they were even decreased (s. Figure 1). The number of neutrophils increased after infusion of both HES solutions. Number of Lymphocytes decreased until 6 h (HES 200/0,5) respectively 24h (HES 130/0,4) post-infusion, in the following time quantity increased in relation to initial value (s. Figure 2). Quantity of monocytes increased 3,8 to 6,4-times after infusion of HES 200/0,5 in comparison to the initial value (s. Figure 3). In contrast, increase of monocytes was not significant after infusion of HES 130/0,4. Quantity of basophils and eosinophils didn't increase until 24 h (HES 200/0,5) respectively 48 h (HES 130/0,4) post infusion.

Discussion: As shown by the missing correlation, changes in white blood cell count are not only explainable by haemodilutional effects. On the other hand, some changes can be explained by influences of narcosis and surgical procedure. However, it is known that in the first line monocytes absorb HES in association with storage. Up to now, it was unknown that the quantity of monocytes increases directly post-infusion in contrary to the haemodilutional effect of the administered solution. This effect was less pronounced after infusion of HES 130/0,4 than after infusion of HES 200/0,5.

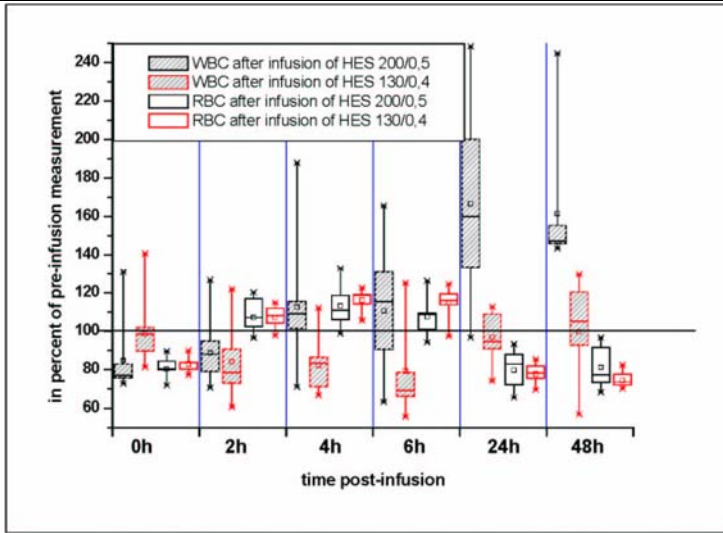


Figure 4:
Comparison of RBC and WBC after infusion of two different HES preparations

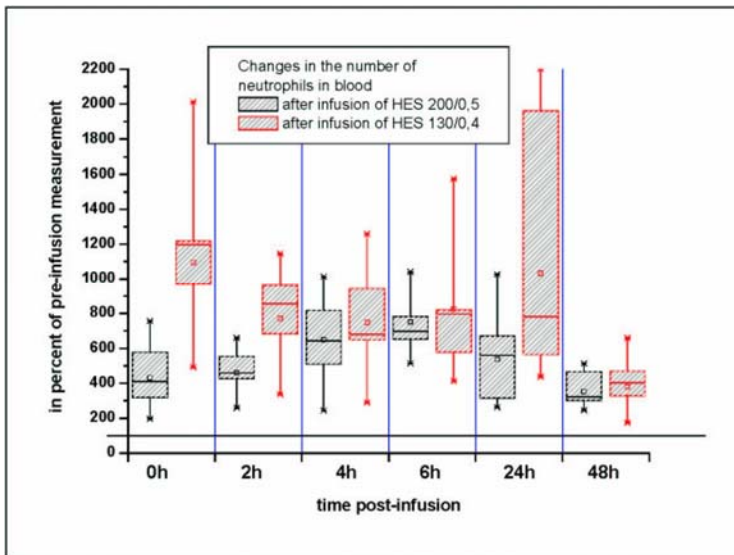


Figure 5:
Changes in the number of neutrophils after infusion of two different HES preparations

Changes in differential haemogram after infusion of mean and low molecular weight hydroxyethyl starch (HES) in rats

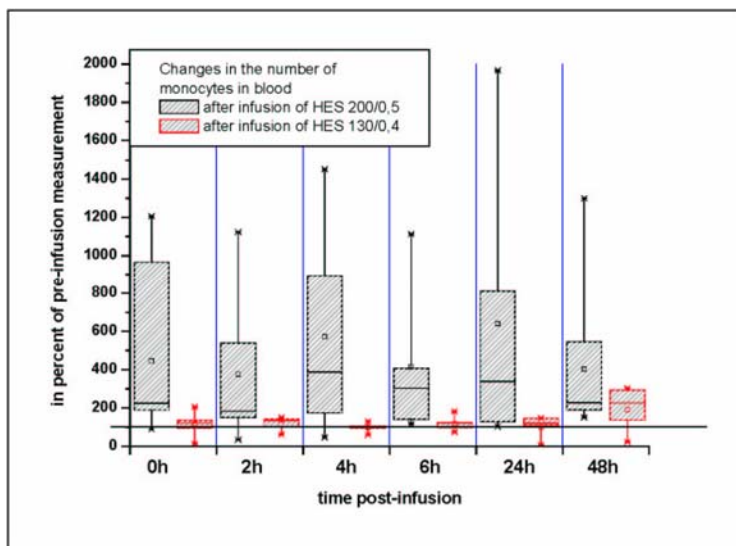


Figure 6:

Changes in the number of monocytes after infusion of two different HES preparations

Middle cerebral artery occlusion during MR-imaging (in-bore occlusion) -A new stroke model in rats

M. Walberer, T. Gerriets, E. Stolz, C. Müller, A. Kluge, A. Bachmann, M. Kaps,
G. Bachmann

Dep. of Radiology / Experimental Neurology Research Group, Kerckhoff Clinic
Bad Nauheim, Germany, Dep. of Neurology, University Giessen, Germany

Introduction

MR-imaging during hyperacute phase of stroke is difficult to perform since induction of focal cerebral ischemia has to be performed outside the magnet bore and the rats have to be transferred into the MRI-scanner thereafter. Thus, the first measurements can be started approximately 20 to 30 minutes after MCA-occlusion.

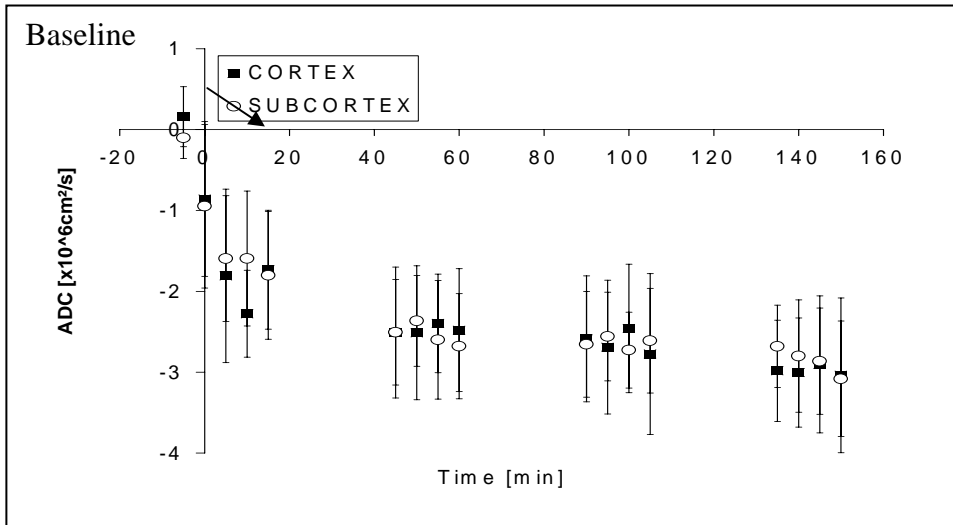
The recently introduced macrosphere-model allows to perform MCA-occlusion inside the MRI-scanner, which permits investigation immediately after infarct induction. Moreover, this method allows a pixel-by-pixel comparison between pre- and postischemic images since the animal has not to be repositioned after baseline measurements.

Material

This study was performed in 9 Sprague-Dawley rats. PE-50 tubing, filled with Saline and six microspheres (0.315-0.355mm in diameter), was placed into the internal artery. The animals were transferred into an MRI-scanner (Bruker, Pharna-scan, 7.0T) and baseline measurements were performed. Then the microspheres were injected into the internal artery to occlude MCA. This procedure was followed by repetitive diffusion- and T2-imaging for 160 minutes. ADC, which is a marker for cytotoxic brain edema, and T2-relaxation time, which is a marker for vasogenic brain edema, were determined in regions of interests (ROI).

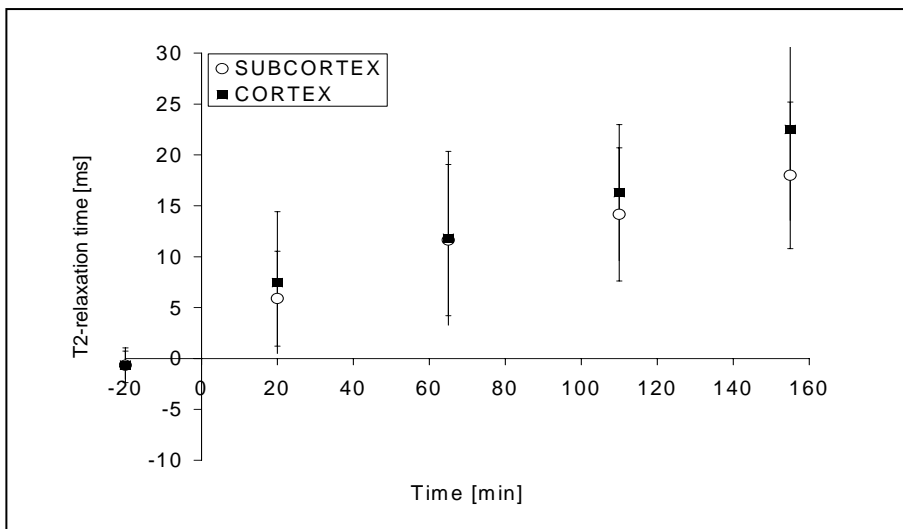
Results

ADC declined significantly as early as 5 to 10 minutes, continued to decrease until 45 minutes after MCA occlusion and remained stable afterwards.



Time-course of ADC-decline (side-to-side differences)

A significant increase in T2-relaxation time and hemispheric swelling could be detected at the first T2-imaging time-point (20-35 minutes after MCA occlusion). T2-relaxation time continued to increase thereafter.



Time-course of T2-relaxation time (side-to-side differences)

After 150 minutes of ischemia, the lesion covered $18.0 \pm 7.4\%$ of the hemispheres.

The model failed to induce MCA occlusion in one out of nine animals (11%).

Conclusion

Decrease of ADC indicated the development cytotoxic brain edema within the first minutes of ischemia.

The increase in T2-relaxation time indicated vasogenic brain edema as early as 20 minutes after MCAO. At this time-point a significant midline-shift was detectable.

The present study demonstrates that the macrosphere models allows in-bore occlusion and thus permits MRI studies immediately after MCA occlusion. This new technique provides important information about the pathophysiological processes during the hyperacute phase of stroke.

Cryopreservation of transgenic mouse embryos

Klaus Wayss, Michaela Klefenz and Johannes Schenkel

Deutsches Krebsforschungszentrum, E 160, Im Neuenheimer Feld 280, D-69120 Heidelberg, FR Germany

About 71.000 predominantly transgenic mouse embryos prepared during the past eight years from 9.727 pregnant female donors were cryopreserved protecting 125 mutant mouse lines against loss. Mainly embryos of transgenic overexpressors were conserved, but targeted mutants, too. In the means 7.26 embryos (8-cellers) per pregnant donor were received. A conservation method leading to a high revitalisation rate was chosen. To reduce the number of animals, just available mice were used if suitable. Therefor breedings exclusively for cryopreservation were omitted.

The advantage of this strategy is that (mutant) mouse lines out of current use must not be kept in a breeding nucleus. More over, this procedure leads to rederivation and makes the export of mice to other facilities easier.

Among others, the data were analysed for influences in the gain of embryos by the genetic background and the different housing conditions. Furthermore, the long time sexual activity of males was investigated, remaining constant over 12 frequent breedings and collapsing afterwards.

After thawing, 81% of the formerly cryopreserved embryos were successfully revitalised.

Our data show that the cryopreservation is a safe technology exhibiting the advantage that (mutated) mouse lines out of current use are not to be kept in a breeding nucleus. In parallel, this procedure leads to rederivation making the export of mice to other facilities easier. The cryopreservation of these 125 lines keeps the potential to save more than 20.000 laboratory mice per year to be bred, if they would be kept in a breeding stock or the permanent occupation of 400 cages. This is a major contribution to the requirements of the "3R"-hypothesis developed by Russel and Burch to reduce the number of laboratory animals used.

Understanding and Controlling For Background Strain Effects on Phenotype

Carol Cutler Linder, PhD, Barbara Witham, BS

JAX Research Systems, The Jackson Laboratory, Bar Harbor, Maine, USA

The Jackson Laboratory has over 70 years of unparalleled experience as a repository and developer of new mouse models for basic and applied research. The phenotypic characteristics of mice carrying spontaneous or genetically engineered mutations are often attributed solely to the gene of interest. We have learned through experience the importance of strain background in influencing the overall phenotype. As increasing numbers of researchers are turning to the mouse to better understand the genetics of human disease, a clear understanding of background strain effects has become essential. Strain effects can be grouped into three basic categories: a) unlinked genes that modify the phenotypic effects of the gene of interest; b) unlinked genes that modify the phenotype without directly affecting the effects of the gene of interest; and c) linked genes carried over during backcrossing. We will provide relevant examples of these three types of effects, overall recommendations to help the researcher determine gene vs. background effects, and a description of online resources available from The Jackson Laboratory. This information will assist researchers in strain selection, utilization, and analysis of mutant mouse models.

Alphabetical author index

Author	Page	Author	Page
Aigner, B.	152	Elste	127
Alekuzei, H.	108	Engelhard, K.	157
Arras, M.	81	Erhard, M.H.	155
Bachmann, A.	39, 172	Ernst, H.	161
Bachmann, G.	39, 47, 172	Exner, C.	83
Ballat, C.	108, 159	Fanghänel, J.	147
Bardenheuer, H. J.	43	Fisher, M.	39, 47
Becker, T.	58	Foerster, H.	77, 169
Beuter, C.	110	Fozard, L.	115
Bleich, A.	111	Frahm, Jens	1
Blobner, M.	157	Friderichs-Gromoll, S.	133
Böhme, H.	141	Gerriets, T.	39, 47, 172
Bolle, I.	113	Gerstmayr, G.	150
Boretius, S.	1	Giesen, K.	95
Brem, G.	64	Grothe, M.	95
Brielmeier, M.	70, 74	Guan, K.	58
Brodbeck, J.	151	Habermann, G.	133
Buchwald, A.B.	58	Hrabé de Angelis, M.	152
Buer, J.	111	Hackbarth, H.	137, 139
Bürge, T.	115	Hasenfuß, G.	58
Buse, E.	133	Hedrich, H.	111, 124
Büttner, D.	141	Heldmaier, G.	83
Christoffel, J.	154	Helppi, J.	131
Chwalisz, W.T.	124	Hemmerlein, B.	132
Compton, S. R.	68	Heuser, Markus	132
Coulibaly, M.	159	Hilken, G.	113
Cutler Lindner, C.	177	Hoffmann, S.	152
Dasenbrock, C.	137, 139, 161	Homberger, Felix	68
Doerge, H.	108, 159	Jacobsen, K.	70, 143
Döring-Schätzl, D.	155	Joost, H.G.	96
Duperon, J.	131	Joswig, N.	110
Eberspächer, E.	157	Kaps, M.	39, 47, 173
Eckel, B.	157	Kaspareit, J.	133
Ehrenreich, H.	30		

Author	Page	Author	Page
Kimmina, S.	136	Natt, Oliver	1
Klefenz	176	Needham, J.	143
Klein, M..	137, 139	Nicklas, W.	104
Klempt, M.	152	Nielsen, P.	148
Klötting, Ingrid	87	Nusser, P.	151
Klötting, Nora	87	Oegma, J.	131
Kluge, A.	39, 172	Ott, S.	92, 101, 150, 151
Kluge, R.	95	Paturzo, F.	68
Klymiuk, N.	64	Peters, D.	143
Knauth, Michael	43, 52	Plaschke, Konstanze	43, 52
König, S.	60	Plum, L.	95
Krause, P.	60	Rathkolb, B.	152
Krüger, C.	141	Reifenberg, K.	92
Kwiatkowski, H.	110	Rettich, A.	81
Lages, D.	58	Rimoldi, G.	154
Lauber, J.	111	Ringert, R.H.	132
Löhler, J.	92	Ruf, S.	157
MacArthur Clark, J.	68	Rülicke, T.	81
Mahabir, E.	70, 72, 143	Schenkel, J.	175
Mähler, M.	111	Schemeck, S.	95
Malek, F.A.	147	Schmid, L.	155
Martin, E.	43	Schmidt, J.	70, 143
Mayer, A.	72	Schmitto, J.	108
Meyer, H.	101, 150, 151	Schmolz, K.	95
Michaelis, Th.	1	Schoendube, F.	108, 159
Milite, G.	145	Schulz-Schaeffer, W.J.	15
Militzer, K.	141	Seidel, K.	70
Mohr, A.	52	Seidlova-Wuttke, D.	154
Mohr, M.	152	Seifert, B.	81
Möritz, K.U.	147	Sellin, C.	159
Mossmann, H.	110, 148	Sirén, Anna-Leena	30
Muehlfeld, C.	159	Soewarto, D.	152
Müller, C.	39, 172	Spindler, G.	150, 151
Müller, M.	64		

Alphabetical author index

Author	Page
Stadelmann	19
Stauffer, U..	110
Steinke, K.	108
Stolz, E.	39, 47, 172
Tandi, Ch.	77, 169
Theisen, A.	77, 163, 169
Tillmann, T.	137, 139, 161
Tsai, P.P.	137, 139
Vogel, F.	133
Wagenblast, M.	77, 163, 169
Wagner, S.	152
Walberer, M.	39, 47, 172
Watanabe, Takashi	1
Wayss, K.	176
Wedekind, D.	124
Werner, C.	157
Wilhelm, P.	70, 74
Winklmaier, H.	163
Witham, B.	177
Wolf, E.	152
Won, S.	58
Wuttke, W.	154
Yamamura, K.	92
Zöller, G.	132
Zyba, V.	58

The main topic of the meeting “Neuroscience” was focussed on the region of Göttingen, due to the different institutes working with laboratory animals such as the Max Planck Institutes for Experimental Medicine and Biophysical Chemistry, the German Primate Center, the European Neuroscience Institute and finally the Georg August University (Medical Department). A large variety of issues was discussed in the course of this congress, e.g. stroke, neurodegenerative disorders, TSE, stem-cells and infectious diseases in laboratory animals, which can be found in the congress book now.



ISBN-10: 3-938616-66-0
ISBN-13: 978-3-938616-66-6

Universitätsdrucke Göttingen